NOTICE

The quality of this microform is heavily dependent upon the quality of the original thesis submitted for microfilming. Every effort has been made to ensure the highest quality of reproduction possible.

If pages are missing, contact the university which granted the degree.

Some pages may have indistinct print especially if the original pages were typed with a poor typewriter ribbon or if the university sent us an inferior photocopy.

Previously copyrighted materials (journal articles, published tests, etc.) are not filmed.

Reproduction in full or in part of this microform is governed by the Canadian Copyright Act, R.S.C. 1970, c. C-30.

AVIS

La qualité de cette microforme dépend grandement de la qualité de la thèse soumise au microfilmage. Nous avons tout fait pour assurer une qualité supérieure de reproduction.

S'il manque des pages, veuillez communiquer avec l'université qui a conféré le grade.

La qualité d'impression de certaines pages peut laisser à désirer, surtout si les pages originales ont été dactylographiées à l'aide d'un ruban usé ou si l'université nous a fait parvenir une photocopie de qualité inférieure.

Les documents qui font déjà l'objet d'un droit d'auteur (articles de revue, tests publiés, etc.) ne sont pas microfilmés.

La reproduction, même partielle, de cette microforme est soumise à la Loi canadienne sur le droit d'auteur, SRC 1970, c. C-30.

Canada

ANALYSIS OF ELECTROMAGNETIC FIELDS IN LOADED TEM CELLS

By

SENG-LEE,FOO,B.A.Sc.

A Thesis submitted to the
School of Graduate Studies and Research
in partial fulfillment of the requirements
for the degree of
Master of Applied Science

Ottawa-Carleton Institute for Electrical Engineering
Department of Electrical Engineering
Faculty of Engineering
University of Ottawa

ISBN 0-315-46760-6

UNIVERSITÉ D'OTTAWA
UNIVERSITY OF OTTAWA

CONTENTS

ACKNOWLEDGEMENT

The author would like to express his sincere gratitude to his supervisors Dr.Stanislaw S.Stuchly and Dr.George Costache,whom the author felt deeply indebted to for their encouragement and guidance throughout the work.

The author also gratefully acknowledge the assistance and support given by the Department of Electrical Engineering ,University of Ottawa.

Finally the author would like to especially thank his wife ,Yin-lan, for her understanding ,patience and support during the study.

ABSTRACT

Physical and electrical characteristics of symmetrical and asymmetrical TEM cells are briefly described .Applications and limitations of TEM cells are discussed .Fabrication details and design curves for constructing a TEM cell are given.

TEM mode operation is assumed for electrostatic analysis. Mathematical formulation and solution of finite difference method and finite element method are presented. Combined method of finite difference and finite element is developed and elaborated .Comparison of the three numerical methods is given.

Actual implementation of all three numerical methods for a loaded TEM cell is presented. Electric field distortions in the TEM cell due to the present of a homogeneous 2-Dimensional telephone is computed using all three methods. Results are analysed and discussed .

Further investigations of the field distortions and electric field variations in a loaded TEM cell is performed for various types of telephone model:A homogeneous telephone, an inhomogeneous telephone and a metallic telephone. Theoretical curves for estimating maximum object size in a given TEM cell are developed for a semicircular cylindrical object in contact with the center conductor.

LIST OF ACRONYMS

CW	Continuous wave
DF	Distortion factor
EM	Electromagnetic
ER	Preset Error criterion for SOR
EMC	Electromagnetic compatibility
EMI	Electromagnetic interference
EMP	Electromagnetic pulse
EMS	Electromagnetic susceptibility
EUT	Equipment under test
FDM	Finite difference method
FDEM	Combined method of finite difference & finite element
FEM	Finite element method
IFI	Instruments for Industry Inc.
NEMP	Nuclear Electromagnetic pulse
NOTR	Total number of triangles in Finite Element Method
RCTL	Rectangular transmission line
RF	Radio Frequency
SOR	Successive overrelaxation method
TEM	Transverse electromagnetic
VSWR	Voltage standing wave ratio

LIST OF SYMBOLS

ϵ	Dielectric constant
ϵ_o	Dielectric constant of free space
ϵ_r	Relative dielectric constant
Φ	Electric potential
Φ_o	Electric potential of the septum
D	Displacement vector
ρ	Electric charge
ρ_s	Surface charge density
$\vec{E}$	Electric field
$\bar{E}$	Normalized electric field intensity
$\vec{n}$	Unit vector normal to the Gaussian Surface
Z_o	Characteristic impedance
υ	Phase velocity
υ_o	Velocity of light
λ	Wavelength
λ_c	Cutoff wavelegth
λ_g	Guide-wavelength
f_c	Cutoff frequency
f_r	Resonant frequency
Δ	Unit step of the finite difference method
C	Capacitance per unit length of the TEM cell
a	One half the width of the TEM cell
b	Distance between the center septum and the outer conductor of the TEM cell
g	The gap between the center septum and the outer conductor of the TEM cell
w	Width of the center septum of the TEM cell

LIST OF TABLES

LIST OF FIGURES

CHAPTER 1

GENERAL INTRODUCTION

1.1 INTRODUCTION

Due to the predominant use of semiconductor technology ,the probability of destruction of unprotected electronic equipments has increased and EMP is today regarded as a major threat ,especially for the military applications.EMP is a pulse sometimes known as nuclear electromagnetic pulse (NEMP).This is a pulse of energy caused by a nuclear explosion that is capable of causing the malfunction or destruction of unprotected equipmqnts such as data and communication links,communication equipment, radars and supply lines.EMP covers a spectrum from approximately 10KHz to several hundred MHz and induces very high voltages and currents into cables,antennas,metal enclosures and structures. It is capable of breaking down insulation and causing highly destructive currents to flow in circuits unless they are suitbly protected.To ensure the proper operation of these solid-state electronic equipments under this serious electromagnetic interference environment the electromagnetic compatibility of these electronic equipments must be determined to a certain accuracy.

Studies the electromagnetic compatibility (EMC) of various electronic equipments require accurate measurement techniques to define their electromagnetic interference (EMI) characteristics . Many measurement techniques have also been developed for performing test of electromagnetic susceptibility (EMS) . The primary measurement techniques include open-field range , shielded enclosure , anechoic chamber and loaded antennas , mode perturbation

, TEM transmission lines ,statistical sampling , compact range , near-field probes and low-Q enclosures as described by M.L.Crowford [3] .

The transverse electromagnetic (TEM) transmission line technique is considered to be a simple,straight forward,relatively inexpensive and easily available technique . This technique was originally proposed and developed by M.L. Crowford [22] at the U.S. National Bureau of Standard in U.S.A.

1.2 TEM CELL

The TEM cell or Crowford cell consists of a section of a TEM-mode rectangular transmission line (RCTL) coupled at each end to a standard 50-Ω coaxial line via a pair of tapered sections . Isometric and cross-sectional views of a regular symmetric TEM cell are shown in Figure 1& 2. The line and the tapered transitions are designed to have a nominal characteristic impedance of 50 Ω along their length to ensure small voltage standing wave ratio (VSWR) in the cell .

The design of the TEM cell is usually based on an approximate equation for the characteristic impedance of a rectangular coaxial transmission line as detailed in Appendix A. Since the rectangular cell is designed to operate in the dominant TEM mode , there is no lower frequency limit.The upper useful frequency of the cell is limited by the distortions in the test fields caused by multimodings and resonances that occur within the cell at frequencies above the cell's multimoding cut-off frequency . Cut-off and resonant frequencies associated with these higher-order modes of an empty cell are given in Appendix B. The influence of these higher-order modes is insignificant until they approach their resonances , at which the cell acts as a high-Q cavity .

Figure (1) ISOMETRIC VIEWS OF TEM CELLS

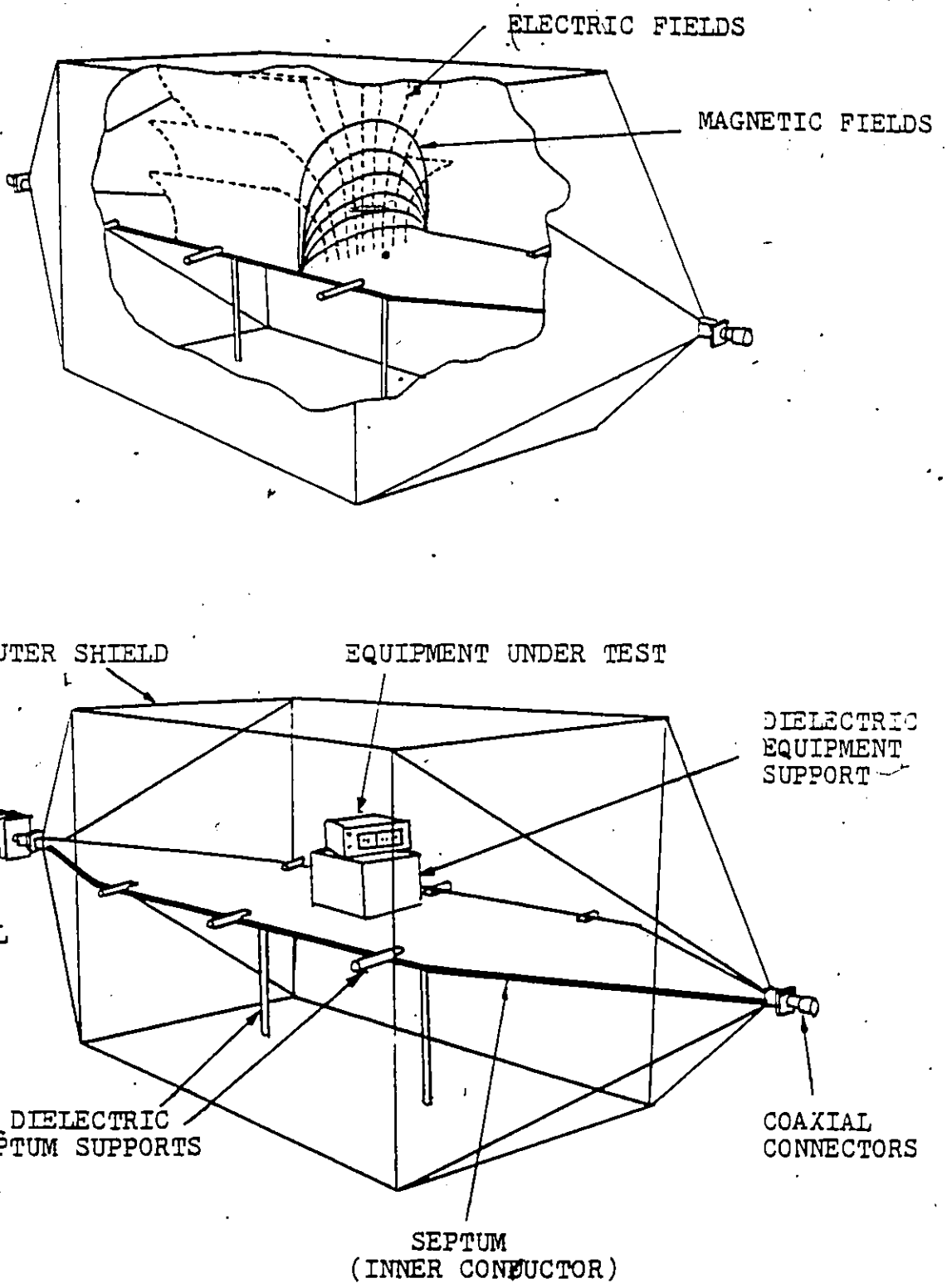

Figure (2) CROSS-SECTIONAL VIEWS OF TEM CELLS

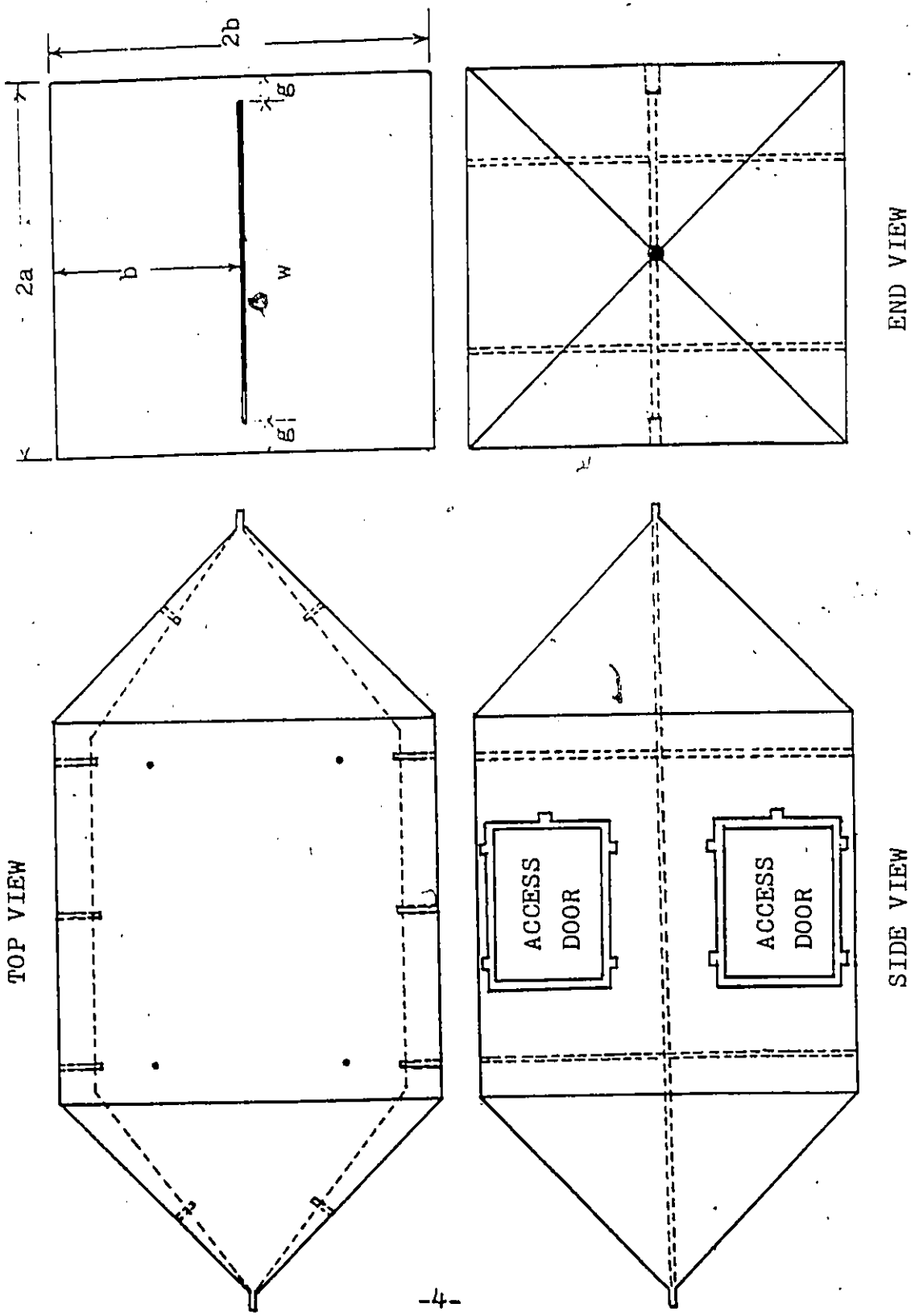

The main limitations of TEM cells is the size of the cell versus the upper useful frequency.The major considerations in the design of TEM cell are ,therefore , to :

1. maximize the usable test cross-section area
2. maximize the upper useful frequency range
3. maximize the uniformity of the EM field pattern
4. minimize the cell impedance mismatch or VSWR

Two major modifications of TEM cells have been proposed to achieve these goals.They are the resonance suppression method and an asymmetrical cell. In the resonance suppression method , the Q-factor of a TEM cell is lowered by placing RF-absorbing material inside the cell . The loading of the RF-absorbing material significantly suppresses high frequency resonances and multimoding phenomena in the cell and thereby extends the upper useful frequency range of the cell . Unfortunately , the loading also attenuates the waves and thus degrade the field uniformity in the cell . The asymmetrical cell is obtained by vertically offsetting the center septum of a regular TEM cell .Unlike the regular TEM cell,it contains two unequal size chambers. The EM fields in the smaller chamber tends to become more uniform and thus is closer simulating a plane wave.This region can therefore be used for accurate calibration of small elements. The larger chamber ,on the other hand , sacrifices field uniformity for greater available test space,and is useful for testing larger equipment without loss of the test bandwidth,or an increase in the overall size of the cell.However, asymmetrical cells have a more complicated modal spectrum .

Since TEM cells operate in a broad frequency range, they can be used for a variety of waveforms including CW,impulse ,pulsed or modulated exposure fields .They are,in princi-

ple,capable of simulating free-space uniform plane-wave ,and electromagnetic pulse (EMP) or detecting emissions from an equipment under test (EUT) placed in the cell .

Compared to others EMI/EMC measurement techniques , TEM cells provide advantages of better accuracy , higher isolation of the test environment , higher sensitivity and wider frequency range .

1.3 PURPOSE OF THE STUDY

Although considerable amount of work has been devoted to the TEM cell , most of it concentrated on the design aspects,higher-order multimoding and resonances ,and various applications of the TEM cell . So far,relatively little effort has been devoted to the field distortions due to the presence of an EUT in the TEM cell .

The purpose of this study is to investigate theoretically the field distortions in a EUT-loaded symmetric TEM cell using numerical methods. The results of this work should allow to determine ;

1. The field distortions in a specific TEM cell .

2. The maximum tolerable object size in a TEM cell for various object characteristics .

3. The field distributions in a loaded and unloaded TEM cell .

The results of this investigation should also be useful to those who are concern about the accuracy of EMC/EMI measurements,especially those involved in measurements of electromagnetic fields using TEM cells .The results should also provide informations leading to improvements of the measurement accuracy of the TEM cell.

CHAPTER 2

METHODS OF NUMERICAL ANALYSIS

2.1 INTRODUCTION

There are several methods leading to an approximate solution of the field distribution in an empty TEM cell . They can be categorized into three basic groups ;

1. *Analytical approach*

   e.g. separation of variables and conformal mapping techniques

2. *Integral equation method*

   e.g. moment method

3. *Differential equation method*

   e.g. finite element method,finite difference method

However , when an arbitrarily-shaped dielectric or metallic object is introduced into the TEM cell , the only practical method to obtain the approximate solution of the field distribution in the cell is by differential equation method using either the finite difference method or the finite element method .

In order to improve the efficiency of computations, both methods: the finite difference

and the finite element methods are combined to form a more versatile and practical method for solving this problem .

For comparison purposes , the three methods ; the finite difference , the finite element and the combined methods are used to obtain the solution of a EUT-loaded TEM cell .

2.2 FINITE DIFFERENCE METHOD

The finite difference method is a relatively old and simple numerical method for solution of the boundary value problems . By discretizing the region into an array of finite grid points and approximating the derivatives in the governing differential equation by difference equations , an equivalent system of equations for the problem is obtained . The complex analytical problem is thus reduced to solving a set of simultaneous linear equations using a digital computer .

2.2.1 MATHEMATICAL FORMULATION OF THE FINITE DIFFERENCE METHOD

Mathematical analysis of this method has been extensively investigated and presented by many authors ,Green[30] ,Schneider[31],Wexler[32] ,Botha and Pinder [34] .The principle of the procedure is simple. It consists of two major steps ; discretization of the region and reduction of differential equations .

A. *Discretization of the region*

In order to solve a 2-dimensional problem in cartesian coordinates,the whole physical region is subdivided into a square-mesh by a net of interlaced rows and columns.The continuous dielectric boundary is replaced by an approximate interface consisting of several

steps as shown in Fig.3.

B. *Reduction of differential equations*

For every node at the boundary , a difference equation in terms of the potential of the node and its four neighborhood nodal potentials can be deduced as an approximated representation of the governing differential equation (Laplace equation) at the node .There are several different types of nodal equations ;

1. INTERIOR NODE (free-node)

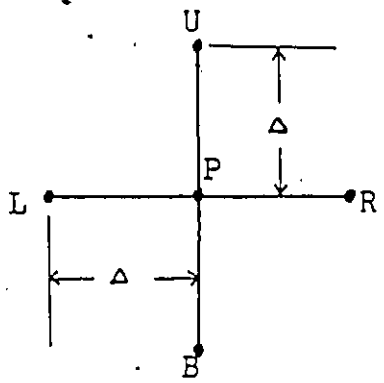

Applying Taylor's expansion in the horizontal ,x, direction,

$$\Phi(x-\Delta) = \Phi(x) + \Delta \cdot \frac{\partial \Phi}{\partial x} + \frac{\Delta^2}{2} \cdot \frac{\partial^2 \Phi}{\partial x^2} + \cdots \quad (1)$$

$$\Phi(x+\Delta) = \Phi(x) - \Delta \cdot \frac{\partial \Phi}{\partial x} + \frac{\Delta^2}{2} \cdot \frac{\partial^2 \Phi}{\partial x^2} - \cdots \quad (2)$$

and adding eq.(1) and (2)

$$\frac{\partial^2 \Phi}{\partial x^2} = \frac{1}{\Delta^2}[\Phi(x-\Delta) + \Phi(x+\Delta) - 2 \cdot \Phi(x) - \frac{\Delta^4}{12} \cdot \frac{\partial^4 \Phi}{\partial x^4} + \cdots$$

$$\approx \frac{1}{\Delta^2} \cdot (\Phi_R + \Phi_L - 2\Phi_P) \quad (3)$$

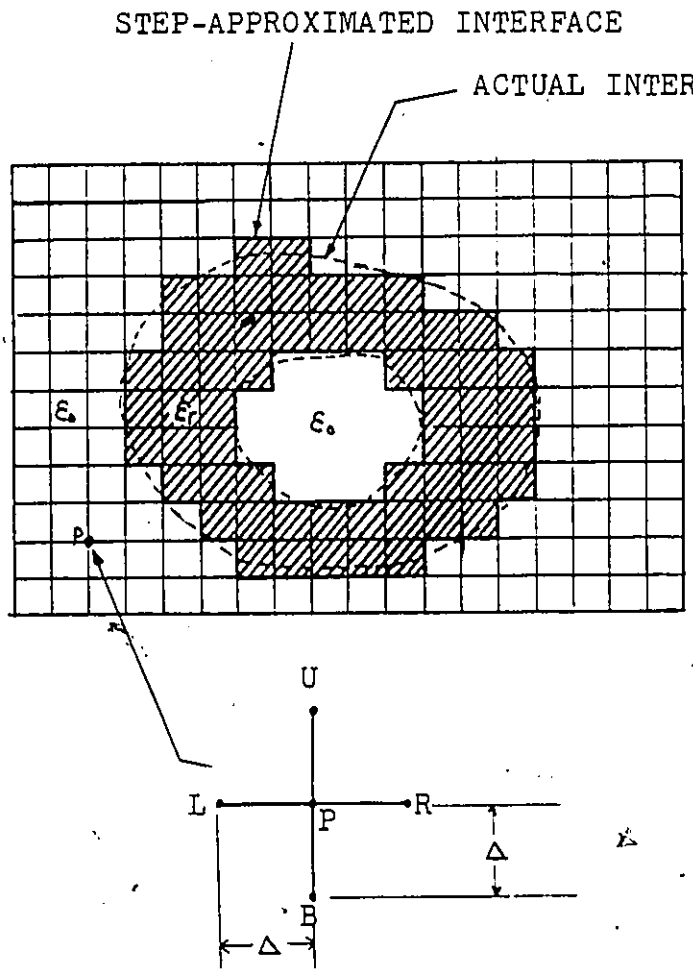

Figure (3) FINITE DIFFERENCE SCHEME

Therefore,an approximation for the second derivative of Φ with respect to x is obtained to the accuracy of the order of resolution Δ^2 . Applying the same procedure to the vertical,y,direction ,a similar approximation for the second derivative of Φ with respect to y is obtained as follows ;

$$\frac{\partial^2 \Phi}{\partial y^2} \approx \frac{1}{\Delta^2}(\Phi_U + \Phi_B - 2\Phi_P) \tag{4}$$

Combining eq.(3) and (4) ,the difference equation for any free node is found as follows :

$$\Phi_B + \Phi_U + \Phi_L + \Phi_R - 4 \cdot \Phi_P = 0 \tag{5}$$

This expression is also known as a five-points finite difference operator of regular nodes.

2. DIRICHLET BOUNDARY CONDITIONS

The potentials on these boundaries ,by definition ,are constant and therefore are set to some given values Φ_o

$$\Phi_P = \Phi_o$$

3 NEUMANN BOUNDARY CONDITIONS

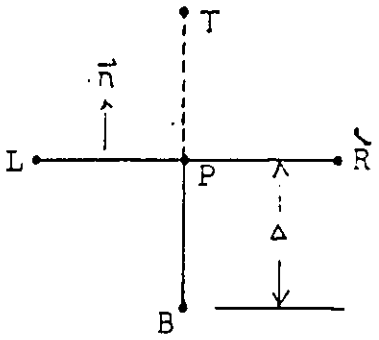

By definition, potentials on Neumann boundaries have the unique property of vanishing normal derivatives of potential along these boundaries.

$$\frac{\partial \Phi}{\partial n} = 0$$

The corresponding difference equation of this differential equation is

$$\frac{\Phi_T - \Phi_B}{2\Delta} = 0$$

The necessary condition for potentials at these boundaries is therefore,

$$\Phi_T = \Phi_B \tag{6}$$

Since potentials at these boundaries must also satisfy the five points difference operator, the difference equation for these nodes can therefore be found by adding eq.(5) and (6) as given below:

$$\Phi_P = \frac{1}{4}(\Phi_R + \Phi_L + 2\Phi_B) \tag{7}$$

4 SIMPLE DIELECTRIC INTERFACE

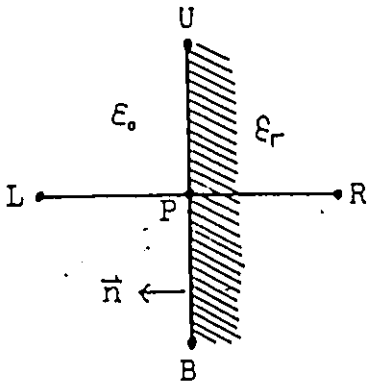

The difference equation for these points can be obtained by enforcing the continuity of the normal component of the displacement vector at the interface as follow;

$$D_{n1} - D_{n2} = \rho_s$$

,where ρ_s is the surface charge density on the interface. Since the surface charge density is generally equal to zero for poor conductors,the normal component of the displacement vector must therefore be continuous on the interface . Thus,

$$D_{n1} = D_{n2}$$

or

$$-\epsilon_1 \cdot \frac{\partial \Phi_P}{\partial n} = -\epsilon_2 \cdot \frac{\partial \Phi_P}{\partial n}$$

,where $\epsilon_1 = \epsilon_0$ and $\epsilon_2 = \epsilon_r \cdot \epsilon_0$,

in difference expression

$$\epsilon_1(\frac{\Phi_R - \Phi_L}{2\Delta}) = \epsilon_2(\frac{\Phi_R - \Phi_L}{2\Delta})$$

* The necessary condition at these boundaries is therefore,

$$\Phi_R = \Phi_L \tag{8}$$

Substituting eq.(8) into five points difference operator equation for both media leads to:

$$\Phi_U + \Phi_B + 2\Phi_L - 4\Phi_P = 0 \tag{9}$$

$$\epsilon_r(\Phi_U + \Phi_B + 2\Phi_R - 4\Phi_P) = 0 \tag{10}$$

Adding eq.(9) and (10) give the difference equation for these nodes as given below :

$$\Phi_P = \frac{\Phi_U + \Phi_B}{4} + \frac{\Phi_L + \epsilon_r \Phi_R}{2(1+\epsilon_r)} \tag{11}$$

There are three other variations of this type of interface condition and the difference equations are the simple permutations of eq.(11) as given in Table I.

5 ACUTE DIELECTRIC ANGLE

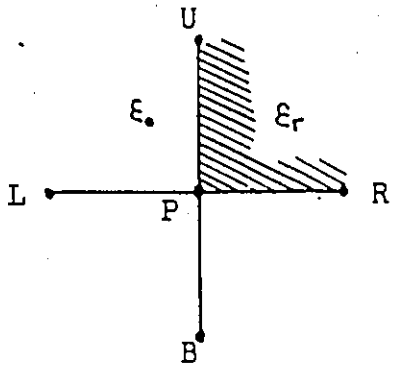

Using the continuity conditions of the normal component of the displacement vector in both x and y directions at these boundaries and applying the same procedure as before ,the necessary conditions of potentials at these nodes are then found to be :

$$\Phi_L = \Phi_R$$

$$\Phi_U = \Phi_B$$

Substituting these conditions into the five points difference operator equations for both media leads to,

$$\Phi_L + \Phi_B - 2\Phi_P = 0 \tag{12}$$

$$\epsilon_r(\Phi_U + \Phi_R - 2\Phi_P) = 0 \tag{13}$$

The difference equation for these nodes is therefore obtained by adding eq.(12) and (13) to the five-points difference operator equation as given below:

$$\Phi_P = \frac{\Phi_B + \Phi_L}{(3+\epsilon_r)} + \frac{(1+\epsilon_r)(\Phi_U + \Phi_R)}{2(3+\epsilon_r)} \tag{14}$$

6 OBTUSE DIELECTRIC ANGLE

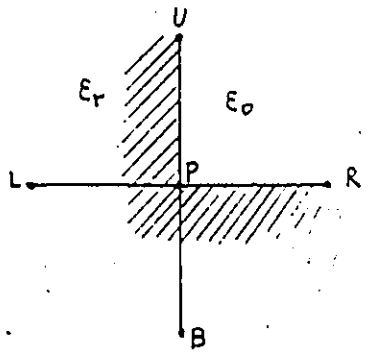

Applying the exact same procedure and conditions as in acute dielectric angle case , the following necessary conditions of potentials at these boundaries are then found to be :

$$\Phi_L = \Phi_R$$

$$\Phi_U = \Phi_B$$

Substituting the conditions into the five points operator equation for both media leads to,

$$\Phi_U + \Phi_R - 2\Phi_P = 0 \tag{14}$$

$$\epsilon_r(\Phi_L + \Phi_B - 2\Phi_P) = 0 \tag{15}$$

Also the five points operator must also be satisfied in media 2 as follow ;

$$\epsilon_r(\Phi_U + \Phi_R + \Phi_B + \Phi_L - 4\Phi_P) = 0 \tag{16}$$

The difference equation for these nodes is thus obtained by adding eq.(14),(15) and (16):

$$\Phi_P = \frac{\epsilon_r(\Phi_L + \Phi_B)}{(1 + 3\epsilon_r)} + \frac{(1 + \epsilon_r)(\Phi_U + \Phi_R)}{2(1 + 3\epsilon_r)} \tag{17}$$

There are three other variations of this type of interface condition as given in Table I .

The difference equations for all types of interface conditions were given by H.E. Green [30] as shown in Table I .

2.2.2 SOLUTION OF THE FINITE DIFFERENCE METHOD

Once all difference equations for every possible node in the region under consideration are found,the approximate difference solution is then readily obtained by solving the matrix of system of equations using a digital computer .Since the finite difference method results in a huge and sparse matrixes ,direct method of solving the system of equations requires very large computer storage and therefore is not generaly suitable and is usually very limited . Among all the techniques for solving simultaneous equations, a successive over-relaxation (SOR) iterative technique is found to be the best suited to handle such large and sparse matrixes efficiently.

The general form of the final system of equations of the finite difference method in matrix representation is as follow :

$$\begin{pmatrix} s_{11} & s_{12} & \dots & s_{1n} \\ s_{21} & s_{22} & \dots & s_{2n} \\ \vdots & \vdots & \ddots & \vdots \\ s_{m1} & s_{m2} & \dots & s_{mn} \end{pmatrix} \begin{pmatrix} \Phi_1 \\ \Phi_2 \\ \vdots \\ \Phi_n \end{pmatrix} = \begin{pmatrix} b_1 \\ b_2 \\ \vdots \\ b_n \end{pmatrix}$$

The k^{th} equation of the system of equations is :

$$\sum_{j=1}^{n} \Phi_j S_{kj} = b_k$$

rearranging the equation gives :

$$\Phi_k = \frac{b_k}{s_{kk}} - \sum_{\substack{j=1 \\ j \neq k}}^{n} \left(\frac{s_{kj}}{s_{kk}} \right) \Phi_j \qquad (k = 1 \dots n)$$

TABLE I
FINITE DIFFERENCE EQUATIONS

DESCRIPTION	FIGURE	DIFFERENCE EQUATION
NEUMANN BOUNDARY CONDITIONS	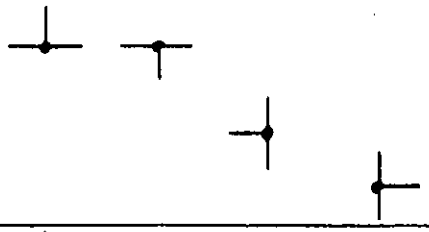	$\Phi_L + \Phi_R + 2\Phi_U - 4\Phi_P = 0$ $\Phi_L + \Phi_R + 2\Phi_B - 4\Phi_P = 0$ $\Phi_U + \Phi_B + 2\Phi_L - 4\Phi_P = 0$ $\Phi_U + \Phi_B + 2\Phi_R - 4\Phi_P = 0$
SIMPLE DIELECTRIC INTERFACE	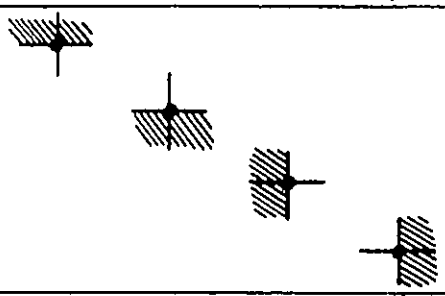	$\Phi_P = \frac{\Phi_L+\Phi_R}{4} + \frac{\epsilon_r\Phi_U+\Phi_B}{2(1+\epsilon_r)}$ $\Phi_P = \frac{\Phi_L+\Phi_R}{4} + \frac{\epsilon_r\Phi_B+\Phi_U}{2(1+\epsilon_r)}$ $\Phi_P = \frac{\Phi_U+\Phi_R}{4} + \frac{\epsilon_r\Phi_L+\Phi_R}{2(1+\epsilon_r)}$ $\Phi_P = \frac{\Phi_U+\Phi_R}{4} + \frac{\epsilon_r\Phi_R+\Phi_L}{2(1+\epsilon_r)}$
ACUTE DIELECTRIC INTERFACE	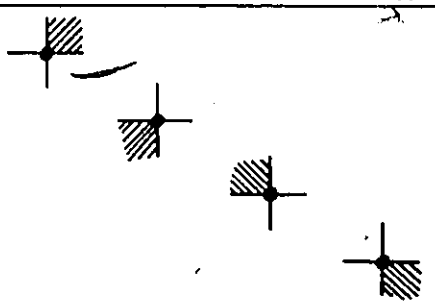	$\Phi_P = \frac{\Phi_R+\Phi_L}{(3+\epsilon_r)} + \frac{(1+\epsilon_r)(\Phi_U+\Phi_R)}{2(3+\epsilon_r)}$ $\Phi_P = \frac{\Phi_U+\Phi_R}{(3+\epsilon_r)} + \frac{(1+\epsilon_r)(\Phi_R+\Phi_L)}{2(3+\epsilon_r)}$ $\Phi_P = \frac{\Phi_R+\Phi_R}{(3+\epsilon_r)} + \frac{(1+\epsilon_r)(\Phi_U+\Phi_L)}{2(3+\epsilon_r)}$ $\Phi_P = \frac{\Phi_U+\Phi_L}{(3+\epsilon_r)} + \frac{(1+\epsilon_r)(\Phi_R+\Phi_R)}{2(3+\epsilon_r)}$
OBTUSE DIELECTRIC INTERFACE	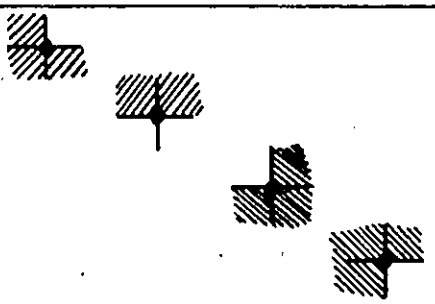	$\Phi_P = \frac{\epsilon_r(\Phi_L+\Phi_R)}{(1+3\epsilon_r)} + \frac{(1+\epsilon_r)(\Phi_U+\Phi_R)}{2(1+3\epsilon_r)}$ $\Phi_P = \frac{\epsilon_r(\Phi_U+\Phi_R)}{(1+3\epsilon_r)} + \frac{(1+\epsilon_r)(\Phi_R+\Phi_L)}{2(1+3\epsilon_r)}$ $\Phi_P = \frac{\epsilon_r(\Phi_R+\Phi_R)}{(1+3\epsilon_r)} + \frac{(1+\epsilon_r)(\Phi_U+\Phi_L)}{2(1+3\epsilon_r)}$ $\Phi_P = \frac{\epsilon_r(\Phi_U+\Phi_L)}{(1+3\epsilon_r)} + \frac{(1+\epsilon_r)(\Phi_R+\Phi_R)}{2(1+3\epsilon_r)}$

In the successive relaxation method, initial values $\Phi_j^{(0)}$ are assigned arbitrarily to each variable Φ_j at the beginning of each calculation .They are then corrected successively by scanning through all equations for all $j = 1 \ldots, n$. At end of each scan the old variables are replaced by the corresponding new variables. The disadvantage of this technique is that it requires $2 \times n$ computer storage locations.

To reduce the size of computer storage requirement an overrelaxation technique is employed .Instead of storing all the old variables values until all equations are scanned ,each old variable is replaced by the corresponding new variable right after the computation of the revised value.The new variable is also used to update the other variables Φ_j as soon as it replaces the old variable.Mathematically, the expression used for the computation is as follow :

$$\Phi_k^{m+1} = -\sum_{j=1}^{k-1} \left(\frac{s_{kj}}{s_{kk}}\right) \Phi_j^{m+1} - \sum_{j=k+1}^{n} \left(\frac{s_{kj}}{s_{kk}}\right) \Phi_j^{m} + \frac{b_k}{s_{kk}}$$

The first term of the summation shows the anticipation of the newly updated values in the computation of successive correction process for iteration $(m + 1)$.

For more efficient computations an accelerating factor ω has been proposed to improve the iteration cycles as follow ;

$$\Phi^{m+1} = \Phi^m + \omega[\Phi^{m+1} - \Phi^m]$$

It has been shown that the computation converges the most rapidly for some value of ω between 1 and 2 that has to be determined experimentally.

The termination of the computation is determined by a preset error criterion . At the

completion of each iteration cycle ,an error factor is calculated as follow :

$$ER = \frac{\sum_{i=1}^{n} | \Phi_i^{m+1} - \Phi_i^m |}{\sum_{i=1}^{n} \Phi_i^{m+1}}$$

It is then compared to the preset error criterion value before the next computation cycle.If the error factor is smaller than the preset error criterion , the computation is terminated automatically .

2.3 FINITE ELEMENT METHOD

The finite element method is a relatively new numerical procedure for solving physical or mathematical problems governed by a differential equation . It has been proven to be a powerful,versatile and efficient numerical technique in many fields of science and engineering. It is especially useful in solving anisotropic, arbitrarily-shaped and inhomogeneous problems. Furthermore, the required mathematics analysis is frequently relatively simple and it is easy to program on a digital computer.

The basic first-order finite element method using triangular elements is the most widely used for 2-dimensional problems and is of the main interest here.

2.3.1 MATHEMATICAL FORMULATION OF THE FINITE ELEMENT METHOD

The fundamental operations and procedures associated with the finite element method are simple and similar to other numerical approximation processes .However, the method possesses two distinct and unique characteristics that are different from the other numerical procedures.They are the utilization of the integral formulation technique to generate a system of algebraic equations and the use of continuous piecewise-smooth functions to approximate the unknown quantity.

The finite element method consists of three discrete steps .First the division of the whole problem region into many small element regions, discretization. Second the construction of the trial function in terms of the unknown nodal values .Third the performance of the mathematical analysis in each of these elements in order to obtain a system of equations for the problem by

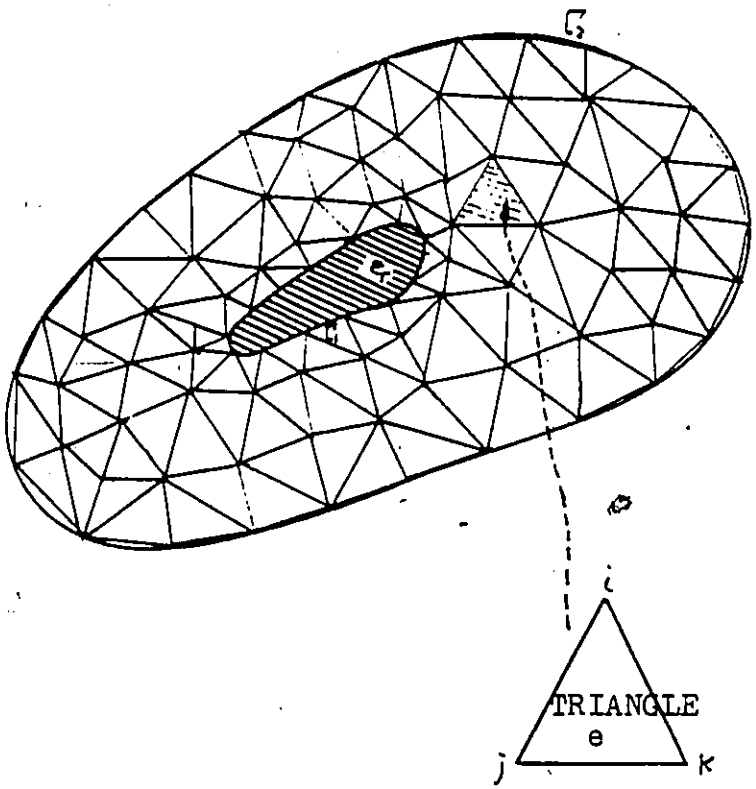

Figure (4) FINITE ELEMENT METHOD

taking into account contributions from all elements . Each of these steps is described in the following paragraphs .

1. DISCRETIZATION

Before any numerical process can be applied to a problem the whole problem must first be properly subdivided into a finite numbers of subregions .In the 2-dimensional finite element method, the problem region can be divided into any shape of subregions .For a simple first-order finite element method , the problem region is subdivided into many linear triangular elements . There is no restriction on the triangle shape as long as they consists of three nodes and are connected by three straight segments .However , it must be emphasized that the shape and size of the triangles does affect the accuracy . Once the division of the problem region is completed ,it is necessary to specify the element number to each element ,assign node numbers to each node and record the coordinates of each node numerically.

2. CONSTRUCTION OF THE TRIAL FUNCTION

Fig.4 depicts a linear triangular element, e, with three straight sides and three nodes as follow:

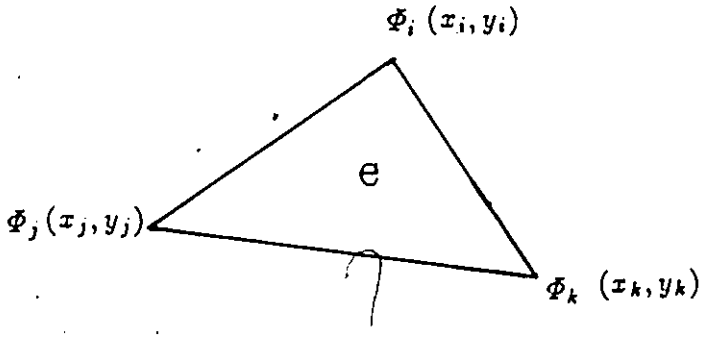

The nodes are denoted by $i,j,$ and k ,and nodal values of variables Φ are Φ_i, Φ_j and Φ_k whereas the nodal coordinates are represented by $(x_i, y_i), (x_j, y_j)$ and (x_k, y_k) . For linear

approximation, the parameters Φ vary linearly between nodes and the interpolation polynomial for Φ can be expressed as :

$$\Phi^e = c_1 + c_2 x + c_3 y \tag{18}$$

where c_1, c_2, c_3 are constants

Subject to the nodal conditions of

$$\Phi^e = \begin{cases} \Phi_i, & \text{if } x = x_i, \quad y = y_i \\ \Phi_j, & \text{if } x = x_j, \quad y = y_j \\ \Phi_k, & \text{if } x = x_k, \quad y = y_k \end{cases}$$

which is a complete linear polynomial because it contains a constant term and all possible linear terms with respect to x and y. As a result , this allows the arbitrary orientation of triangular element while the continuity between any adjacent elements is still satisfied .

Substitution of the nodal conditions into eq.18 , results in the following system of equations:

$$\Phi_i^e = C_1 + C_2 x_i + C_3 y_i$$

$$\Phi_j^e = C_1 + C_2 x_j + C_3 y_j$$

$$\Phi_k^e = C_1 + C_2 x_k + C_3 y_k$$

Rearranging the equations :

$$\begin{aligned} C_1 &= \frac{1}{2A}[(x_j y_k - x_k y_j)\Phi_i + (x_k y_i - x_i y_k)\Phi_j + (x_i y_j - x_j y_i)\Phi_k] \\ C_2 &= \frac{1}{2A}[(y_j - y_k)\Phi_i + (y_k - y_i)\Phi_j + (y_i - y_j)\Phi_k] \\ C_3 &= \frac{1}{2A}[(x_k - x_j)\Phi_i + (x_i - x_k)\Phi_j + (x_j - x_i)\Phi_k] \end{aligned} \tag{19}$$

where the area of the element triangle e is :

$$2A = \begin{vmatrix} 1 & x_i & y_i \\ 1 & x_j & y_j \\ 1 & x_k & y_k \end{vmatrix}$$

By substituting eq.19 to eq.18 and rearranging the final equations , an equation for Φ in terms of three *shape functions* or *interpolation functions* N_i, N_j and N_k and nodal values Φ_i, Φ_j and Φ_k as follow :

$$\Phi^e = N_i^e \Phi_i + N_j^e \Phi_j + N_k^e \Phi_k \tag{20}$$

where the shape functions are :

$$N_i = \frac{1}{2A}[a_i + b_i x + c_i y]$$

$$N_j = \frac{1}{2A}[a_j + b_j x + c_j y]$$

$$N_k = \frac{1}{2A}[a_k + b_k x + c_k y]$$

the subscripts indicate that the node with which the shape function is associated to and the constants a's ,b's and c's are functions of the coordinates of the three nodes as follow:

$$a_i = x_j y_k - x_k y_j \qquad b_i = y_j - y_k \qquad c_i = x_k - x_j$$

$$a_j = x_k y_i - x_i y_k \qquad b_j = y_k - y_i \qquad c_j = x_i - x_k$$

$$a_k = x_i y_j - x_j y_i \qquad b_k = y_i - y_j \qquad c_k = x_j - x_i$$

It is interesting to note that the shape functions are always polynomials of the same type as the original interpolation equation.Since the original interpolation equations of Φ are linear functions ,the scalar quantity of Φ is therefore related to the nodal values by a set of shape functions that are linear in position. This means that the gradient of Φ with respect to x and y remains constant within an element and this implies that many small linear elements are required to accurately approximate area where large gradients of Φ are expected .

3. FORMULATION OF THE SYSTEM OF EQUATIONS

Once the trial function is established ,the immediate objective is to determine the individual element matrixes using integral formulation . There are basically two kinds of integral formulation methods available for this specific application. The variational principle and the weighted residual method . Although the variational method is not applicable to problems with differential equation containing first derivative terms[38][39][40], it is the most popular approach in many finite element formulation especially in elliptic , hyperbolic or parabolic problems and it is the basis of formulation used here.

Minimization of the energy functional of the corresponding differential equation by use of some interpolation functions can generate a system of algebraic equations . According to the variational principle, if there exists a functional F in a domain V with boundary S such that:

$$F = \int_v G(\Phi)dV + \int_s g(\Phi)dS$$

where $G(\Phi)$ is a valid differential equation in V , $g(\Phi)$ is the given boundary conditions on S , Φ is the unknown function to be determined . Then the function Φ is the solution of the differential equation $G(\Phi)$ when the functional F is minimized.

In this problem, the governing equation is the Laplace equation

$$G(\Phi) = \Delta^2\Phi$$

The unknown trial function Φ is chosen to satisfy the Dirichlet boundary conditions with the Neumann conditions given as:

$$g(\Phi) = \frac{\partial \Phi}{\partial n} = 0$$

The corresponding functional for the Laplace equation is found as:

$$F = \int_v \epsilon_r (\Delta \Phi)^2 dV$$

In this case ,the whole region is divided into many triangles with the potential of each triangle approximated by eq.20. Substitution of the trial function eq.20 into the functional F of the Laplace equation , results in the functional for the element e as follow:

$$F_e = \epsilon_r \int_\Omega (\Delta N_i \Phi_i + \Delta N_j \Phi_j + \Delta N_k \Phi_k)^2 d\Omega.$$

$$F_e = \epsilon_r \int_\Omega [(\Delta N_i \Phi_i)^2 + (\Delta N_j \Phi_j)^2 + (\Delta N_k \Phi_k)^2 + 2(N_i N_j \Phi_i \Phi_j + N_j N_k \Phi_j \Phi_k + N_i N_k \Phi_i \Phi_k)] d\Omega$$

The functional is then minimized against each vertex potential:

$$\frac{\Delta F_e}{\Delta \Phi_i} = 2\epsilon_r \int_\Omega \Delta N_i \Delta N_i \Phi_i d\Omega + 2\epsilon_r \int_\Omega \Delta N_i \Delta N_j \Phi_j d\Omega + 2\epsilon_r \int_\Omega \Delta N_i \Delta N_k \Phi_k d\Omega = 0$$

$$\frac{\Delta F_e}{\Delta \Phi_j} = 2\epsilon_r \int_\Omega \Delta N_j \Delta N_i \Phi_i d\Omega + 2\epsilon_r \int_\Omega \Delta N_j \Delta N_j \Phi_j d\Omega + 2\epsilon_r \int_\Omega \Delta N_j \Delta N_k \Phi_k d\Omega = 0$$

$$\frac{\Delta F_e}{\Delta \Phi_k} = 2\epsilon_r \int_\Omega \Delta N_k \Delta N_i \Phi_i d\Omega + 2\epsilon_r \int_\Omega \Delta N_k \Delta N_j \Phi_j d\Omega + 2\epsilon_r \int_\Omega \Delta N_k \Delta N_k \Phi_k d\Omega = 0$$

Where,

$$\Delta N_i = \frac{1}{2A}[(y_j - y_k)\hat{i} + (x_k - x_j)\hat{j}]$$

$$\Delta N_j = \frac{1}{2A}[(y_k - y_i)\hat{i} + (x_i - x_k)\hat{j}]$$

$$\Delta N_k = \frac{1}{2A}[(y_i - y_j)\hat{i} + (x_j - x_i)\hat{j}]$$

The system of equations for each subregion is then obtained in the matrix form as follow:

$$2A\epsilon_r \begin{bmatrix} 0 & \dots & 0 & \dots & 0 & \dots & 0 & \dots & 0 \\ \vdots & \dots & \vdots & \dots & \vdots & \dots & \vdots & \dots & 0 \\ 0 & \dots & \Delta N_i \Delta N_i & \dots & \Delta N_i \Delta N_j & \dots & \Delta N_i \Delta N_k & \dots & 0 \\ \vdots & \dots & \vdots & \dots & \vdots & \dots & \vdots & \dots & 0 \\ 0 & \dots & \Delta N_j \Delta N_i & \dots & \Delta N_j \Delta N_j & \dots & \Delta N_j \Delta N_k & \dots & 0 \\ \vdots & \dots & \vdots & \dots & \vdots & \dots & \vdots & \dots & 0 \\ 0 & \dots & \Delta N_k \Delta N_i & \dots & \Delta N_k \Delta N_j & \dots & \Delta N_k \Delta N_k & \dots & 0 \\ \vdots & \dots & \vdots & \dots & \vdots & \dots & \vdots & \dots & 0 \\ 0 & \dots & 0 & \dots & 0 & \dots & 0 & \dots & 0 \end{bmatrix} \begin{bmatrix} \Phi_1 \\ \vdots \\ \Phi_i \\ \vdots \\ \Phi_j \\ \vdots \\ \Phi_k \\ \vdots \\ \Phi_n \end{bmatrix} = \begin{bmatrix} 0 \\ \vdots \\ 0 \\ \vdots \\ 0 \\ \vdots \\ 0 \\ \vdots \\ 0 \end{bmatrix}$$

The final system of equations can then be obtained by summing all the contributions from all subregions,

$$\begin{bmatrix} s_{11} & s_{12} & \cdots & s_{1n} \\ s_{21} & s_{22} & \cdots & s_{2n} \\ \vdots & \vdots & \ddots & \vdots \\ s_{n1} & s_{n2} & \cdots & s_{nn} \end{bmatrix} \begin{bmatrix} \Phi_1 \\ \Phi_2 \\ \vdots \\ \Phi_n \end{bmatrix} = \begin{bmatrix} 0 \\ 0 \\ \vdots \\ 0 \end{bmatrix}$$

where

$$S_{ij} = \sum_{k=1}^{NOTR} (2A_k \epsilon_r \Delta N_i \Delta N_j)$$

where NOTR is the total number of elements.

It is instructive to notice that some of the quantities $\Phi's$ in the final system of equations above are fixed values due to the Dirichlet boundary conditions.In such cases,these associated rows may be eliminated by shifting the effects of of these nodes to the right-hand-side of the matrix of the other rows .The final system of equations will then become a smaller matrix with all the free-nodes at the left-hand-side and a non-zero column at the right-hand-side .

2.3.2 SOLUTION OF THE FINITE ELEMENT METHOD

While the finite difference method most frequently employ iterative techniques ,the finite element method uses the direct or Gauss method . The Gauss method consists of two basic steps namely triangulation and back substitution .

(1.) TRIANGULATION

A general algebraic system of equations for the finite element method can be represented in the matrix form as follow :

$$\begin{bmatrix} s_{11} & s_{12} & \cdots & s_{1n} \\ s_{21} & s_{22} & \cdots & s_{2n} \\ \vdots & \vdots & \ddots & \vdots \\ s_{n1} & s_{n2} & \cdots & s_{nn} \end{bmatrix} \begin{bmatrix} \Phi_1 \\ \Phi_2 \\ \vdots \\ \Phi_n \end{bmatrix} = \begin{bmatrix} 0 \\ 0 \\ \vdots \\ 0 \end{bmatrix}$$

The triangulation process involves convertion of the general matrix into a matrix in the following form :

$$\begin{bmatrix} s_{11} & s_{12} & \cdots & s_{1n} \\ 0 & s_{22} & \cdots & s_{2n} \\ \vdots & \vdots & \ddots & \vdots \\ 0 & 0 & \cdots & s_{nn} \end{bmatrix} \begin{bmatrix} \Phi_1 \\ \Phi_2 \\ \vdots \\ \Phi_n \end{bmatrix} = \begin{bmatrix} 0 \\ 0 \\ \vdots \\ 0 \end{bmatrix} \tag{21}$$

The triangulation process can be described by the following three fundamental operations;

(a) *PIVOTING*

Selecting of the row containing the largest nonzero first entry as the pivoting equation.

(b) *NORMALIZING PIVOTING EQUATION*

Division of the pivoting equation by the coefficient of its first entry.

(C) *ELIMINATION*

Elimination of the first entry of all other equations by multiplying the normalized pivoting equation by the coefficient of the first entry of each equation and subtracting it to the corresponding equation ,respectively .

Apply the three steps to the system of equations repeatly and leave the pivoting equation unchanged in each operation . When the procedure is completed , the final matrix of the system of equations will be triangulated as shown in eq.21.

(2) BACK SUBSTITUTION

Once the triangulated system of equations is obtained ,the solution is readily found by

substituting the numerical value of the last equation back through all the equations and each unknown are computed for each substitution .

Since this method requires storage of all matrix elements it can handle only small or medium size systems of equations.For a reasonable large digital computer it is limited to a few hundreds of unknowns only.

2.4 COMBINED METHOD OF THE FINITE DIFFERENCE AND THE FINITE ELEMENT

Despite of the successes and popularity of the finite difference and the finite element methods ,there remains some defficiencies in both methods .In the finite difference method severe difficulties are encountered in solving problems with complicated geometries ; either there are difficulties in fitting the grid to the shape of the boundaries ,or there is a requirement of very fine grid to approximate the interface properly which results in a large truncation error in the computation processes and very long computation time .In the finite element method the vital problem is encountered in the requirements of huge effort in data input by the operator and large computer storage. Therefore , in some cases,it is advantageous to solve a problem with the combined finite difference and finite element method to eliminate difficulties encountered in each method used seperately. The combined method of finite difference and finite element retains the same flexibility in boundary geometry as in the finite element method and yet provides the simplicity in data input characteristic for the finite difference method ,furthermore, it allows further flexibility in trading-off the computation cost ,computer storage requirements and result accuracy.

The fundamental idea of the combined method of finite difference and finite element is

to split a given boundary into two major subdomains :the finite difference region and the finite element region . The idea of this method is to apply the finite difference scheme over most of the problem boundary and to employ the finite element scheme only to the areas of complicated geometry .

2.4.1 MATHEMATICAL FORMULATION OF THE COMBINED METHOD

Combined approach consists in formulating the equation of the boundary-value problems in terms of both variational and finite difference expressions.The problem region under consideration is first subdivided into two main subdomains ; the finite difference region and the finite element region as shown in Fig.5. In the finite difference region ,V_2 ,the basis of the finite difference scheme is applied .This domain is replaced by a grid of discrete points .A set of algebraic equations is obtained with unknown functions ,$\Phi_2's$ by collecting the difference equations of G for every point in V_2,including points on the boundary $h(s)$.In the finite element region,V_1,the fundamental operations and procedures of the finite element method are applied . This domain is further subdivided into many first order triangular elements .A set of algebraic equations is also obtained with unknowns $\Phi_1's$ by minimizing the functionals F of G with the boundary conditions $h(s)$ and $g(s)$. The system of equations for the problem can be obtained in the matrix form by assembling the contributions from both regions with unknown Φ as follow:

$$s\Phi = b$$

where,

$$\Phi = \Phi_1 + \Phi_2$$

$$s = s_1 + s_2$$

$$b = b_1 + b_2$$

Figure (5) MATHEMATICAL REPRESENTATION OF THE COMBINED METHOD

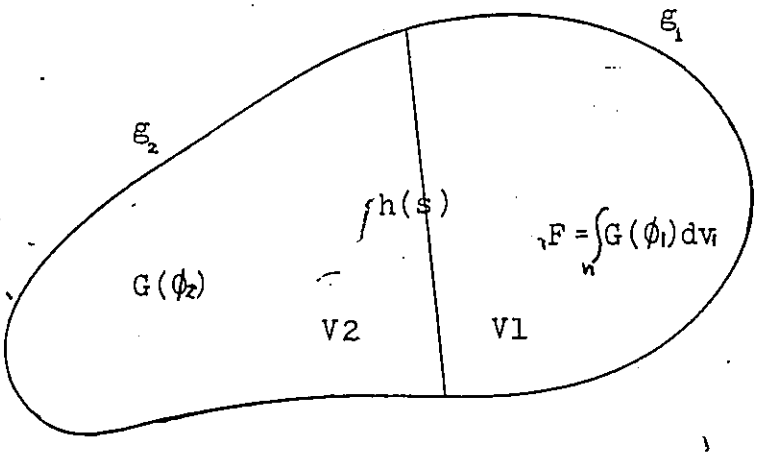

F — A functional of G

G — A valid differential equation in V1 and V2

h — Dynamic interface condition

V1 — Subregion one, Finite element region

V2 — Subregion two, Finite difference region

g_1 — Dirichlet boundary condition of V1

g_2 — Dirichlet boundary condition of V2

ϕ_1 — Unknown functions to be determined in V1

ϕ_2 — Unknown functions to be determined in V2

where contributions from the finite difference region are represented by

$$s_1 \Phi_1 = b_1$$

and contributions from the finite element region are represented by

$$s_2 \Phi_2 = b_2$$

2.4.2 SOLUTION FOR THE COMBINED METHOD

For the combined method ,the numbers of unknowns are too limited to solve the final system of equations by the direct method .It is also difficult to use the iterative method .In order to solve the final system of equations efficiently, the direct method and the overrelaxation method are combined .

In order to understand the operation of solving the system of equations properly, a few concepts are defined as follow (refer to Fig.6):

(1) FINITE DIFFERENCE REGION

Area to be grided and solved by the finite difference method.

(2) FINITE ELEMENT REGION

Area to be subdivided into triangles and solved by the finite element method.

(3) TRANSITION REGION

Area containing the Dynamic Dirichlet boundary conditions of the finite element and the finite difference regions.

Figure (6) SCHEME OF THE COMBINED METHOD

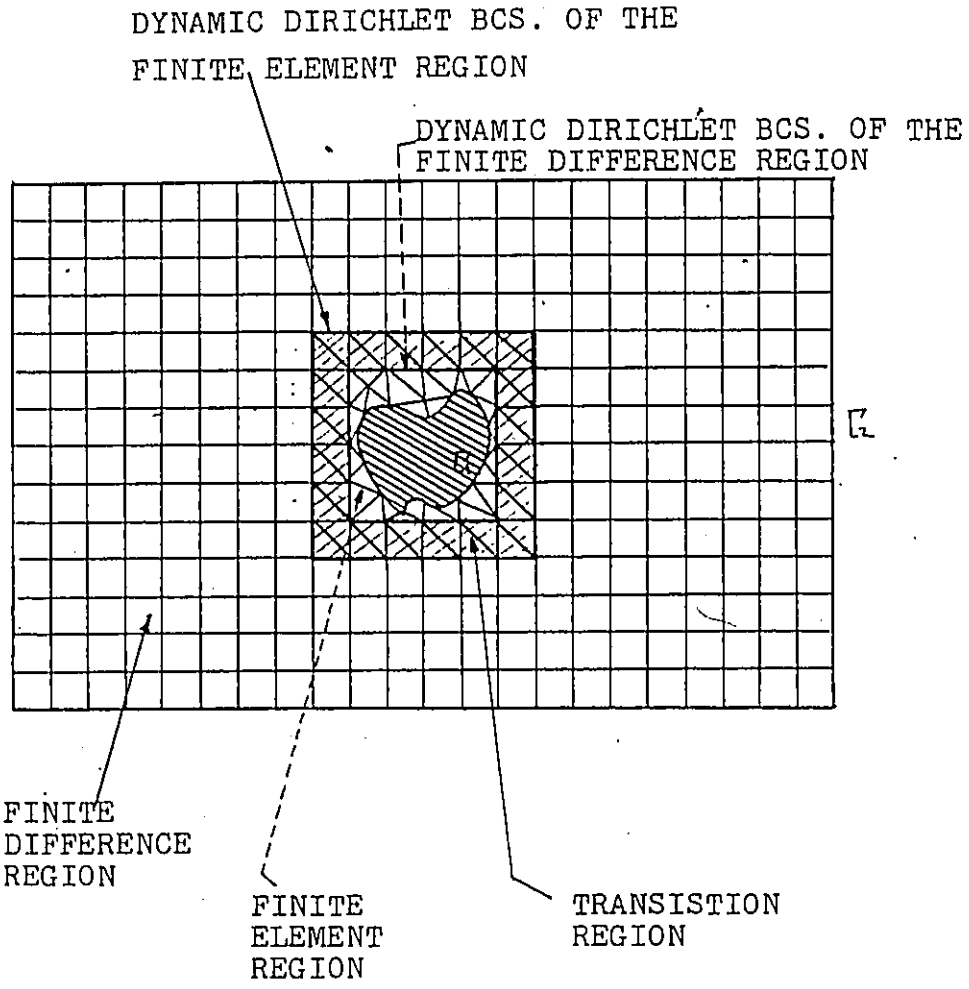

The procedure of solving the system of equations is simple. The parts of the system of equations arise from the discretization of the Laplace's equation with the finite difference method are solved by the SOR method and the parts of the system of equations obtained by the finite element method are solved by Gauss's elimination method. The two operations proceed alternatively and independently for each iteration of the SOR through transition region.One of the regions, the finite element region or the finite difference region is replaced by its equivalent Dynamic Dirichlet boundary condition while the other is operating during each iteration.The operation begins with assigning initial values to all Dynamic Dirichlet boundary values in the transition region and all potential nodes in the finite difference region .These values are changed by solving the linear algebraic system of equations of the finite difference and the finite element regions, alternatively. After a certain numbers of iterations, the values converge and the solution is obtained .

2.5 DISCUSSION

Of the three numerical methods discussed in this chapter, the finite difference method is considered to be the most straightforward and the easiest to apply in practice .This is especially true for equations defined over rectangular domains .However, its efficiency deteriorates considerably when the region under consideration is irregular in geometrical shape.Large errors are usually involved in this method as a result of grid approximation in the discretization process, step approximation on the dielectric interface, and numerical truncation in the computation process.

The finite element method using variational formulation is ideally suited for the solution of the Laplace equation in an irregular or regular shaped domain . This method offers good accuracy and good computation efficiency .However, it involves massive manipulation of the

input data .

The combined method of the finite difference and the finite element is proposed to combine the advantages of the two methods for more general application .It is a mathematically and practically efficient numerical procedure for solving boundary value problems with irregular boundary conditions.

CHAPTER 3

IMPLEMENTATION OF THE NUMERICAL METHODS TO THE TEM CELL

3.1 INTRODUCTION

TEM cells are currently used in a variety of EMI/EMC measurements [6][13][14][15][17][22]. For these applications TEM cells are used to simulate free-space uniform plane-wave . When an object under test is introduced into the cell , the uniform fields in the cell is disturbed due to the scattering fields produced by the EUT and the mutual coupling between the object and the TEM cell. In order to analyse the loading effect on electromagnetic fields caused by the EUT , the electric field strength in an empty TEM cell and in an EUT-loaded TEM cell are computed numerically .The ratios of the electric field strength of an EUT-loaded cell to that of an empty cell at the same location are then computed to estimate the field distortions in the cell .

Similar problems have been investigated by M.Kanda[12],Wilson[7],Das&Mohan[4] with an EUT simulated by a metallic rectangular cylinder . Moment method and conformal mapping methods were used with a common assumption of relatively small separation between the septum and the outer wall .Unfortunately it is extremely difficult to extend these developments for an arbitrarily-shaped dielectric objects which are most commonly encountered situations in actual engineering applications .

3.2 MATHEMATICAL MODEL

By confining the wave propagation in the cell to the dominant TEM mode , the transverse field distribution in the cell can be obtained from the solution of a related electrostatic problem since the electric fields in these planes satisfy Laplace equation .

The mathematical model and the normalized cross-sectional dimensions of an unloaded TEM cell are shown in Fig.7 . The model number of this particular TEM cell used in this analysis is an IFI cc101.5s manufactured by Instruments for Industry Inc. .The physical dimensions of the IFI cc101.5s TEM cell are given in Appendix C. There are two kinds of boundary conditions in this model : prescribed potential values along the conductive metal surfaces(Dirichlet conditions),and vanishing normal derivative values (Neumann conditions) along the symmetry planes, the distance between the center septum and the outer wall . Subject to these boundary conditions , the electric potential itself in the TEM cell is governed by the Laplace equation $\Delta^2\Phi = 0$ .In the TEM cell loaded with a 2-Dimensional EUT , again the Laplace equation still holds in the interior of the cell , and the scalar potential has fixed values along metal walls and the center septum .However,the symmetry of field distribution between the upper and lower chambers is perturbed and the vanishing normal derivatives conditions at the septum planes may not apply any longer . In order to ensure the vanishing normal derivative conditions at the septum planes , the cross-sectional dimension of the EUT is confined to a certain limit such that the loading effect of EUT is insignificant in these planes. The mathematical model of a loaded TEM cell is shown in Fig.8 with an assumption that the cross-sectional dimensions of the EUT are relatively small compared to that of the TEM cell.The specific EUT model used in the analysis in this chapter is a 2-dimensional homogeneous telephone with dielectric constant $\epsilon_r = 2.2$ as shown in Fig.9.

Indeed, with the assumption of vanishing normal derivative conditions at the septum

Figure (7) MATHEMATICAL MODEL OF AN UNLOADED TEM CELL

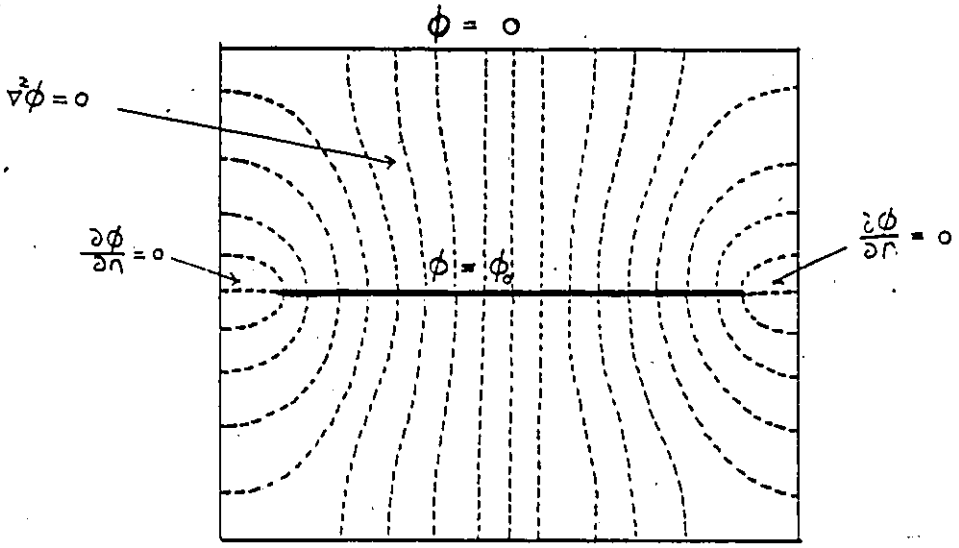

Figure (8) MATHEMATICAL MODEL OF A LOADED TEM CELL

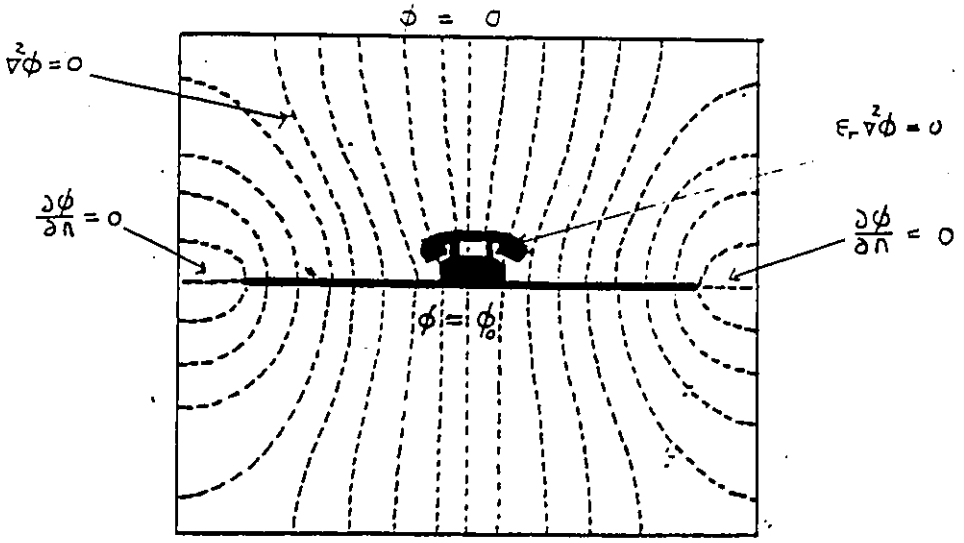

Figure (9) A 2-DIMENSIONAL HOMOGENEOUS TELEPHONE MODEL

$\varepsilon_r = 2.2$

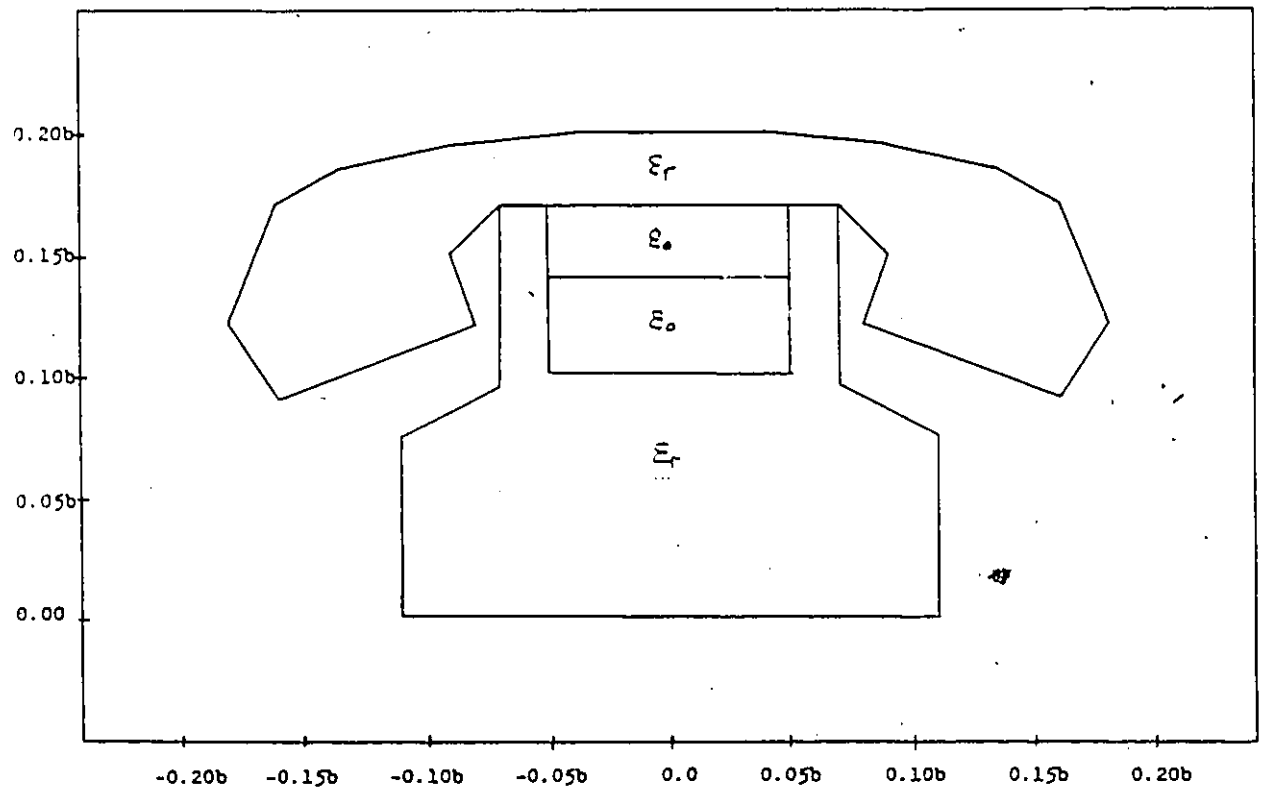

planes for both loaded and unloaded TEM cell , only one-quarter of the actual problem needs to be analysed for a symmetrical object;However,the analysis covers one-half space either upper or lower chamber, of the cell to generalize the computer program for asymmetrical objects as well .

3.3 NUMERICAL ANALYSIS USING THE FINITE DIFFERENCE METHOD

When solving problems by using the finite difference method with regular mesh , the key consideration is the proper selection of the grid size . In order to optimize the approximation operation , the grid size of the mesh should be chosen as large as possible to avoid long computation time and high truncation error . On the other hand , it must be chosen to be small enough to approximate all boundary or interface conditions properly and to meet the accuracy requirement .

The finite difference scheme for this problem is shown in Figures 10a& 10b. The grid size is chosen as 0.01 (normalized value to the distance between center septum and outer wall) which is the maximum possible step-size to well approximate the telephone boundary . The resulting system of equations is a 101×201 matrix . The converging rate of the solution of this large system of equations by iteration methods is slow . For a preset error criterion of 10^{-5},the required computation time is about 246 cpu seconds for unloaded case and is about 248 cpu seconds for loaded case . For the error criterion of 10^{-6}, the computation time is about 404 cpu seconds for the unloaded case ,and is about 386 cpu seconds for the loaded case . This demonstrates the inefficiency of solving this problem by using the finite difference method .

Once the node potentials are determined , the electric field intensity value at location (x, y) can be calculated as follows:

Figure (10) FINITE DIFFERENCE SCHEME OF THE TEM CELL

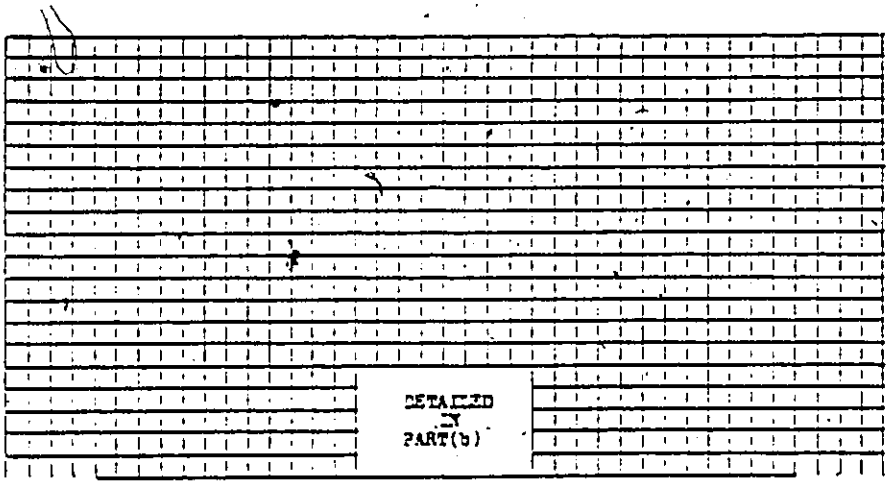

(a) PRINCIPAL FINITE DIFFERENCE SCHEME

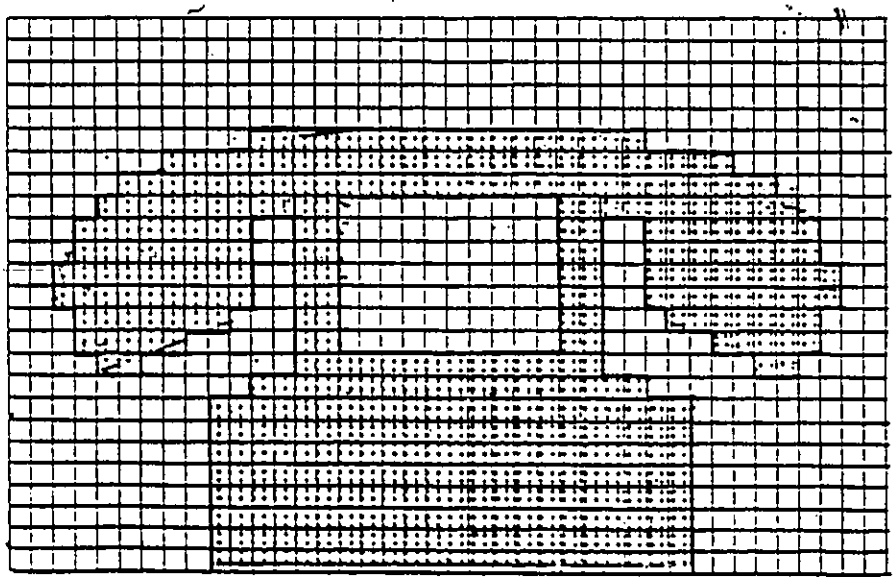

(b) DETAIL FINITE DIFFERENCE SCHEME AT THE DIELECTRIC INTERFACE

$$|E(x,y)| = \sqrt{|E_x|^2 + |E_y|^2}$$

where

$$E_x = -\frac{\partial \Phi}{\partial x}$$

$$E_y = -\frac{\partial \Phi}{\partial y}$$

The electric field intensity in unloaded TEM cells and loaded cells with a homogeneous telephone is computed at some points of interest as shown in Table II.

3.4 NUMERICAL ANALYSIS USING THE FINITE ELEMENT METHOD

The most critical step in the finite-element analysis is the construction of the finite dimensional subspaces . In this process , the basic element is chosen as a linear triangle . Each element-triangle can take any size and orientation to suit any shape of the boundary and interface geometries,as long as it has three straight sides and three nodes .It is essential to note that each triangle contains a constant electric field intensity or potential gradient. Therefore,the size and shape of triangles must be carefully chosen especially in the area where large potential gradients are expected ,to obtain a good result accuracy.

The finite element model of a TEM cell is shown in Figures 11a&11b. Higher density of triangles is used in the area close to the center of the cell where the largest gradients of the potential are expected .There are 326 triangles and 184 nodes used in this analysis. The required computation time for the calculation for both loaded and unloaded cases are less than 20 cpu seconds.

Table (II) RESULTS OF THE FINITE DIFFERENCE SCHEME

* HOMOGENEOUS TELEPHONE
* $\varepsilon_r = 2.2$
* ERROR CRITERION 10^{-5}.

LOCATION	E_{loaded}	$E_{unloaded}$	DISTORTION FACTOR	
			%	dB
1	100.60	102.30	-1.66	-0.15
2	101.70	101.90	-0.20	-0.02
3	102.40	101.30	1.09	0.09
4	102.60	101.30	1.28	0.10
5	98.40	96.10	2.39	0.21
6	96.70	92.70	4.31	0.37
7	96.40	90.80	6.17	0.52
8	96.30	90.10	6.88	0.57
9	96.10	90.60	6.07	0.51
10	96.50	92.40	4.43	0.37
11	98.40	95.90	2.61	0.22
12	102.90	101.50	1.38	0.12
13	102.20	101.10	1.09	0.09
14	100.90	101.20	-0.30	-0.03
15	99.10	101.10	-1.98	-0.18

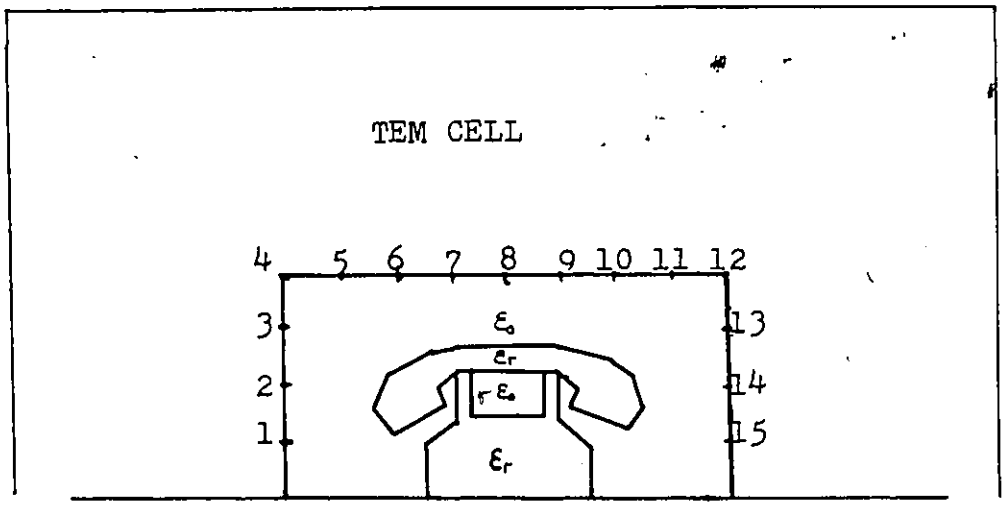

Figure (11) FINITE ELEMENT SCHEME OF THE TEM CELL

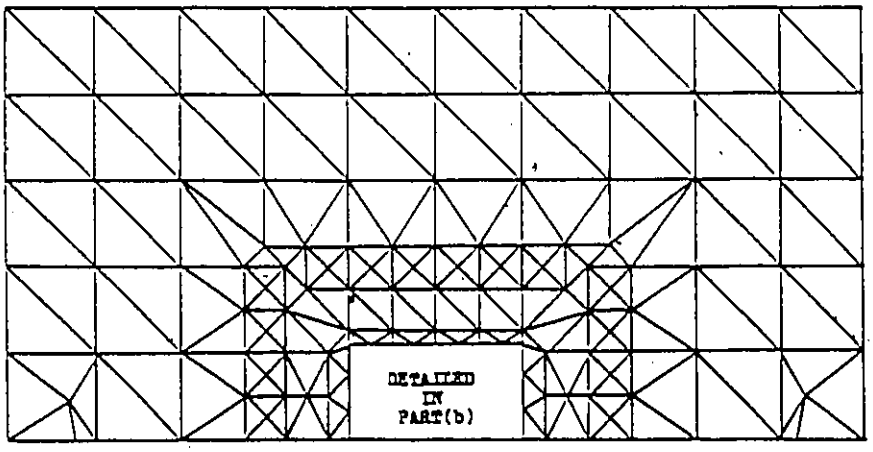

(a) PRINCIPAL FINITE ELEMENT SCHEME

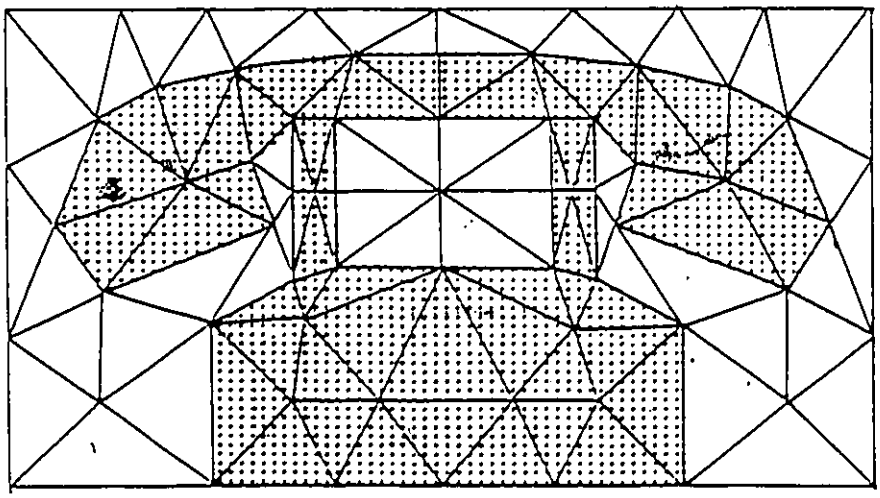

(b) DETAIL FINITE ELEMENT SCHEME AT THE DIELECTRIC INTERFACE

The electric field intensity at some points of interest in the cell are calculated with the same procedure used in the finite difference method :

$$|E(x,y)| = \sqrt{|E_x|^2 + |E_y|^2}$$

where

$$E_x = -\frac{\partial \Phi}{\partial x}$$

$$E_y = -\frac{\partial \Phi}{\partial y}$$

Results are given in Table III.

3.5 NUMERICAL ANALYSIS USING THE COMBINED METHOD

In the combined method , knowledge and operations of the finite element method and the finite difference method are used in a mixed way to provide the best efficiency of computation .It is therefore ,essential to properly subdivide the given region into finite element regions and finite difference regions to optimize the computation efficiency .Generally speaking , the finite difference regions should occupy as much space as possible and the finite element regions should cover minimum areas to reduce amount of data input from element numbering .The boundary between finite difference and finite element regions should be rectangular to fit the regular grid of the finite difference .

With the same consideration as in the finite difference method ,the grid sizes of the finite difference regions are chosen to be small enough to meet the accuracy requirement and yet maximized to provide a good computation efficiency . Since the number of triangle elements in the finite element regions strongly influences the total computation time , it is kept at a minimum possible value to minimize the computation time.

Table (III) RESULTS OF THE FINITE ELEMENT SCHEME

* HOMOGENEOUS TELEPHONE

* $\varepsilon_r = 2.2$

LOCATION	E_{loaded}	$E_{unloaded}$	DISTORTION FACTOR	
			%	dB
1	134.40	139.20	-3.57	-0.31
2	129.60	131.30	-1.29	-0.11
3	121.20	120.60	0.50	0.04
4	110.70	108.80	1.75	0.15
5	110.60	107.30	3.08	0.26
6	111.90	106.00	5.57	0.47
7	114.00	105.70	7.85	0.66
8	114.80	105.00	9.33	0.78
9	113.70	105.60	7.67	0.64
10	111.60	106.00	5.28	0.45
11	110.60	107.20	3.17	0.27
12	110.70	108.70	1.84	0.16
13	121.40	120.50	0.66	0.06
14	129.30	131.00	-1.30	-0.11
15	133.90	138.60	-3.39	-0.30

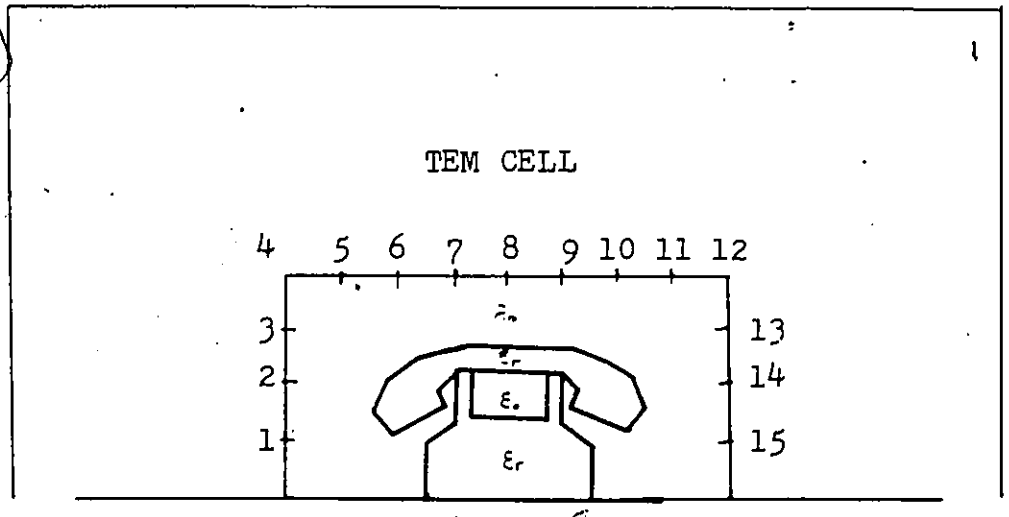

The scheme of the combined method for analysing this problem is shown in Figures 12a&12b . Grid size of the finite difference region is chosen as 0.05 .Number of triangles and nodes in the finite element region are 126 and 96, respectively . The total required computation time for loaded and unloaded cases is only 104 cpu seconds which is almost 500%*to*800% more efficient than the finite difference method and yet giving better result accuracy.

Again,the electric field intensity in the cell is calculated with the same procedure as used in the finite difference method:

$$|E(x,y)| = \sqrt{|E_x|^2 + |E_y|^2}$$

where

$$E_x = -\frac{\partial \Phi}{\partial x}$$

$$E_y = -\frac{\partial \Phi}{\partial y}$$

Results are given in Table IV.

3.6 COMPARISON OF RESULTS

Results computed using all three methods ,the finite difference, the finite element ,and the combined methods are plotted in Fig.13.

In terms of accuracy , the three methods applied to this problem do not differ from each other as shown in Fig.13. However, there are enormous differences in terms of other parameters such as the computer time ,storage requirements , and the number of data input points.

For a given irregular-shaped telephone model , the finite difference method apply step approximation on the irregular boundary and produce a comparable result as the other two

Figure (12) SCHEME OF THE COMBINED METHOD OF THE TEM CELL LOADED WITH A HOMOGENEOUS TELEPHONE

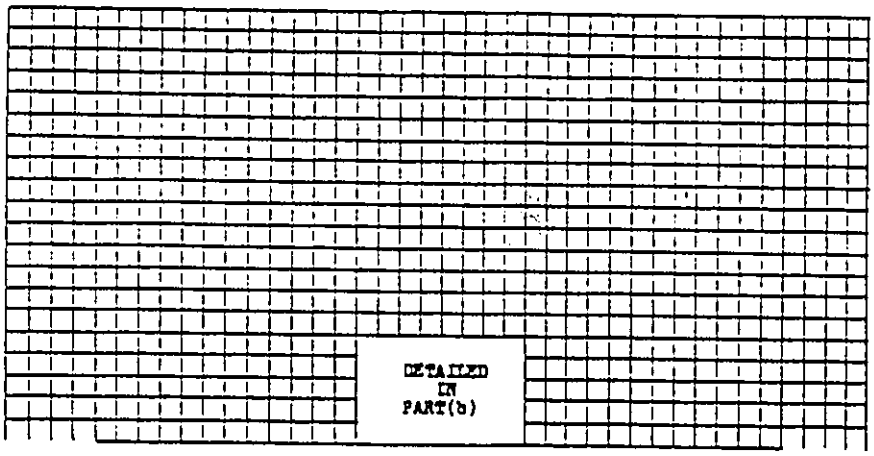

(a) PRINCIPAL SCHEME OF THE COMBINED METHOD

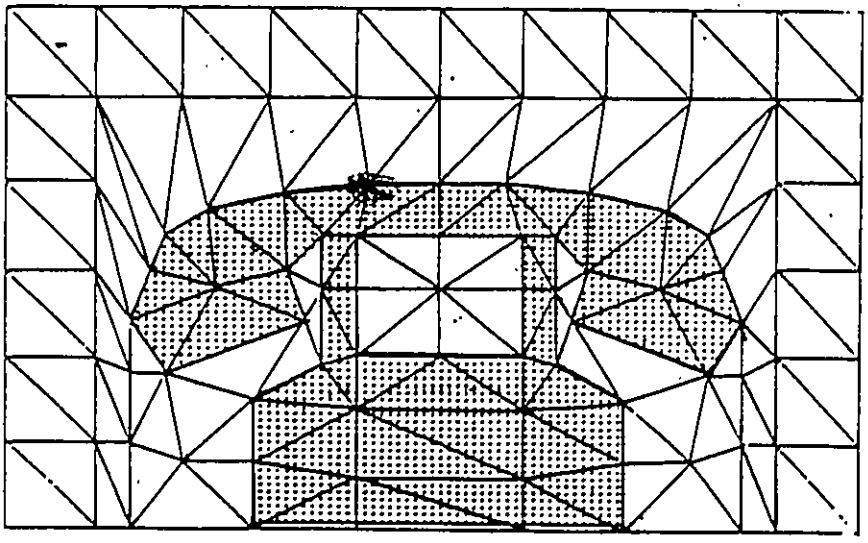

(b) DETAIL SCHEME OF THE COMBINED METHOD AT THE DIELECTRIC INTERFACE

Table (IV) RESULTS OF THE SCHEME OF THE COMBINED METHOD

* HOMOGENEOUS TELEPHONE

* $\varepsilon_r = 2.2$

LOCATION	E_{loaded}	$E_{unloaded}$	DISTORTION FACTOR	
			%	dB
1	131.00	135.75	-3.50	-0.31
2	126.80	128.85	-1.60	-0.14
3	120.00	119.39	0.50	0.04
4	111.16	109.17	1.80	0.16
5	110.20	106.81	3.20	0.27
6	111.00	105.30	5.40	0.46
7	112.53	104.50	7.70	0.64
8	113.15	104.30	8.50	0.71
9	112.77	104.70	7.70	0.64
10	111.38	105.70	5.40	0.46
11	110.40	107.40	2.80	0.24
12	111.74	109.70	1.86	0.16
13	121.00	120.35	0.50	0.05
14	128.15	130.10	-1.50	-0.13
15	132.35	137.16	-3.50	-0.31

NOTE : ERROR CRITERION OF COMPUTATION IS 10^{-5}

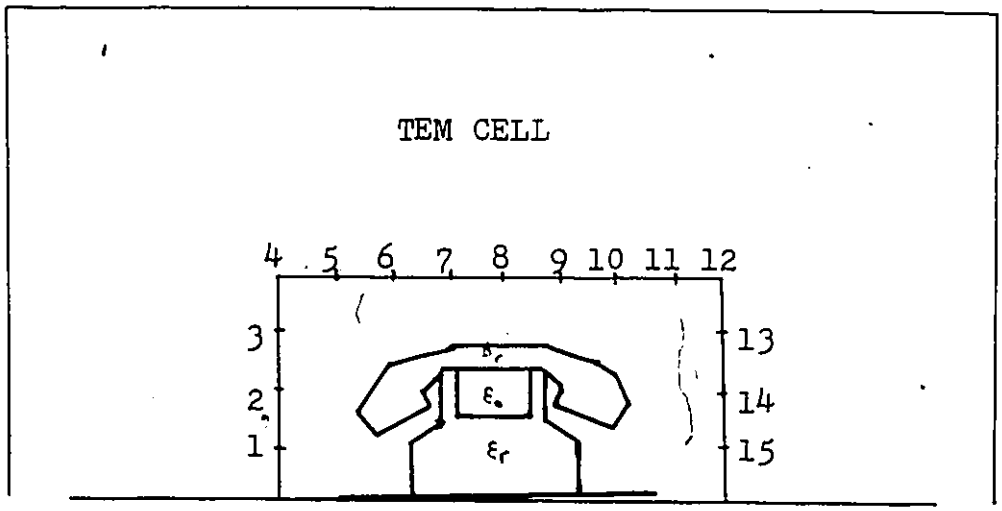

methods but only if a small enough grid size (≤ 0.01) is used . Consequently, it requires solution of a very large size system of equations .In solving such a large size system of equations, the convergence rate is slow,and thus a very long computation time is required .For instance, for a preset error criterion of 10^{-8},the total computation time for the finite difference method is 790 cpu seconds with the grid size of 0.01 . For about the same accuracy, the combined method requires only 104 cpu seconds with the grid size of 0.05 and preset error criterion of 10^{-5}.For the finite element method , the required computation time to achieve the same accuracy is less than 20 cpu seconds.It is,therefore,evident that the finite difference method is the most costly and inefficient method among the three methods for such irregular-shaped objects. Nevertheless, it does provide a simple way of solving complicated problems with a minimum data input by the operator.

The finite element method produces accurate results with the shortest computation time. However,the amount of the accompanied data is massive , especially when high precision from the results is required . Moreover,relatively large computer storage is needed to store the coordinates and the node numbers of the elements.

The combined method of the finite difference and finite element combines the advantages of the finite element and the finite difference methods. It does not require step approximations on irregular-shaped boundaries .Also,the amount of data input required is relatively small and flexible. It further provides flexibility of the trade-off in accuracy, computation time , computer storage ,and data input points .This method is especially suitable for EMI/EMC measurements with a TEM cell,since it requires only a minimum amount of change in the data by the operator when changing the EUT model while the accuracy and the computation time can be kept constant.

Figure (13) ELECTRIC FIELD DISTORTION IN A TEM CELL LOADED WITH HOMOGENEOUS TELEPHONE WITH DIELECTRIC CONSTANT $\varepsilon_r = 2.2$.

——— FEM RESULT
••••••• FDM RESULT WITH ERROR CRITERION OF 10^{-8}
------- RESULTS OF COMBINED METHOD WITH ERROR CRITERION OF 10 E-5
-·-·-·- FDM RESULT WITH ERROR CRITERION OF 10^{-5}

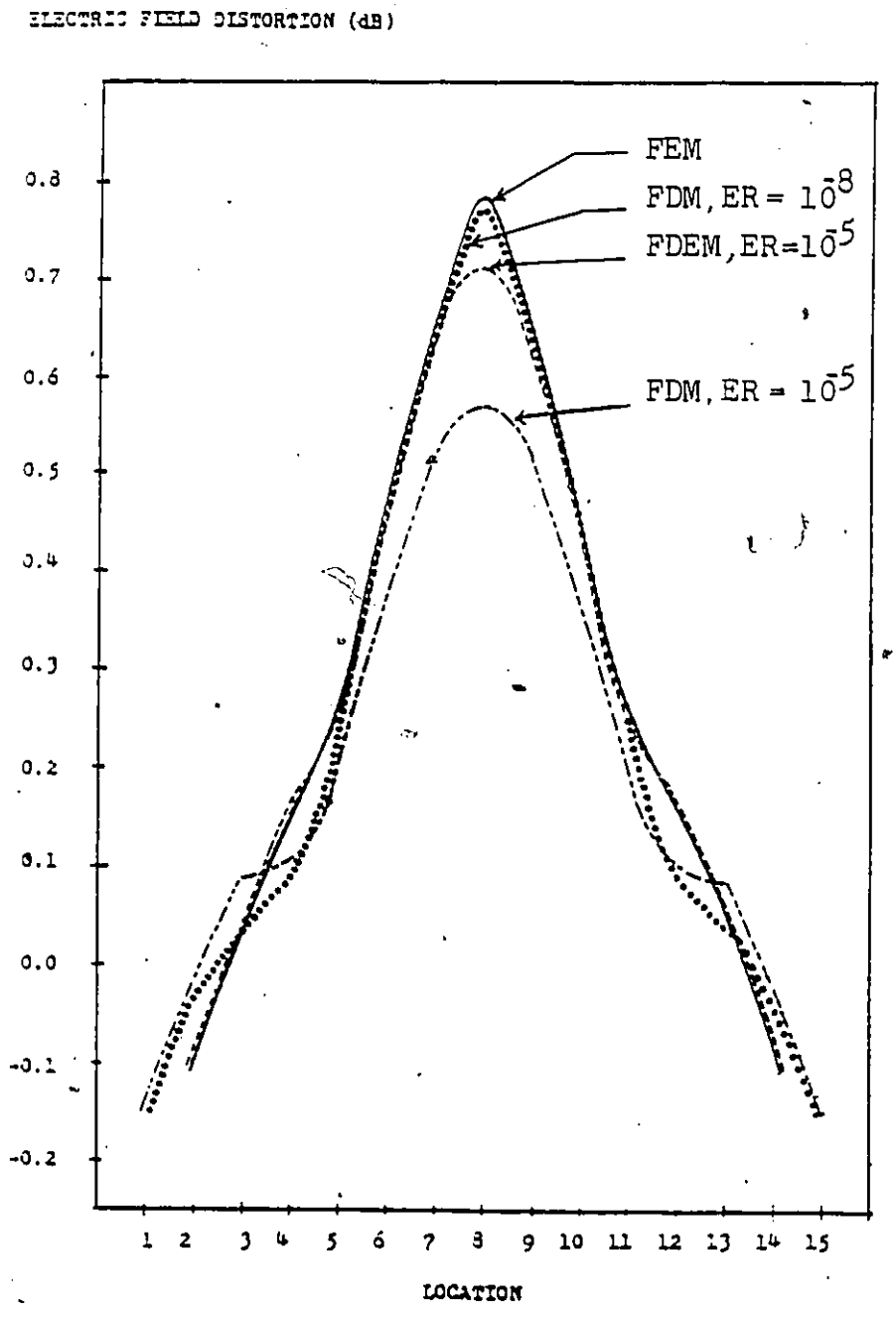

CHAPTER4

RESULTS FOR VARIOUS LOADS

4.1 INTRODUCTION

One of the major points in this investigation is to estimate the electromagnetic field distortions in a TEM cell due to the presence of a regular home telephone in the cell. Since the telephone can be considered as an inhomogeneous dielectric object ,the field distortions in the TEM cell due to the present of such an object can therefore be estimated by investigating the field distortions in a TEM cell due to the present of various types of dielectric telephone .

Another objective of this investigation is to provide a theoretical curve of field distortions in a TEM cell versus the size of EUT for various dielectric properties of the EUT . This is performed by using a circular cylinder object with various diameters .

4.2 INHOMOGENEOUS TELEPHONE

An inhomogeneous telephone model as shown in Fig.14 can be used to simulate a 2-dimensional inhomogeneous , homogeneous or metallic telephone . In this analysis , a homogeneous telephone is simulated by taking the dielectric constant of the entire telephone as a constant of $\epsilon_r = 2.2$ .On the other hand ,an inhomogeneous telephone is simulated by using three different types of dielectric constant of ;$\epsilon_{r1} = 2.2, \epsilon_{r2} = 10$, $\epsilon_{r3} = 20$.

First of all, it is essential to select an appropriate numerical scheme for the solution of this problem . Based on the knowledge acquired in the previous chapter it is obvious that the finite

Figure (14) A 2-DIMENSIONAL INHOMOGENEOUS TELEPHONE MODEL

$\varepsilon_{r1} = 2.2$
$\varepsilon_{r2} = 10$
$\varepsilon_{r3} = 20$

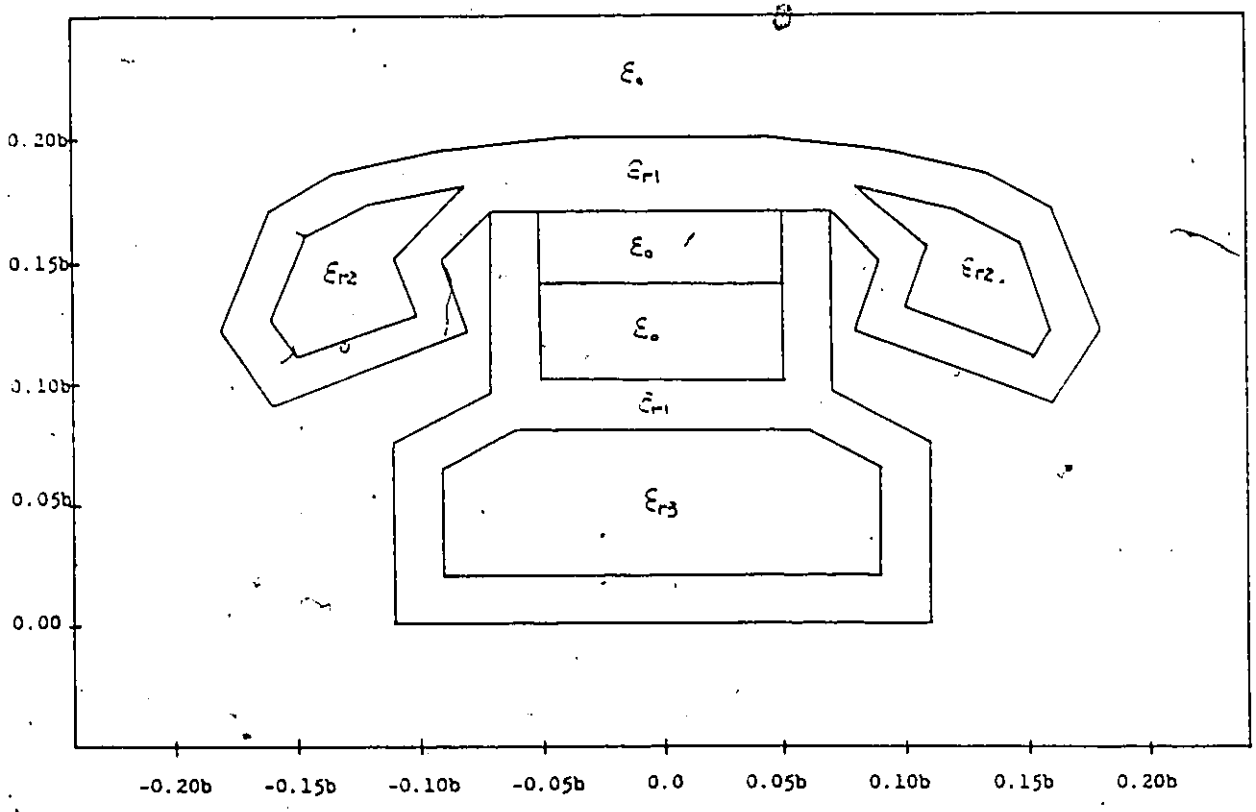

difference method may be the most inefficient and the most difficult method to implement to this inhomogeneous problem .The finite element method tends to require tremendous numbers of domain subdivisions.Consequently ,enormous numbers of data are needed to be handled by the operator. There is no doubt that of the three methods discussed in chapter 3 , the combined method of the finite difference and finite element is the most appropriate for the solution of this inhomogeneous problem .

The actual implementation of the combined method in this problem is shown in Figures 15a&15b.The grid size of the finite difference region is taken as 0.05 such that there are enough values of potential nodes computed for the prediction of electric field distribution . In the finite element region ,a total of 173 triangles and 100 nodes are used to properly approximate the inhomogeneous telephone model .

The electric potential and the electric field intensity in the loaded TEM cell are computed for various types of telephones; A homogeneous telephone,an inhomogeneous telephone and a metallic telephone . For each case,the normalized electric field quantities at various transverse positions located in the cell are then calculated as follow:

$$\tilde{E}(x,y) = \frac{E(x,y)}{\frac{\Phi_o}{b}}$$

where,

$\tilde{E}(x,y)$ is the normalized electric field intensity

$E(x,y)$ is the electric field intensity at location of interest in the transverse plane x,y.

Φ_o is the electric potential at the central plate

b is the vertical distance between the center septum and the outer conductor.

Figure (15) SCHEME OF THE COMBINED METHOD OF A TEM CELL LOADED WITH AN INHOMOGENEOUS TELEPHONE

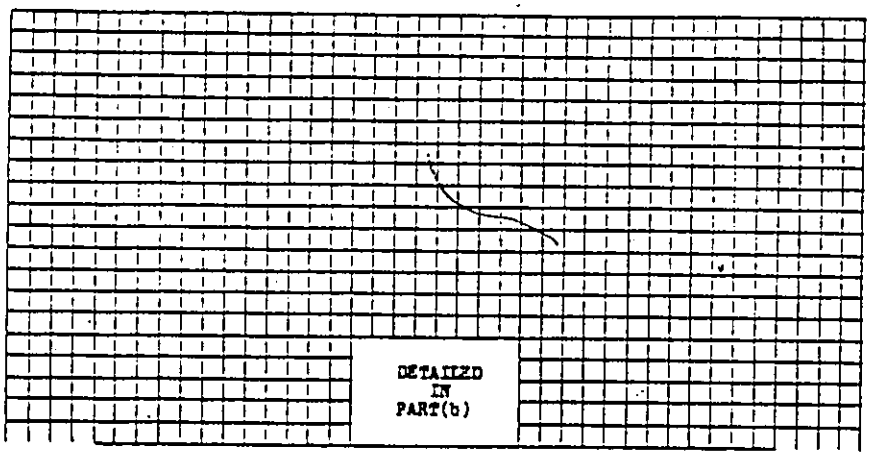

(a) PRINCIPAL SCHEME OF THE COMBINED METHOD

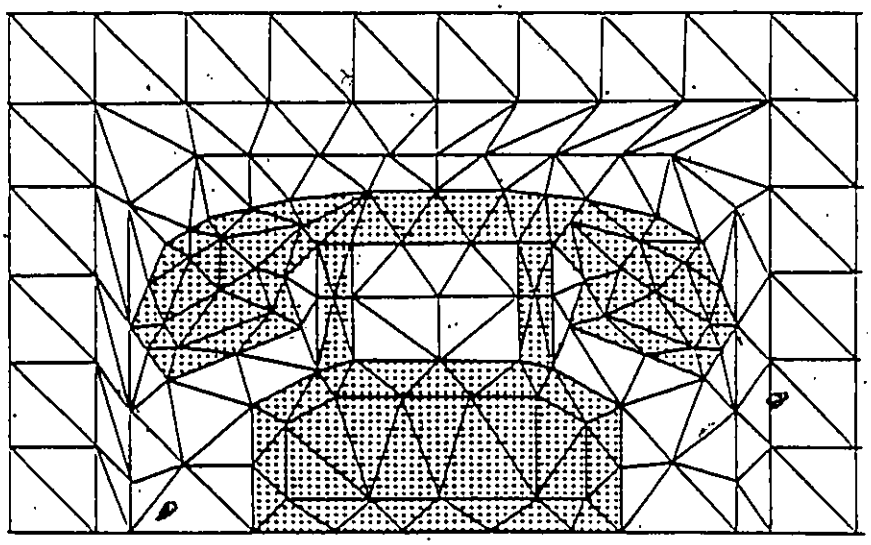

(b) DETAIL SCHEME OF THE COMBINED METHOD AT THE DIELECTRIC INTERFACE

The electric field distortion factor is then computed as a ratio of the normalized electric field strength of an EUT-loaded cell to that of an empty cell at the same location (x,y),to estimate the electric field distortions in the TEM cell due to the loading by the EUT. To express the distortion factor in dB , the field distortions in the loaded TEM cell is calculated using the following equation :

$$\text{Distortion factor DF} = 20Log\frac{E_{loaded}}{E_{unloaded}}$$

The results are plotted in Figures (16) through (26).

Figures 16&17 show the electric field strength and the field distribution in an empty TEM cell . According to Fig.16 which shows the electric field distribution in an empty cell ,the electric field E in the cell is essentially vertically polarized in the region near the center of the cell and gradually becomes horizontally polarized at the area closer to the gap of the cell . Fig.17 demonstrates that the electric field components are quite uniform over much of the volume between the septum and the outer wall . The variations of electric field strength is within 2.7 dB over the area occupied by a typical EUT of $0.4a \times 0.5a$ at the center of the cell.

Figures 18 through 20 show the electric field distributions in a telephone loaded TEM cell. These computer-generated graphs show the nonuniformity of electric component due to the insertion of an EUT.

Figures 21 through 23 show that the distributions of the electric field strength in a typical EUT area in a loaded TEM cell are greatly affected by the insertion of a telephone. The variations of electric field increase from 2.7 dB in an unloaded cell to 3.5 dB in TEM cell loaded with an homogeneous telephone , to 4.15 dB in a TEM cell loaded with an inhomogeneous telephone and to 5.4 dB in an TEM cell loaded with a metallic telephone .

Figure (16) ELECTRIC FIELD DISTRIBUTION IN AN UNLOADED TEM CELL

PLATE POTENTIAL = 100 V

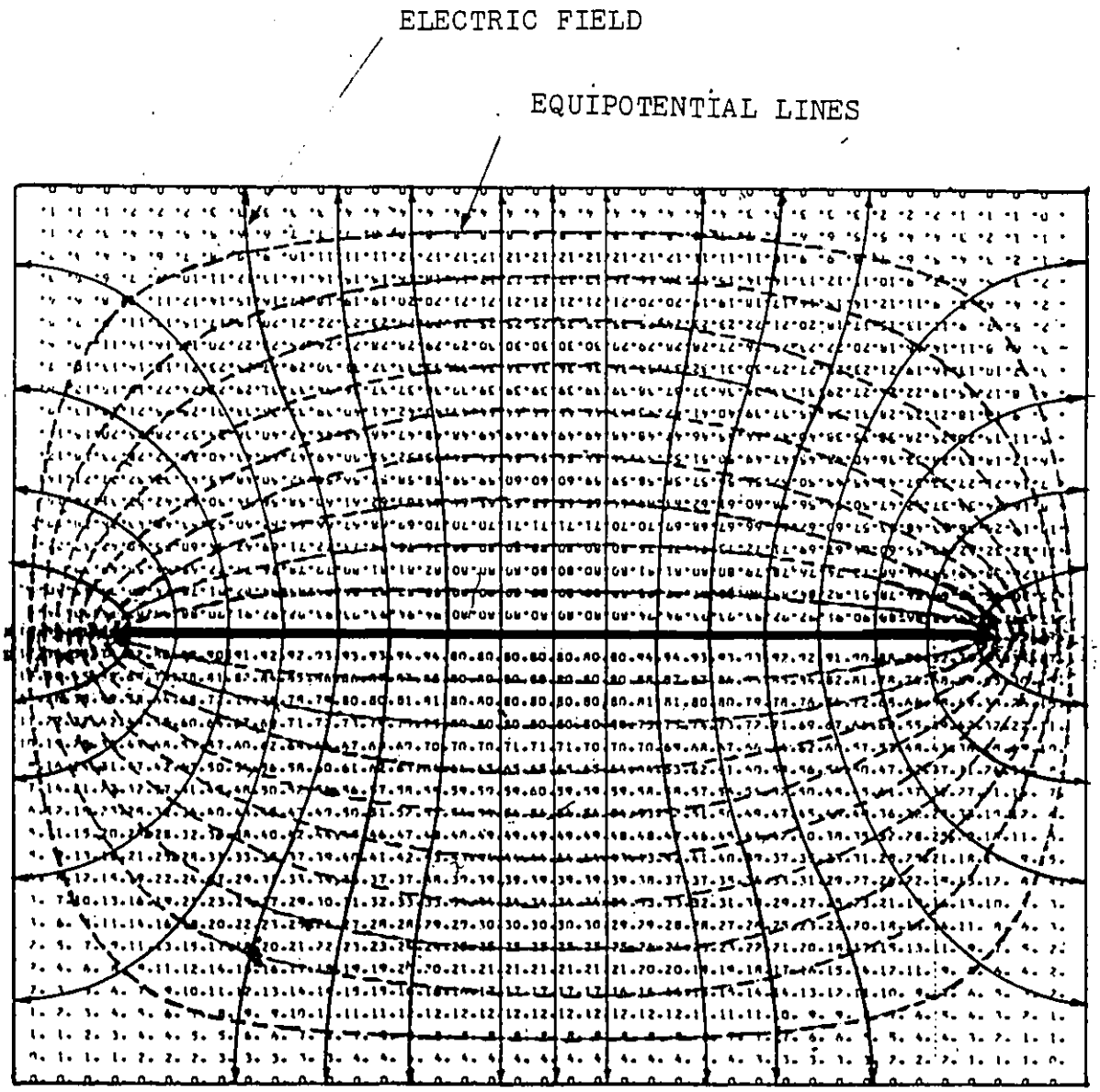

Figure (17) ELECTRIC FIELD INTENSITY IN AN UNLOADED TEM CELL

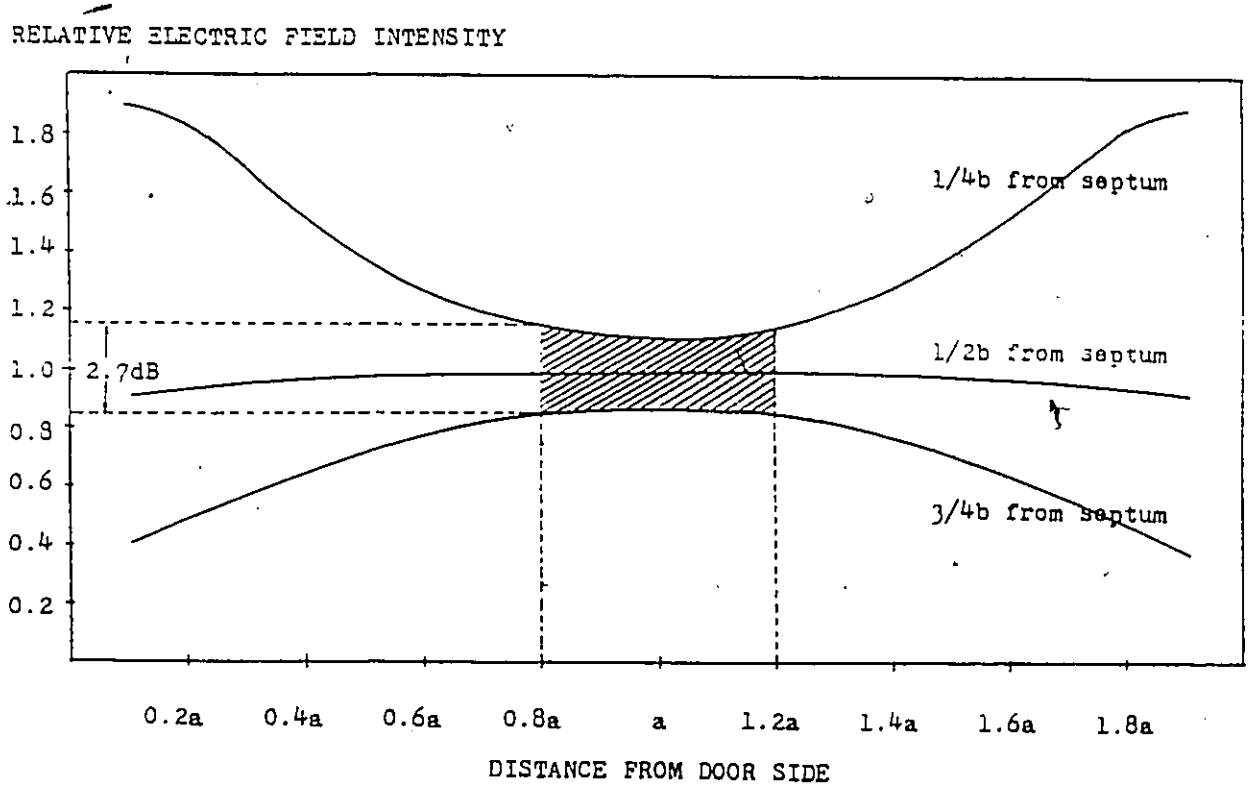

Figure (18) ELECTRIC FIELD DISTRIBUTION IN A TEM CELL LOADED WITH A HOMOGENEOUS TELEPHONE

PLATE VOLTAGE = 100 V

$\varepsilon_r = 2.2$

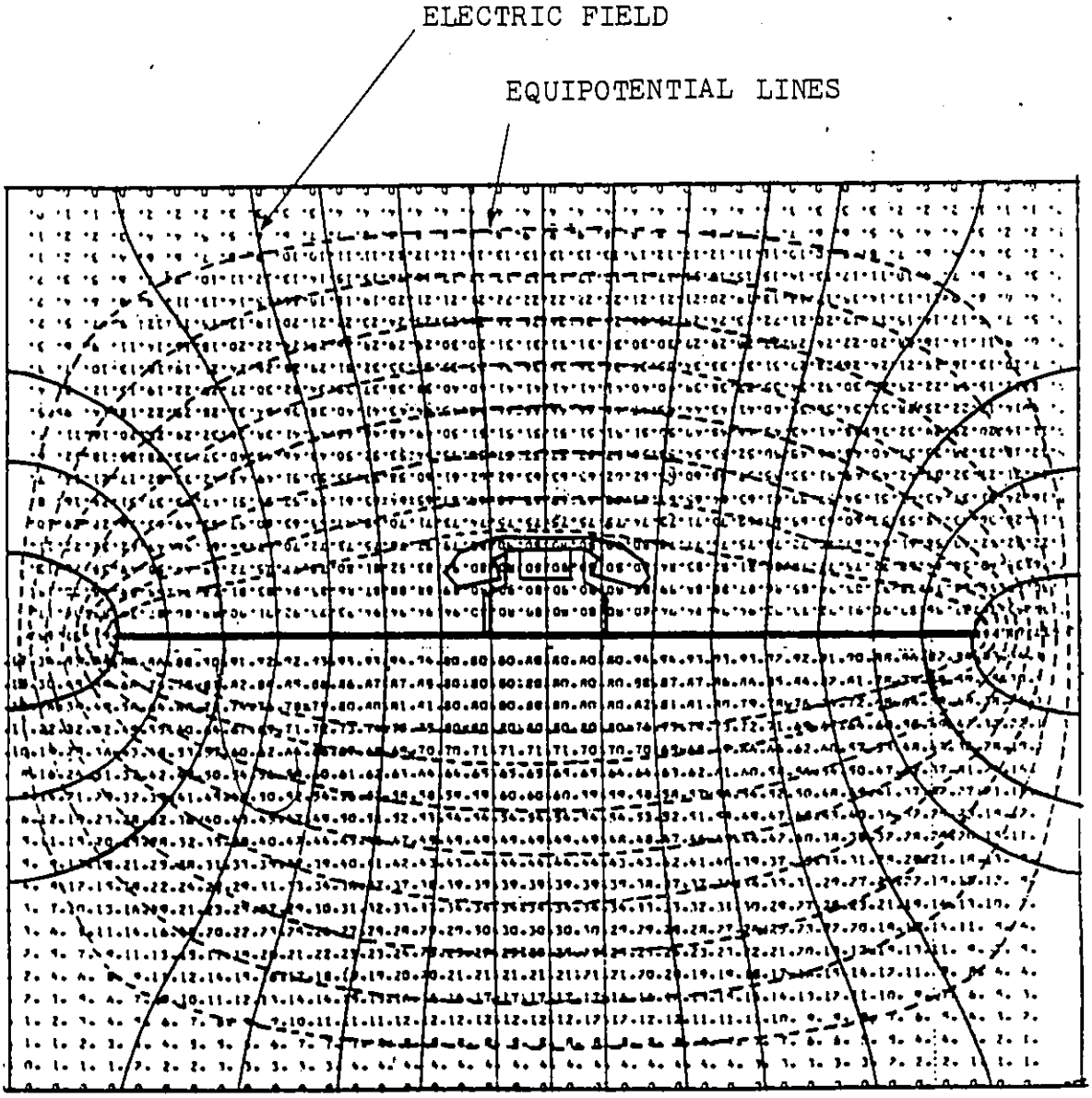

Figure (19) ELECTRIC FIELD DISTRIBUTION IN A TEM CELL LOADED WITH AN INHOMOGENEOUS TELEPHONE

PLATE POTENTIAL = 100V

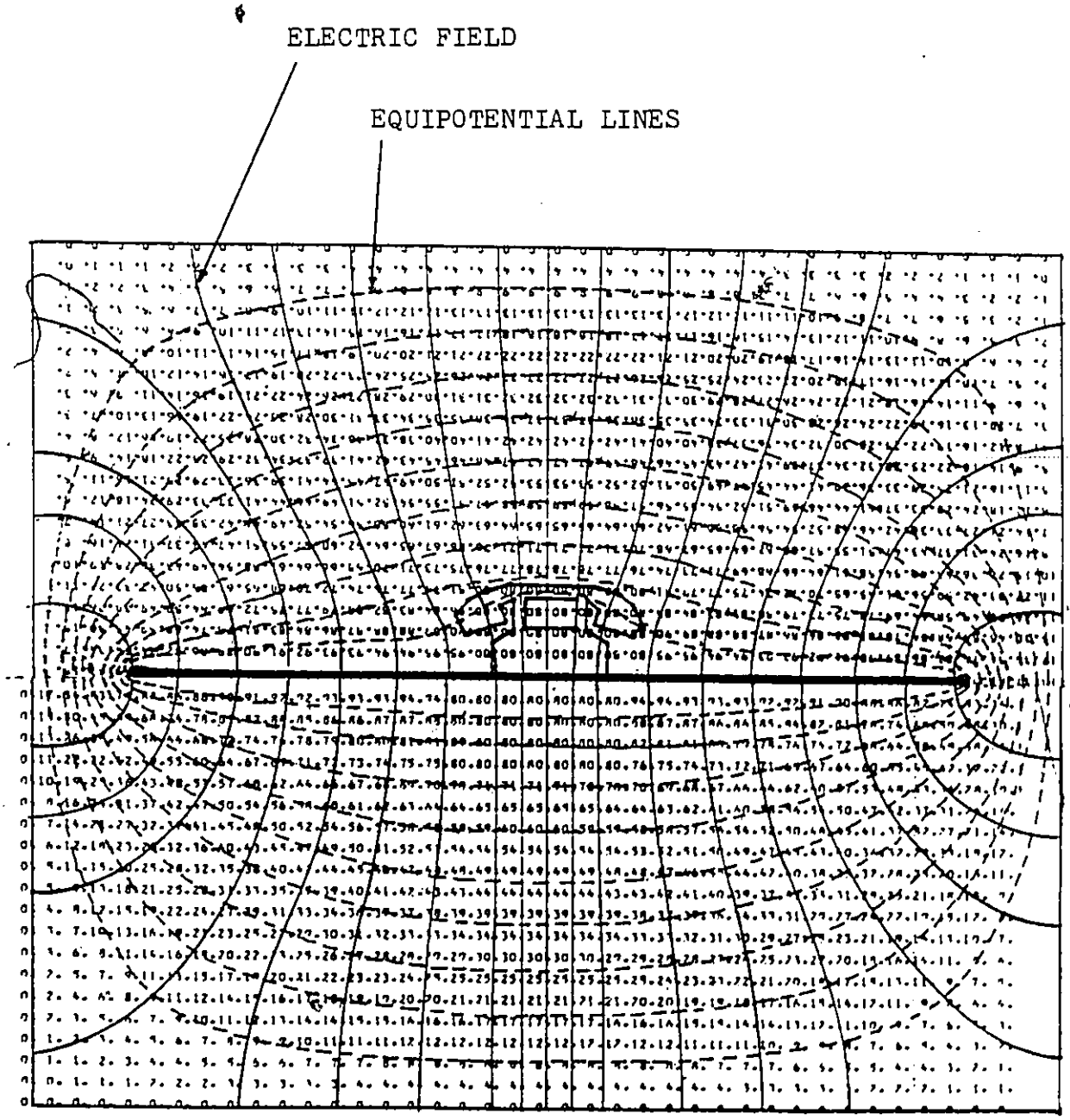

Figure (20) ELECTRIC FIELD DISTRIBUTION IN A TEM CELL LOADED WITH A CONDUCTIVE TELEPHONE

PLATE POTENTIAL = 100 V

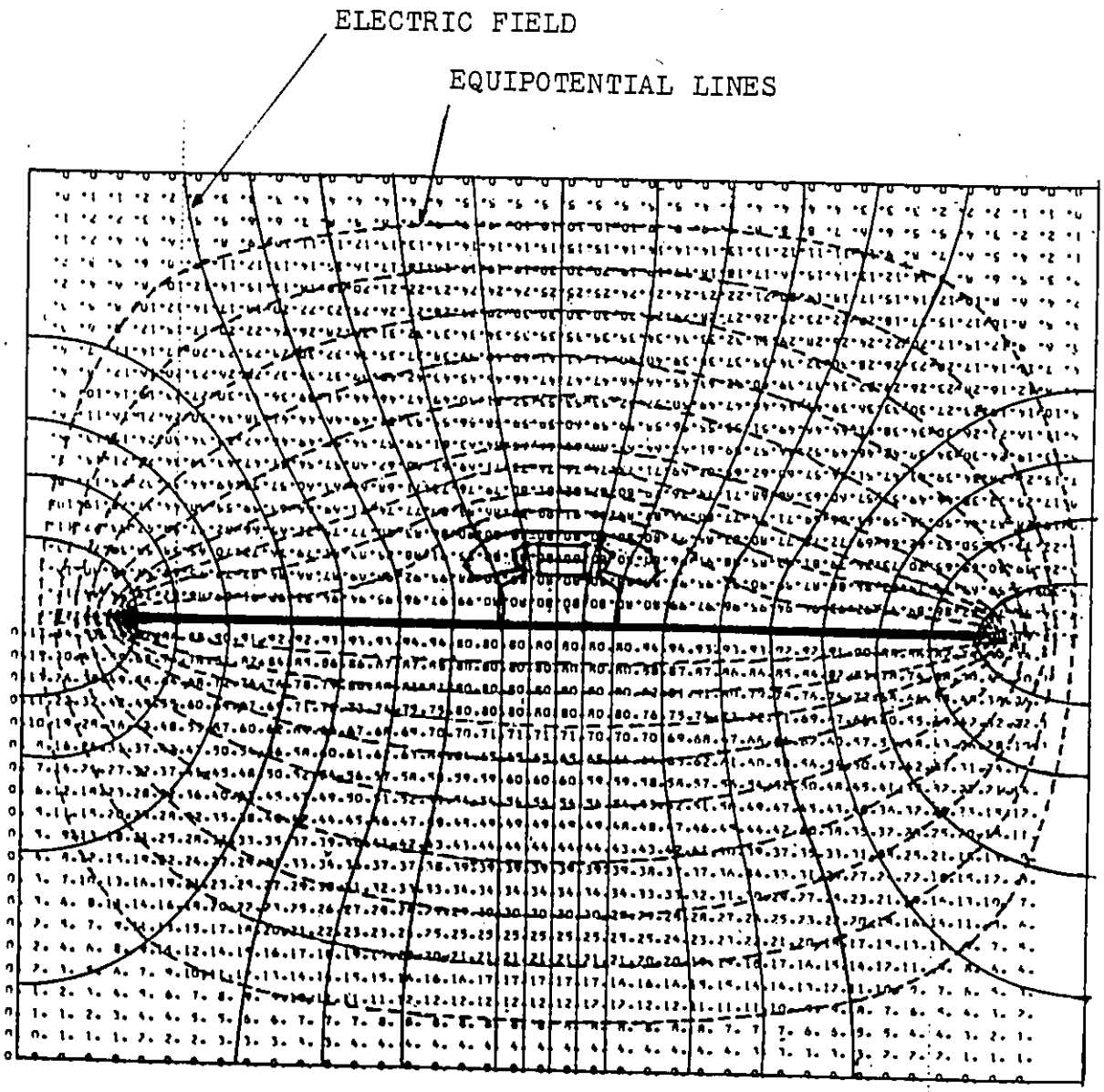

Figure (21) ELECTRIC FIELD INTENSITY IN A TEM CELL LOADED WITH A HOMOGENEOUS TELEPHONE

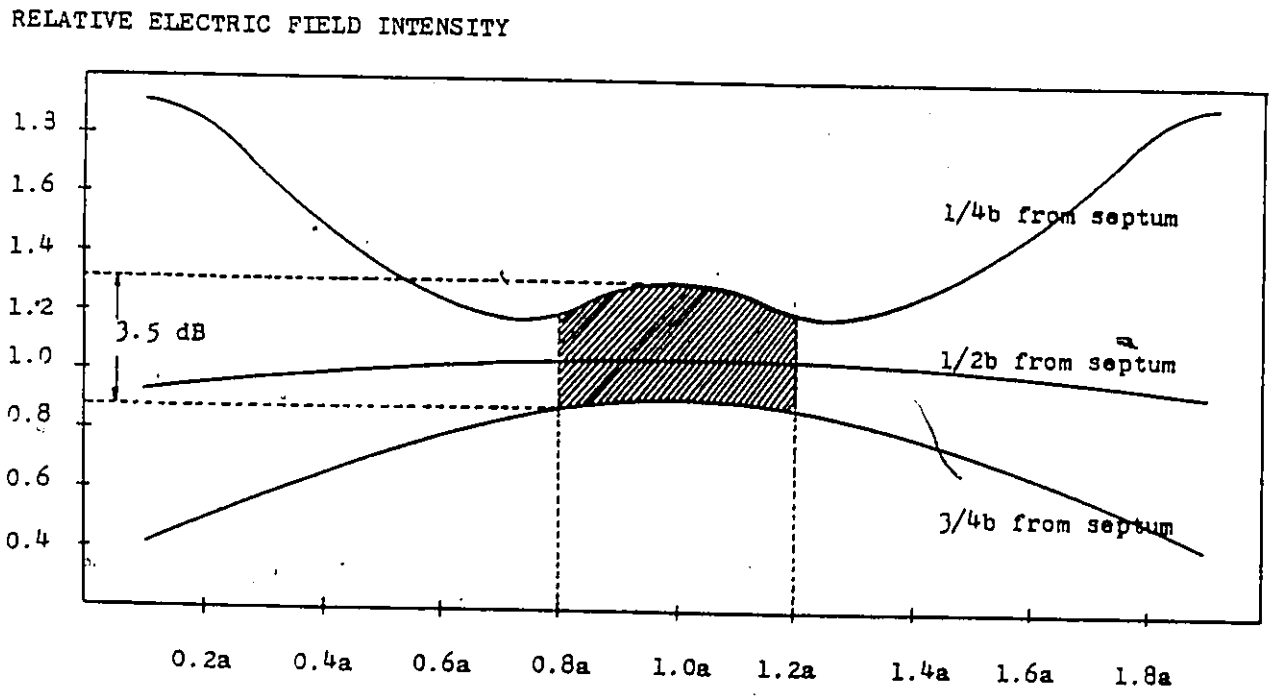

Figure (22) ELECTRIC FIELD INTENSITY IN A TEM CELL LOADED WITH AN INHOMOGENEOUS TELEPHONE

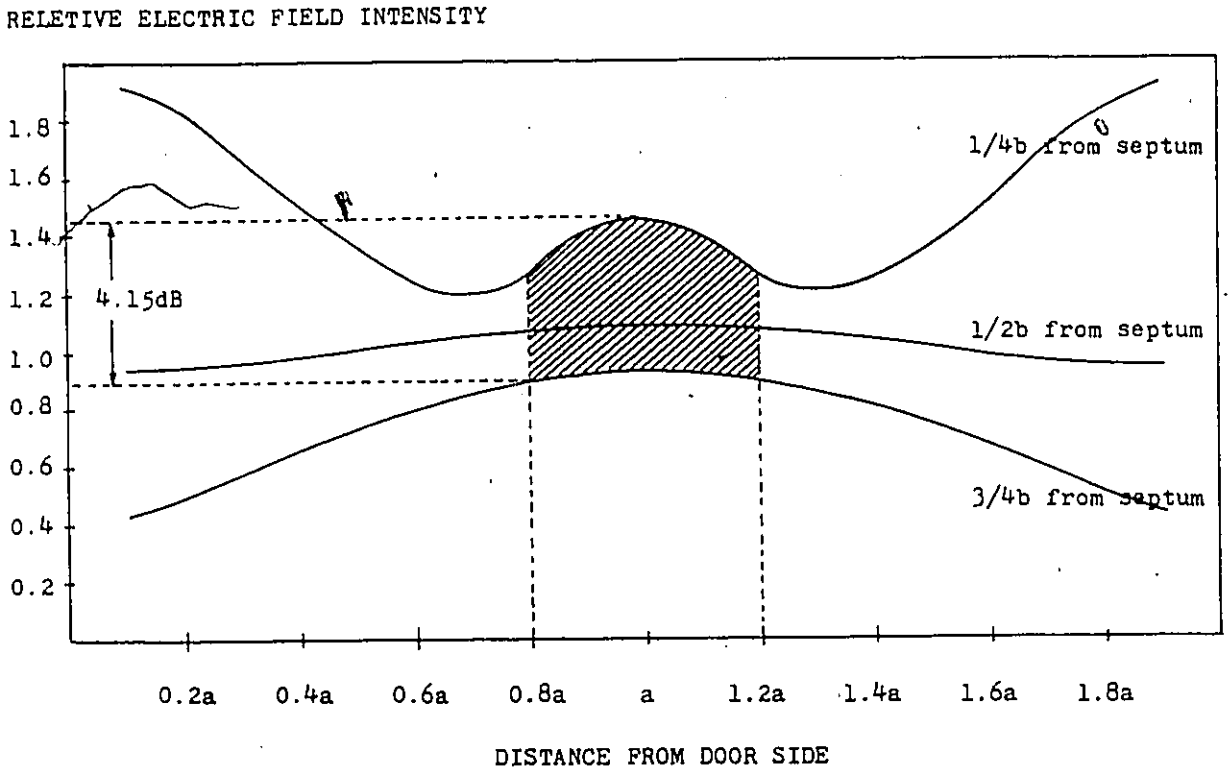

Figure (23) ELECTRIC FIELD INTENSITY IN A TEM CELL LOADED WITH A CONDUCTIVE TELEPHONE

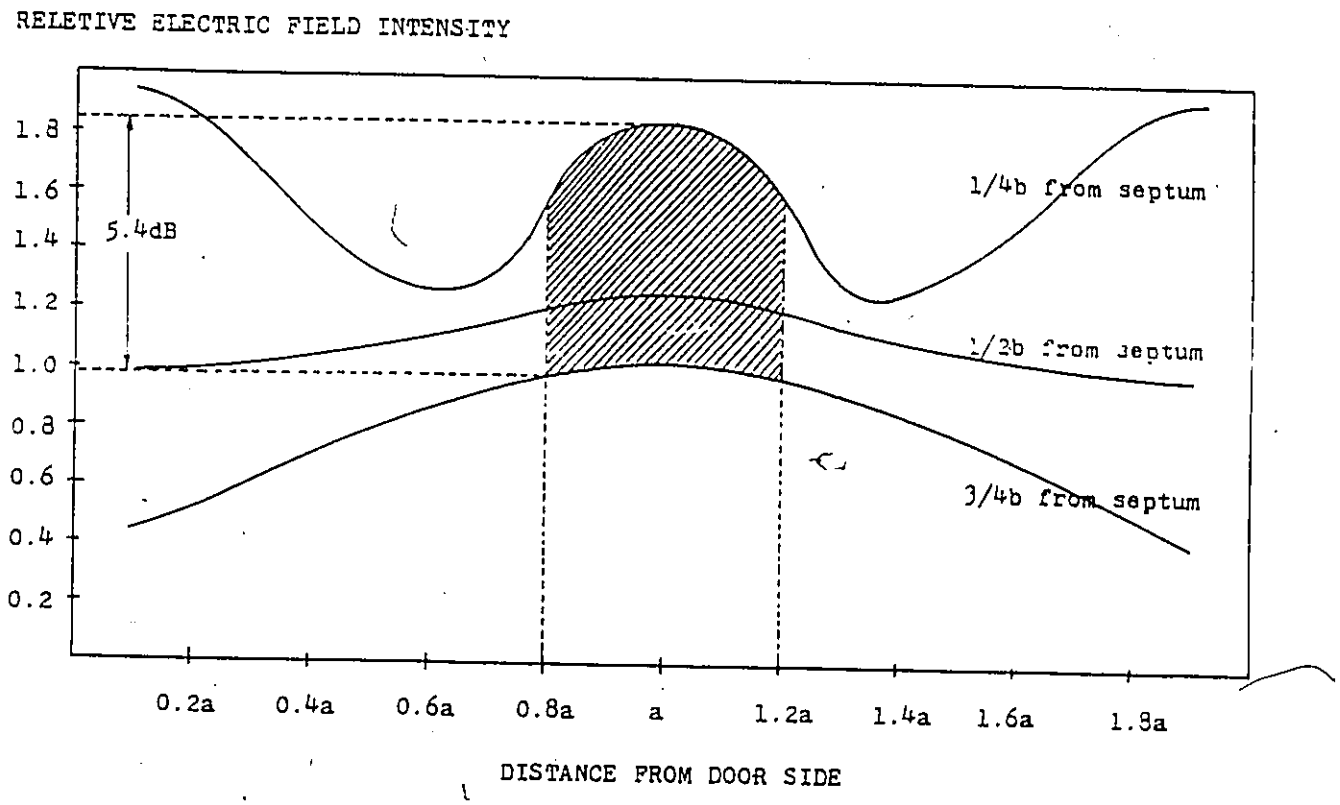

Figure (24) ELECTRIC FIELD DISTORTIONS IN A TEM CELL LOADED WITH A HOMOGENEOUS TELEPHONE

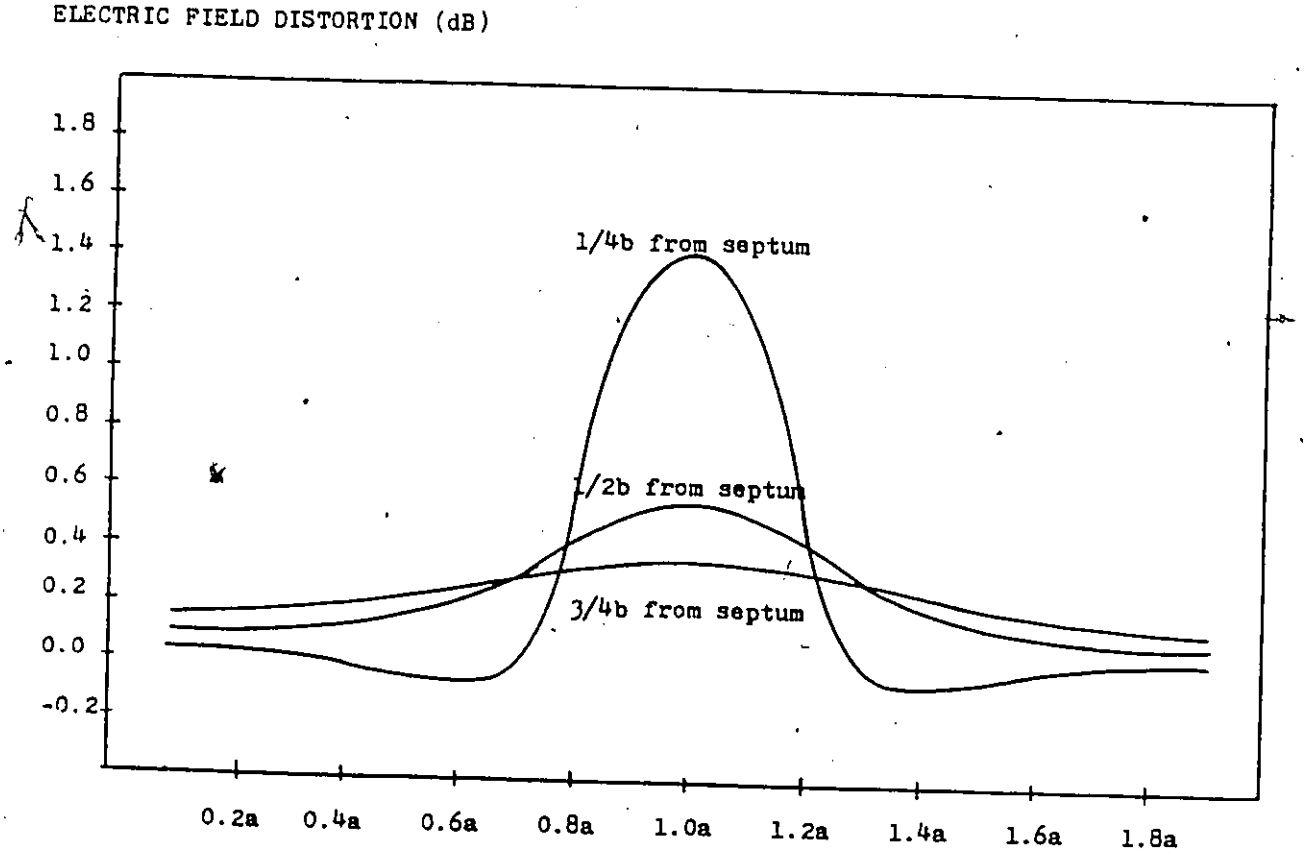

Figure (25) ELECTRIC FIELD DISTORTIONS IN A TEM CELL LOADED WITH AN INHOMOGENEOUS TELEPHONE

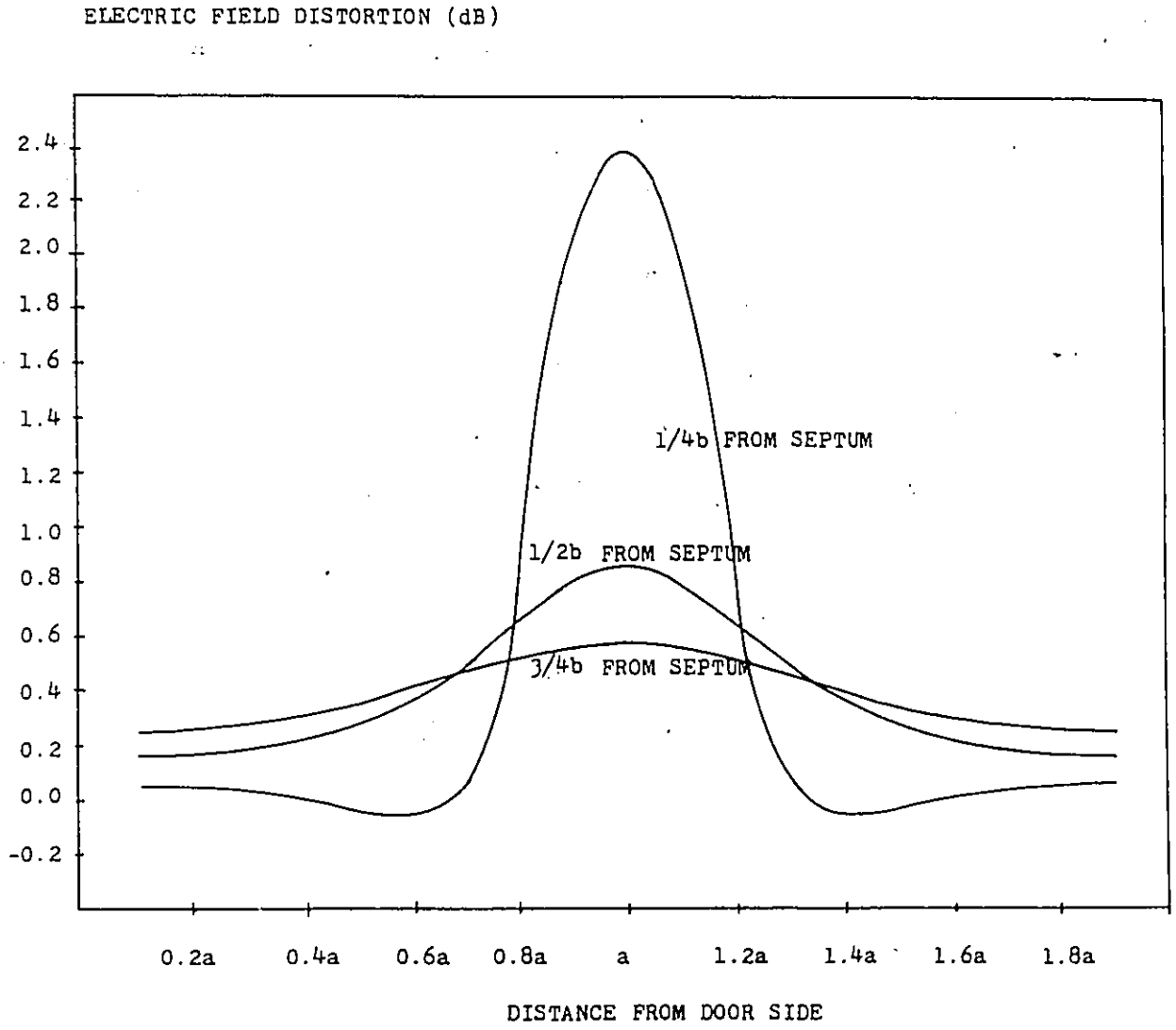

Figure (26) ELECTRIC FIELD DISTORTIONS IN A TEM CELL LOADED WITH A CONDUCTIVE TELEPHONE

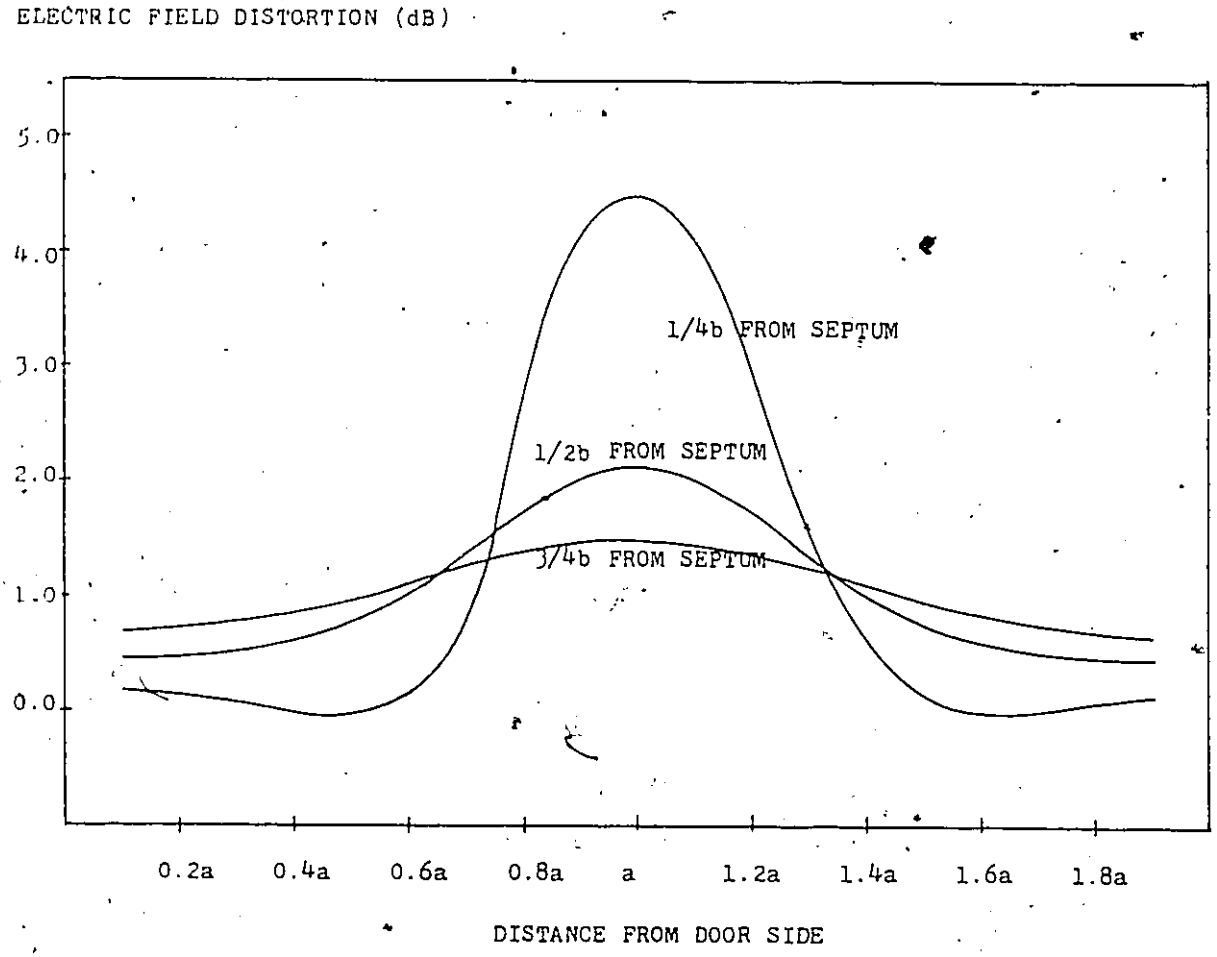

Finally , Figures 24 though 26 show the field distortions in a telephone-loaded TEM cell. These graphs suggest that the greatest nonuniformity of electric field occurs along the vertical axis of the cell due to the electric field gradient in this direction . At a distance of $\frac{1}{4}a$ from the septum, the field distortions in an homogeneous telephone-loaded cell are as high as 1.4dB,and are as high as 2.4dB and 4.5dB in an inhomogeneous telephone loaded cell and a metallic-telephone-loaded cell ,respectively.

From the computer generated datas one can easily compute numerically the characteristic impedances of the loaded and unloaded TEM cells by applying Gauss's Law in the TEM cell.Choosing an approapiate Gaussian surface as shown below :

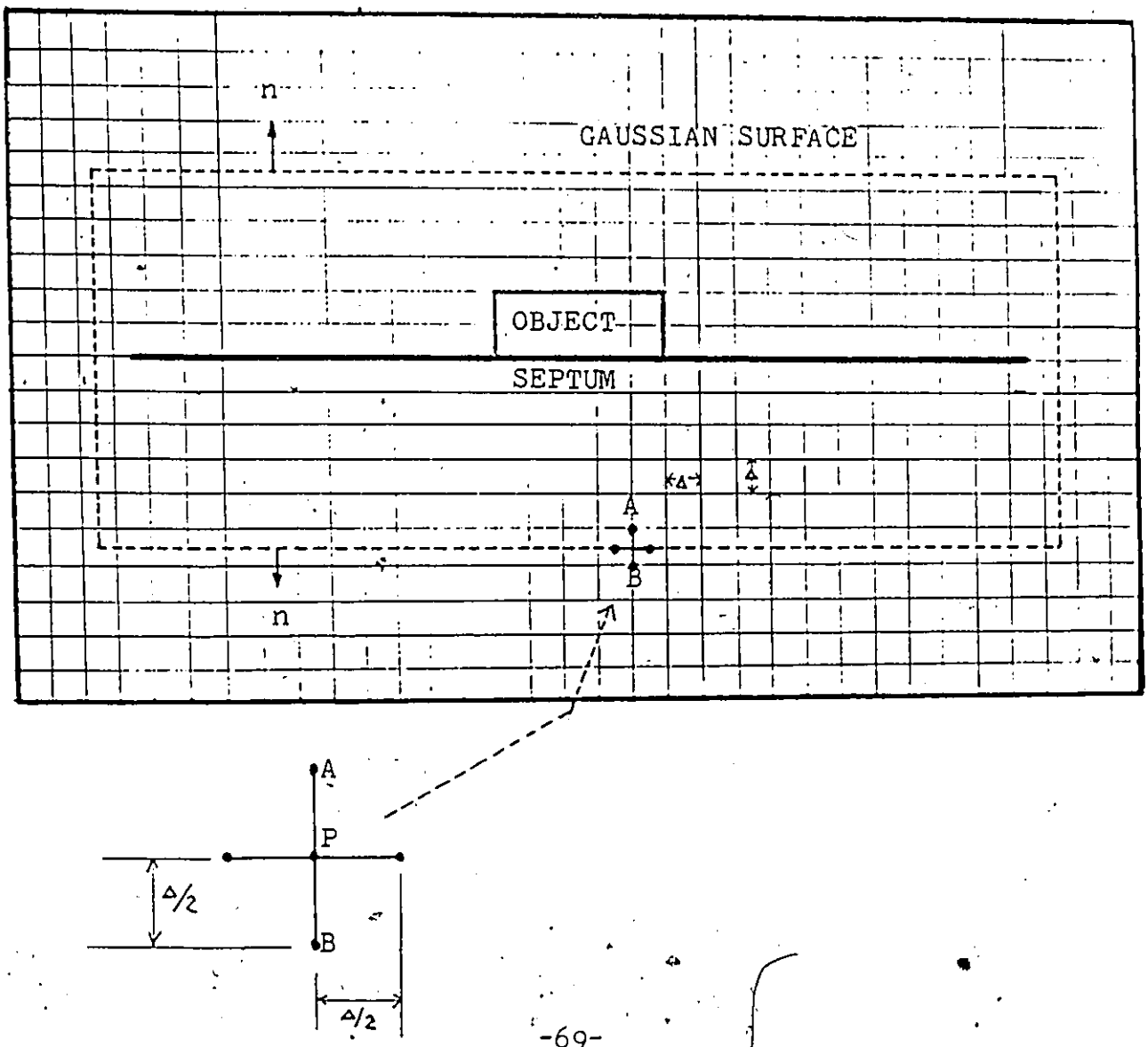

Applying Gauss's Law on the Gaussian surface, s,:

$$\int_s \vec{E} \cdot \vec{n} ds = \frac{\rho}{\epsilon_o}$$

where ρ is the total charges enclosed by the Gaussian surface, $\vec{E}$ is the electric field vector, $\vec{n}$ is the unit vector normal to the Gaussian surface ,but

$$\vec{E} \cdot \vec{n} = -\frac{\partial \Phi}{\partial n}$$

$$= -\frac{\Phi_A - \Phi_B}{\Delta}$$

thus

$$\int_s \vec{E} \cdot \vec{n} ds = -\sum_{Gaussian surface} (\Delta \cdot \frac{\Phi_A - \Phi_B}{\Delta})$$

$$= \sum_{Gaussian surface} (\Phi_A - \Phi_B)$$

Therefore,according to the Gaussian's Law,

$$\rho = \epsilon_o \cdot \sum_{Gaussian surface} (\Phi_{inside} - \Phi_{outside})$$

Once the total charge enclosed in the Gaussian surface in known, the capacitance per unit length in the TEM cell can then be calculated from the following relationship:

$$C = \frac{\rho}{\Phi_o}$$

where , C is the capacitance per unit length in the TEM cell and Φ_o is the electric potential on central plate.

The characteristic impedance of the rectangular line can then be approximated as follow;

$$Z_o = \frac{1}{C \cdot v}$$

$$= \frac{\sqrt{\epsilon_r}}{C \cdot v}$$

$$= \frac{1}{\alpha \cdot v}$$

where, Z_o is the characteristic impedance of the TEM cell ,C is the capacitance per unit length of the TEM cell ,v is the phase velosity in the cell.

Using these relationships the characteristic impedance of an empty IFI cc101.5s TEM cell was found to be about 52.5Ω .When the TEM cell is loaded with some dielectric material the characteristic impedance of the cell is lower due to the increased in capacitance per unit length.The lowest characteristic impedance occurs when a conductive object is inserted.The characteristic impedance of the IFI cc101.5 TEM cell loaded with the metallic-telephone was found to be about 50.8Ω .

4.3 SEMICIRCULAR CYLINDRICAL OBJECT

Further investigations of field distortions in a loaded TEM cell were carried out using semicircular cylindrical object with various diameters and dielectric constants .

The finite element method is considered the best suited procedure for this particular problem . The scheme of the element for this problem is shown in Fig.27. The electric field distortions at the center ($x = a, y \doteq 0.5b$) of the upper chamber is computed for various diameter and dielectric constants of the cylinder . Results are plotted in Fig.28. These curves are generated to estimate the maximum acceptable object size in a given TEM cell.

4.4 DISCUSSION

In this chapter ,field distortions in a TEM cell due to the insertion of various telephone models are computed . The maximum distortion were found to occur along the central vertical axis of the cell and are increasing in the direction toward the septum .At a distance of half way between the outer conductor and the septum , the maximum field distortions in the cell due to the present of various types of telephone is estimated as : 0.6dB for a homogeneous

Figure (27) FINITE ELEMENT SCHEME OF A TEM CELL LOADED WITH A SEMICIRCULAR CYLINDRICAL OBJECT

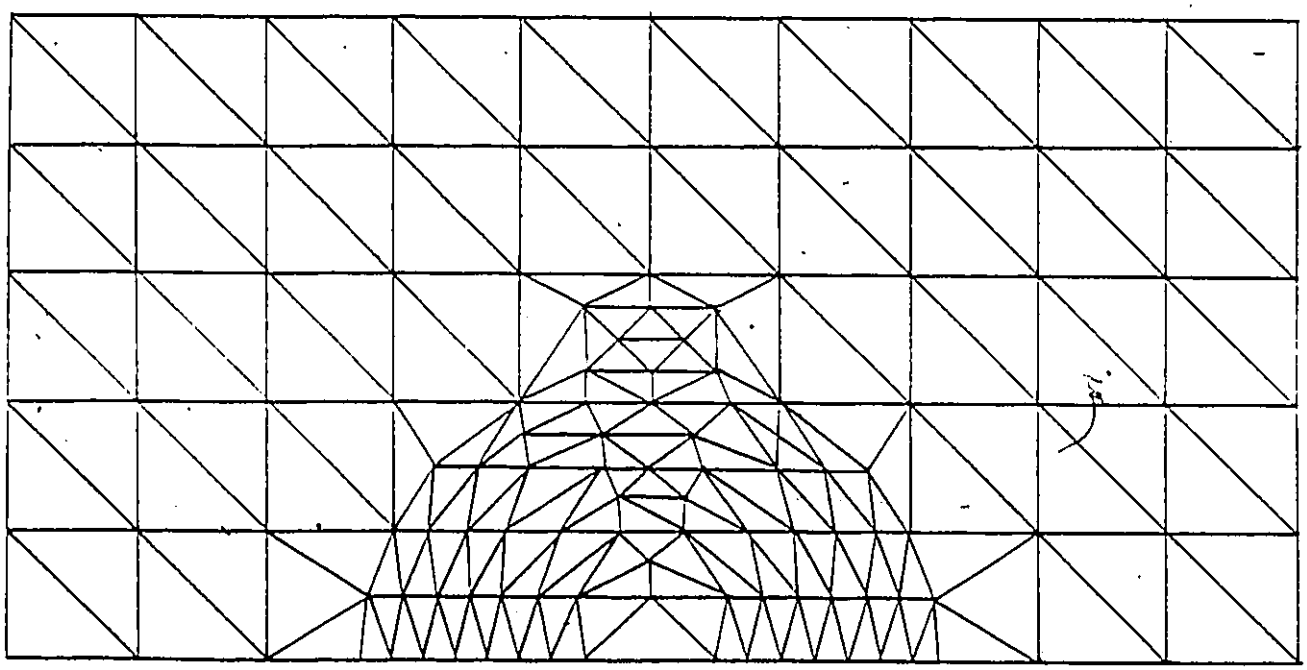

Figure (28) ELECTRIC FIELD DISTORTIONS AT THE CENTER OF THE TEM CELL LOADED WITH A DIELECTRIC SEMICIRCULAR CYLINDER

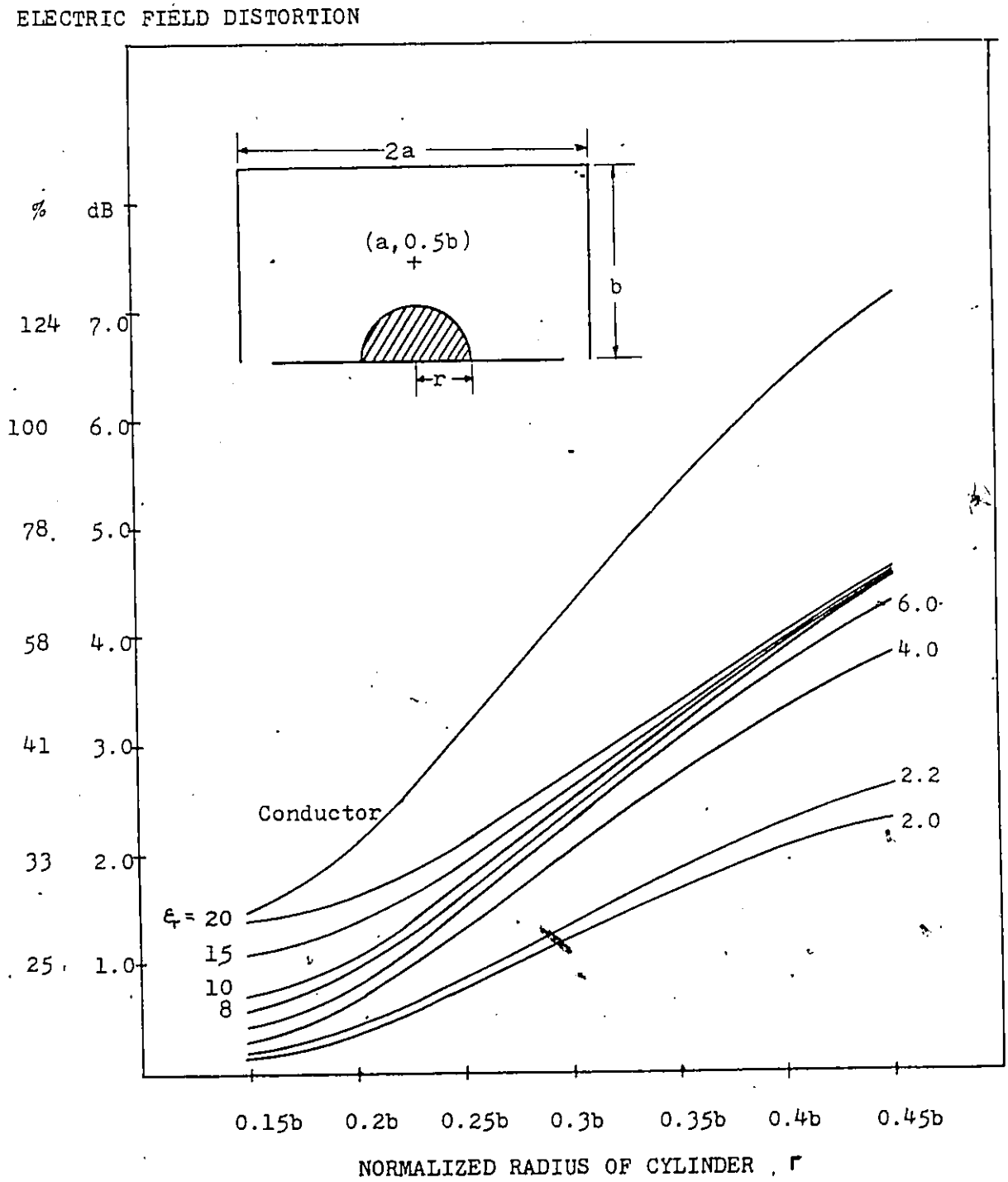

dielectric telephone with dielectric constant $\epsilon_r = 2.2$, 0.9dB for an inhomogeneous telephone with dielectric property approximating a regular home telephone , and 2.0dB for a metallic telephone.

Curves of field distortions at the center of the cell versus the object size for various dielectric constants are plotted using a semicircular cylindrical object.These curves provide useful guidelines for predicting the maximum object size for a given TEM cell . It is interesting to note that results computed in a telephone loaded cell closely agree with the values given here . According to these results, the maximum cross-sectional size for this specific TEM cell model (IFI cc101.5s) loaded with a homogeneous 2-Dimensional telephone with a dielectric constant of $\epsilon_r = 2.2$ is about 0.26 the vertical distance between septum and outer conductor for maximum tolerable field distortions of 1dB and is about 0.4 the vertical distance between the center septum and the outer conductor for the maximum tolerable field distortions of 3dB.

The variations of electric field in the central area of the upper chamber are estimated for various types of telephone loads. In a 0.4X0.5 normalized area at the center of the chamber ,the variations of electric field in an unloaded cell are about 2.7 dB and are increased to 3.5dB for a homogeneous-telephone-loaded cell , 4.15dB for an inhomogeneous-telephone-loaded cell, and 5.4dB for metallic-telephone-loaded cell . It shows that the electric field intensity in the loaded cell is highly nonuniform especially when the inserted load is a metallic object .

CHAPTER 5

DISCUSSION AND CONCLUSIONS

5.1 SUMMARY

When making EMC/EMI measurements in a TEM cell,the electric field pattern inside the cell is distorted due to the loading effect of the equipment under test . The objective of this study was to evaluate field distortions in a EUT-loaded TEM cell to improve the uncertainty of the EMC/EMI measurements using TEM cells. The results allow one to estimate the EMC/EMI characteristics of the object under test more accurately by considering field distortions in the TEM cell .

The mathematical model used in this analysis is based on the pure TEM mode propagation in the TEM cell. Fundamental numerical procedures and operations of the finite element and the finite difference methods are exploited to analyse electromagnetic field distortions in an irregular-shaped-EUT-loaded TEM cell. The finite difference method was recognized as the most straight forward and easiest method to apply in an unloaded TEM cell . However,its efficiency and accuracy deteriorates considerably when applied to a loaded TEM cell ,especially when the EUT has an irregularily-shaped cross-section. The finite element method has the advantage over the finite difference method due to its flexibility in the geometry of boundaries. It is suitable for the analysis of field distortions in a loaded TEM cell. Unfortunately , enormous involvement in manipulation of the input data is usually involved in this method. To overcome the limitations of the above two methods ,the combined method of finite difference and finite element was developed . By dividing the given physical region into two main subdomains, the

finite difference domain and the finite element domain,and simulating an appropiate *"Dynamic Boundary Conditions"* , between the two domains ,the given boundary value problem with any complicated boundary geometries can easily be solved by using the basic operations of the finite difference and the finite element methods. This method combines the advantages and conveniences of the finite element and the finite difference methods , and thereby provides better efficiency , accuracy and flexibility of computations. Computer programs for all three numerical methods were developed and used to compute the field distortions in a homogeneous telephone-loaded TEM cell.

To examine the electric field distortions in a IFI cc101.5s TEM cell during EMC measurements of a home telephone , further investigations on the field distortions in a loaded TEM cell were carried out with EUT's as various types of telephone; a homogeneous telephone, an inhomogeneous telephone and a metallic telephone. Field distributions and field distortions were computed for each cases. Results show that the electric field distortions in the regular telephone-loaded cell is quite high and is not negligible. Variations of the electric field intensity in the loaded cell was as high as 6 dB in the area where the EUT was placed, when metallic telephone was inserted. This suggests that the loading effect in a TEM cell must be taken into account during EMC/EMI measurements on a high dielectric constant object , especially when the cross-section of the object is compatible to that of the TEM cell. Another interesting result from this investigation is that the variation in the line impedance of the telephone-loaded cell is small, within 2 Ω, although the loading effect is quite significant.

To estimate the maximum tolerable object size in a TEM cell for EMC/EMI measurements ,theoretical curves of the field distortions versus cross-sectional object size using semicircular cylindrical were computed for various dielectric constants .Results are plotted in Fig.28. These theroretical curves provide a means of estimating the amount of uncertainty in EMC/EMI

measurements using TEM cells for a known dielectric characteristic and object size.They can also be used as a quick reference guideline to predict the maximum tolerable object size in a TEM cell for a given dielectric material and maximum allowable field distortions.

5.2 FUTURE DEVELOPMENT

There is one imminent problem to be solved that is to expand the two dimension analysis to three dimensional analysis . This can be accomplished by using the combined method of finite difference and finite element and assuming Neumann boundary conditions at the transitions between the tapered and the center septum for relatively small size objects. Since the loaded cell is no longer a uniform transmission line, the loaded cell cannot support a pure TEM wave propagation and thus, cannot be solved by electrostatic analysis. The problem becomes an eigenvalue problem with governing equation as vector Helmoltz equation.

APPENDIX A

COMPUTATION OF THE CHARACTERISTIC IMPEDANCE OF TEM CELLS

The design of a TEM cell can be accomplished by using the expression of the equivalent rectangular coaxial transmission line.

For a given bandwidth requirement, the cross-sectional dimensions of the outer conductor can be determined according to the cutoff frequency expression. The width of the center plate can then be determined by using the characteristic impedance expression found for rectangular transmission lines.

Extensive efforts have been devoted to finding analytical expressions for the characteristic impedance to a rectangular coaxial line. Many different expressions have been propopsed.

The characteristic impedance Z_o of a TEM transmission line can be expressed in terms of its capacitance per unit length, C , as follow;

$$Z_o = \left(\frac{1}{vC}\right)$$

where v is the velocity in the medium .

In a rectangular coaxial line, a substantial part of the capacitance per unit length is attributable to the capacitance between parallel planes ,C_p. The remainder is contributed by the fringing capacitance at the corners ,C_c , plus a correction factor ΔC which accounts for the interaction between the two edges of the center plates. The inter-plate capacitance is

readily found in terms of the cross-sectional dimension $\frac{w}{b}$. The approximated expression for fringing capacitance has been derived by Tippet&Chang[21],Weil[18] using conformal mapping techniques as follow;

$$\frac{C_c}{\epsilon_o} = \frac{2}{\pi} ln[1 + Coth(\frac{\pi g}{2b})]$$

and is expressed in a graphical form by O.R.Cruzan and R.V.Garner[24] as shown in Fig.29. The correction factor Δc is negligible for large gap $\frac{w}{b}$ >0.2 , and it becomes significant for small gap lines. Therefore, for a large-gap TEM cell $\left(\frac{w}{g} > 5\right)$,the characteristic impedance can be approximated as follow;

$$Z_o = \frac{\eta_o}{4[\frac{w}{b} + \frac{c_c}{\epsilon_o}] - \frac{\Delta C}{\epsilon_o}}$$

$$\approx \frac{\eta_o}{4[\frac{w}{b} + \frac{C_c}{\epsilon_o}]}$$

$$\approx \frac{\eta_o}{4[\frac{w}{b} + \frac{2}{\pi} ln[1 + coth(\frac{g}{2b})]]}$$

which is plotted in Fig.30.

It was also approximated by Tippet & Chang[28] as follow;

$$Z_o = \frac{\eta_o}{4[\frac{a}{b} - \frac{2}{\pi} ln(sinh\frac{g\pi}{2b})] - \frac{\Delta C}{\epsilon_o}}$$

$$\approx \frac{\eta_o}{4[\frac{a}{b} - \frac{2}{\pi} ln(sinh\frac{g\pi}{2b})]}$$

Crowford& Workman [27] developed curves for designing a cell with arbitrary cross section and impedance as shown in Fig.31. Typical distributed impedance in an empty cell is traced by time domain reflectometer (TDR) as shown in Fig.32.

Figure (29) FRINGING CAPACITANCE IN A RECTANGULAR COAXIAL TRANSMISSION LINE

*By O.R.Cruzan and R.V.Garner ,reference(24).

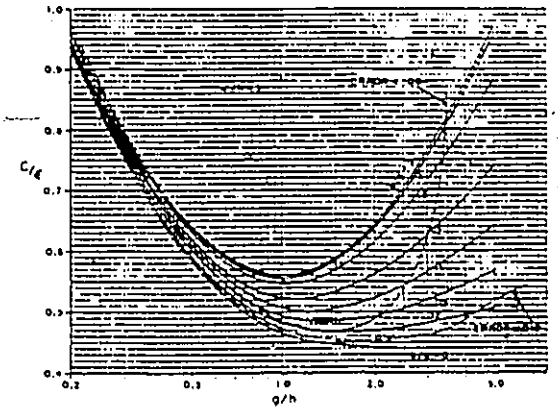

Fig. 6—Corner capacitance for $w/h = 5$.

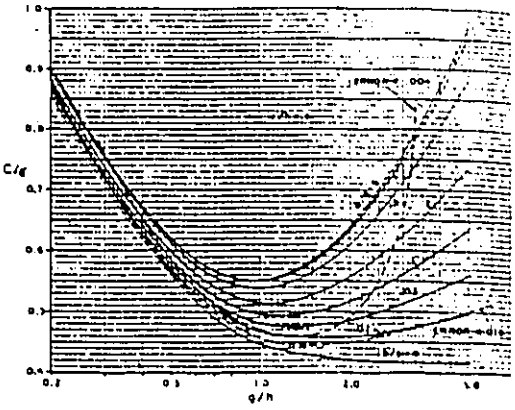

Fig. 9—Corner capacitance for $w/h = 0.6$.

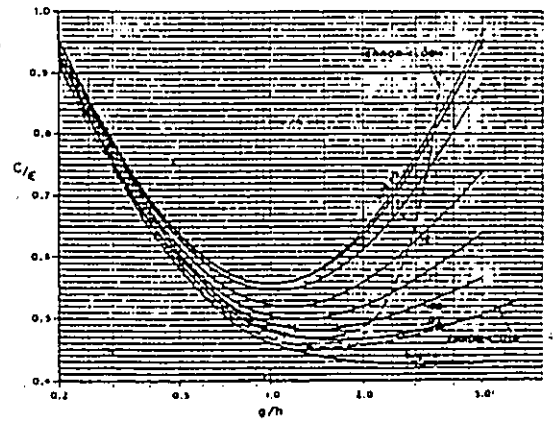

Fig. 7—Corner capacitance for $w/h = 1$.

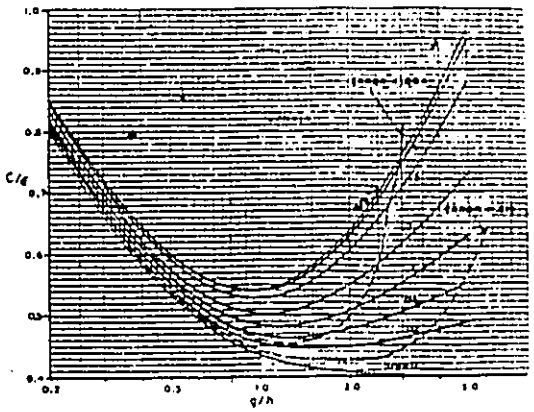

Fig. 10—Corner capacitance for $w/h = 0.4$.

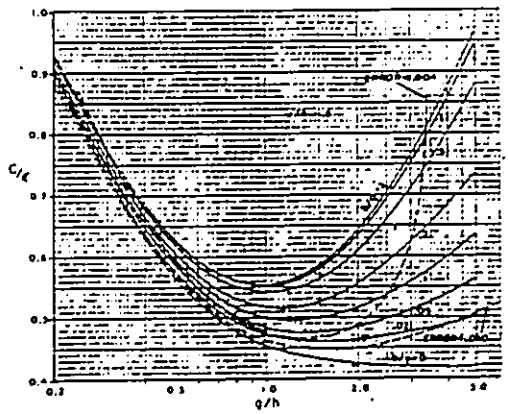

Fig. 8—Corner capacitance for $w/h = 0.8$.

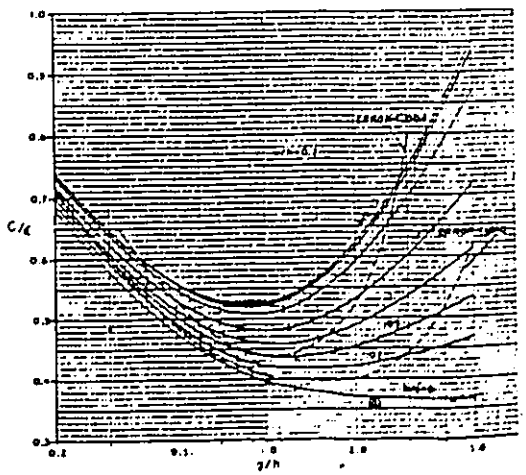

Fig. 11—Corner capacitance for $w/h = 0.2$.

Figure (30) CHARACTERISTIC IMPEDANCE OF A RECTANGULAR COAXIAL TRANSMISSION LINE

*By Claude M. Weil, reference (18).

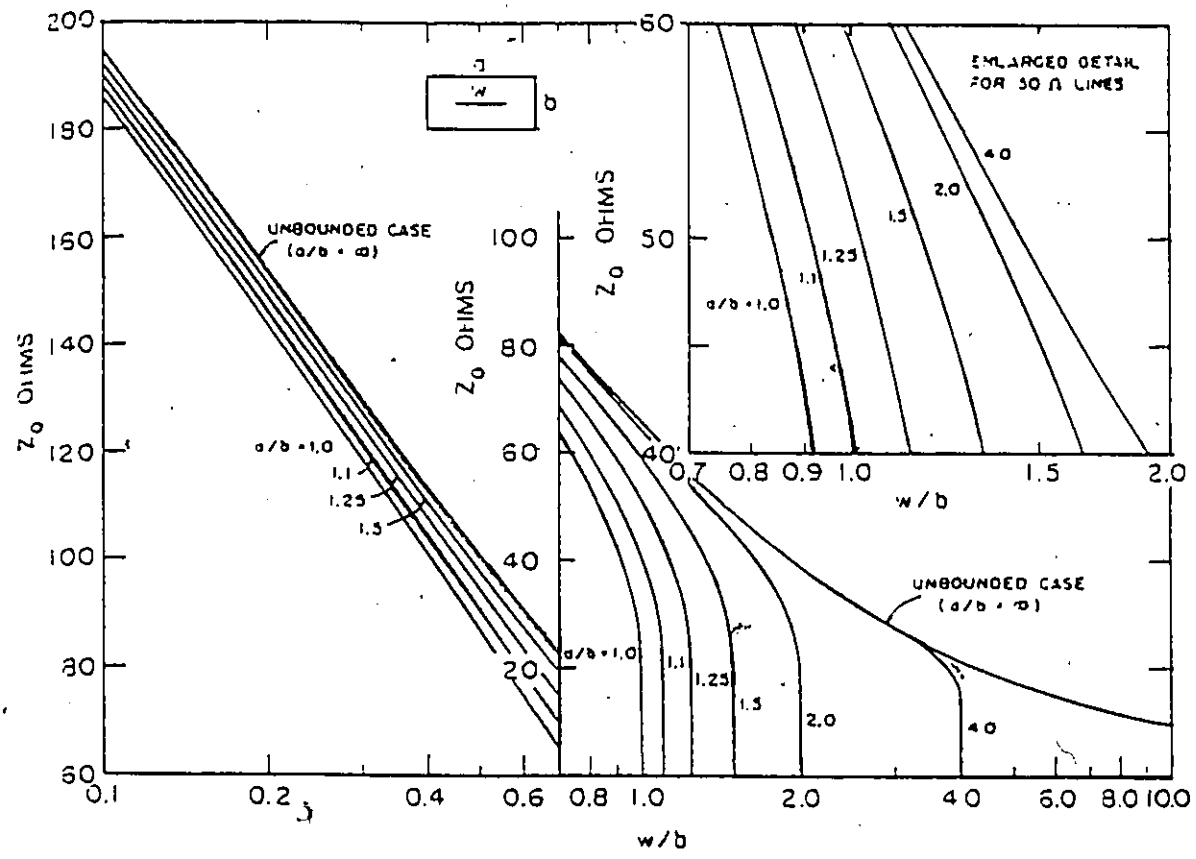

Figure (31) DESIGN CURVES FOR TEM CELLS

*By Crowford and Workman , reference (27).

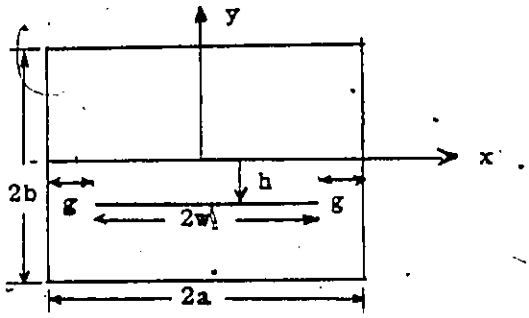

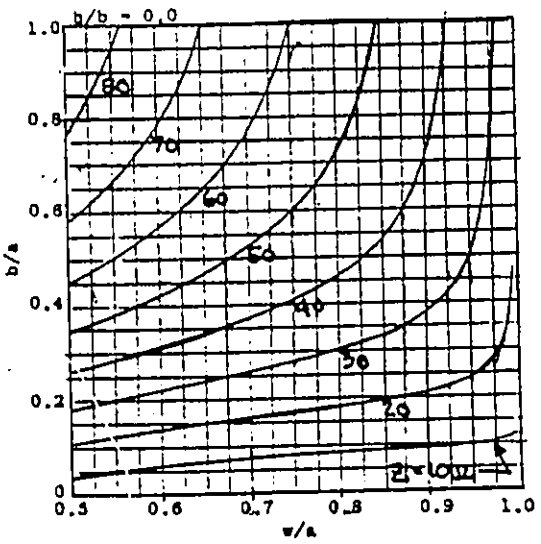

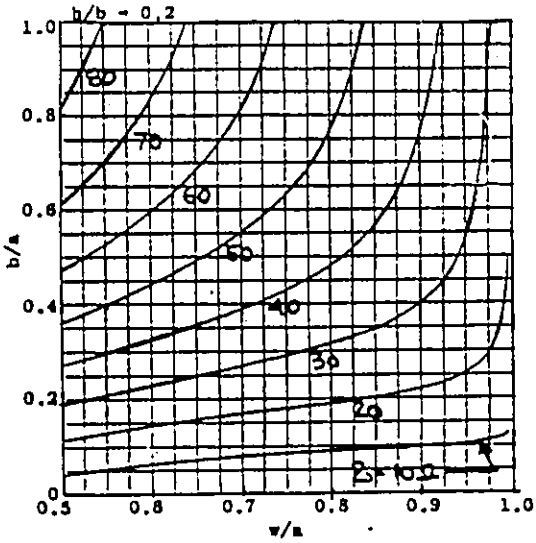

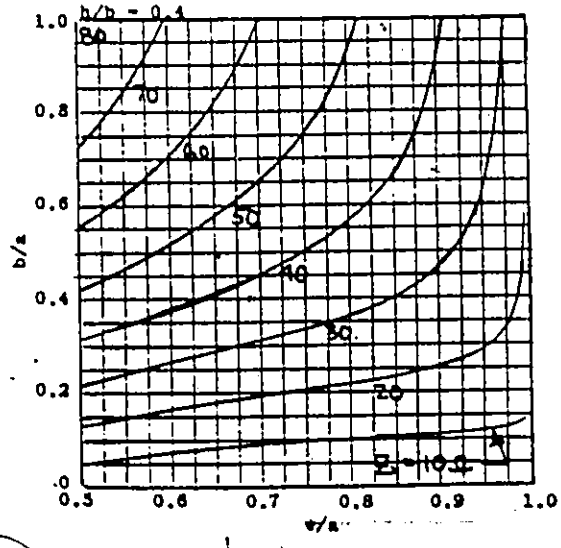

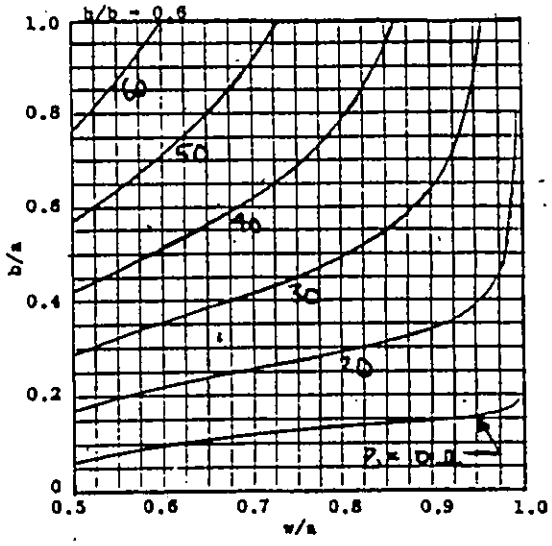

Figure (32) TYPICAL DISTRIBUTED IMPEDANCE IN A TEM CELL

*By Myron L. Crowford , reference (22)

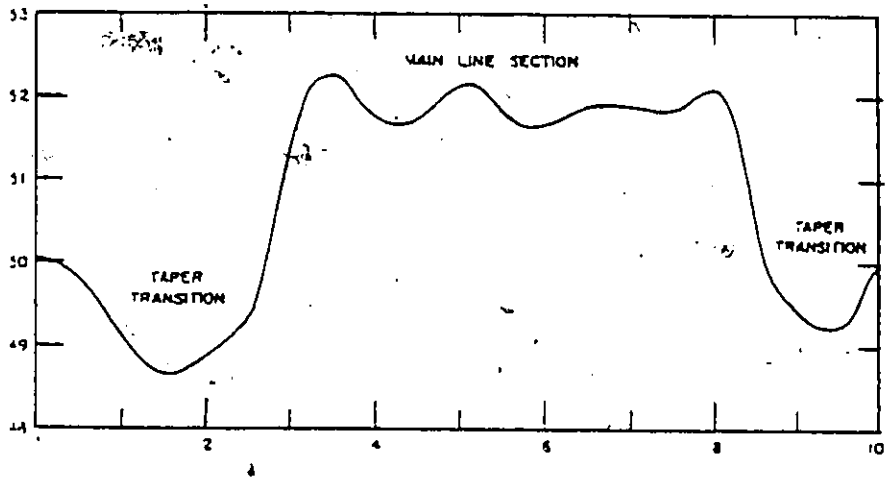

APPENDIX B

MULTIMODING IN THE TEM CELL

Ideally , the TEM cell is designed to allow only TEM mode wave propagation which is characterized by orthogonal electric or magnetic fields that are perpendicular to the direction of propagation along the length of the cell .However,it also supports a set of TE_{mn} and TM_{mn} higher order modes at frequencies above their respective cut-off frequencies.Field patterns for the higher order modes in the TEM cell have been reported by many authors and some of them are given in Fig.33.

It was found that ,depending on the width of the inner conductor and the size of the cell, the dominant cut-off frequency (lowest cut-off frequency) is either the TE_{01} or TE_{10} mode as illustrated in Fig.34. Nevertheless,the TE_{01} mode was found usually to propagate first in practical TEM cells.

Cut-off frequencies of rectangular coaxial waveguides or equivalently TEM cells ,have been investigated and presented by many workers .Modal equations for the first nine higher order modes were summarized by Wilson& MA [1] . Since the cut-off frequency of TE_{10} mode is the lowest cut-off frequency of all higher order modes ,it therefore represents the cut-off frequency of the TEM cell.

. Propagation of higher-order modes does not cause serious field disturbance in a TEM cell until the resonances of the corresponding modes occur .It has been shown that significant perturbation of internal fields within the structure exists primarily at certain discrete frequencies

where resonances of the higher order modes occur .

The TEM mode wave propagates through the tapered ends of the cell without significant alteration. However, each higher order mode wave is always reflected at some point within the tapered section where it becomes too small for the wave to propagate . The energy in the higher order modes,undergoes multi-path reflections within the cell until it is dissipated . At certain frequencies , resonance conditions are satisfied , in which the cell's length for the mode is a multiple integer of half guide wavelength long. At these resonant frequencies,f_R,a TE_{mnp} or TM_{mnp} resonant field pattern exists .For each cut-off frequency, there exists infinite set of resonant frequencies ,$f_R(mnp)$. The resonant frequencies ,$f_R(mnp)$,of the cell can be approximated by using equivalent coaxial box model. The cell is modeled as a transmission line with flat transverse ends instead of tapered ends .The conditions for resonances of TE_{mn} mode is that the effective length of the box for that mode ,L_{mn}, equal an integer number of half guide wavelengths for the mode :

$$L_{mn} = P\left[\frac{\lambda_g(mn)}{2}\right]$$

where, L_{mn} is related to the actual cell dimensions by

$$L_{mn} = L_c + X_{mn}L_E$$

where,

L_C is the actual length of the uniform cross section part of the cell

L_E is the actual length of the tapered end of the cell along the center line

X_{mn} is the fraction of the two ends included in the value of L_{mn}.

Substituting into the relationship for the wavelength in the waveguide

$$\frac{1}{\lambda^2} = \frac{1}{\lambda_g^2} + \frac{1}{\lambda_C^2(mn)}$$

giving an expression for resonant frequencies

$$f_R^2(mnp) = f_c^2(mn) + \left(\frac{Pc}{2l_{mn}}\right)^2$$

where

$$f_c(mn) = \frac{1}{\lambda_c(mn)}$$

The upper useful frequency for a cell is thus determined by the resonance frequency of the dominant higher-order mode ,the TE_{10} mode as given by,

$$f_{res} = \sqrt{f_{c10}^2 + \left(\frac{c}{2l_{10}}\right)^2}$$

where, l_{10} is the equivalent first resonant length of TE_{10} mode ,f_{c10} is the cut-off frequency of the TE_{10} mode

$$f_{c10} \approx \frac{75}{a}\sqrt{1 + \frac{4ab}{\pi b_1 b_2\ ln(\frac{8a}{\pi g})}}$$

L_{mn},the effective cell length ,is an adjustable parameter which is the same for all resonances of a given mode. L_{10}, the effective cell length seen by the TE_{10} mode propagation is usually determined experimentally .It usually exceeds the actual physical length of the transmission line due to the propagation of fringing fields at the line terminations.

Figure (33) FIELD PATTERNS FOR HIGHER ORDER MODES IN A TEM CELL

*From reference (29) and (11)

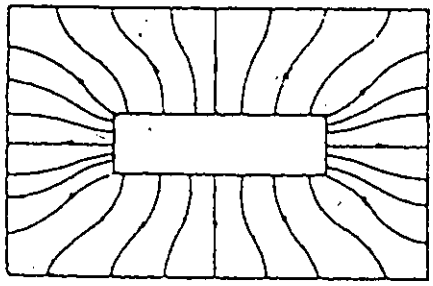

ELECTRICAL FIELD LINES OF THE TEM MODE

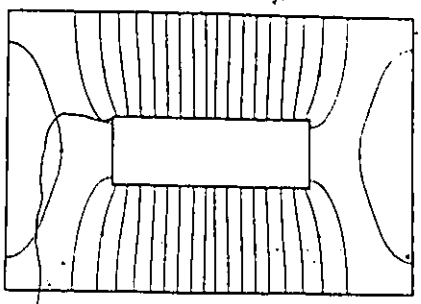

ELECTRICAL FIELD LINES OF THE TE_{10} MODE.

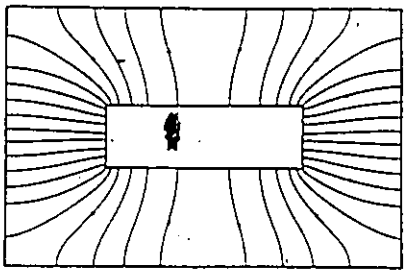

ELECTRICAL FIELD LINES OF THE TE_{01} MODE

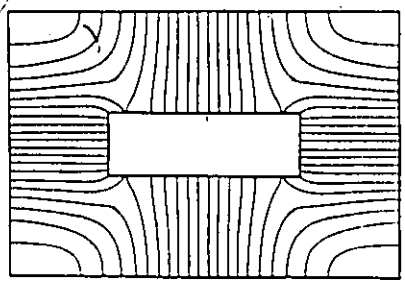

ELECTRICAL FIELD LINES OF THE TE_{11} MODE.

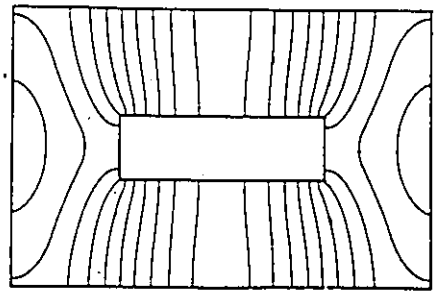

ELECTRICAL FIELD LINES OF THE TE_{20} MODE.

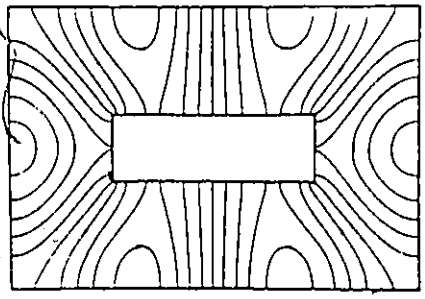

ELECTRICAL FIELD LINES OF THE TE_{30} MODE.

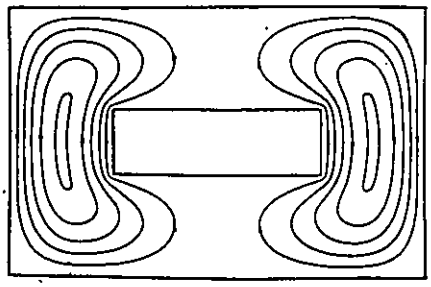

MAGNETIC FIELD LINES OF THE TM_{21} MODE.

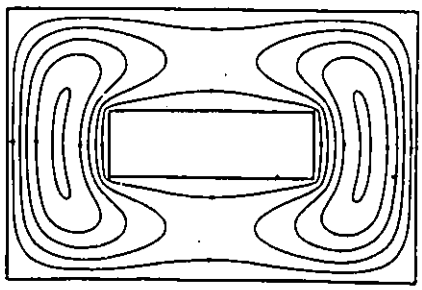

MAGNETIC FIELD LINES OF THE TM_{11} MODE.

Figure (34) DOMINANT HIGHER ORDER MODES IN TEM CELLS

*By Motohsia Kanda , reference (12)

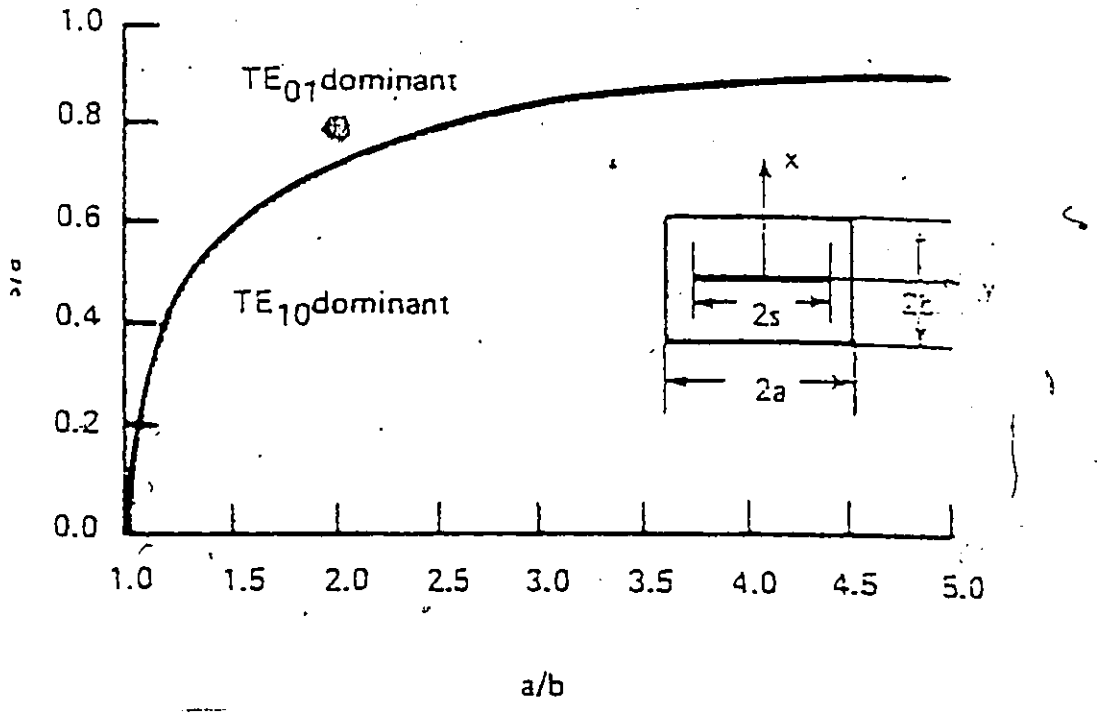

APPENDIX C

SPECIFICATIONS OF IFI cc101.5s TEM CELL

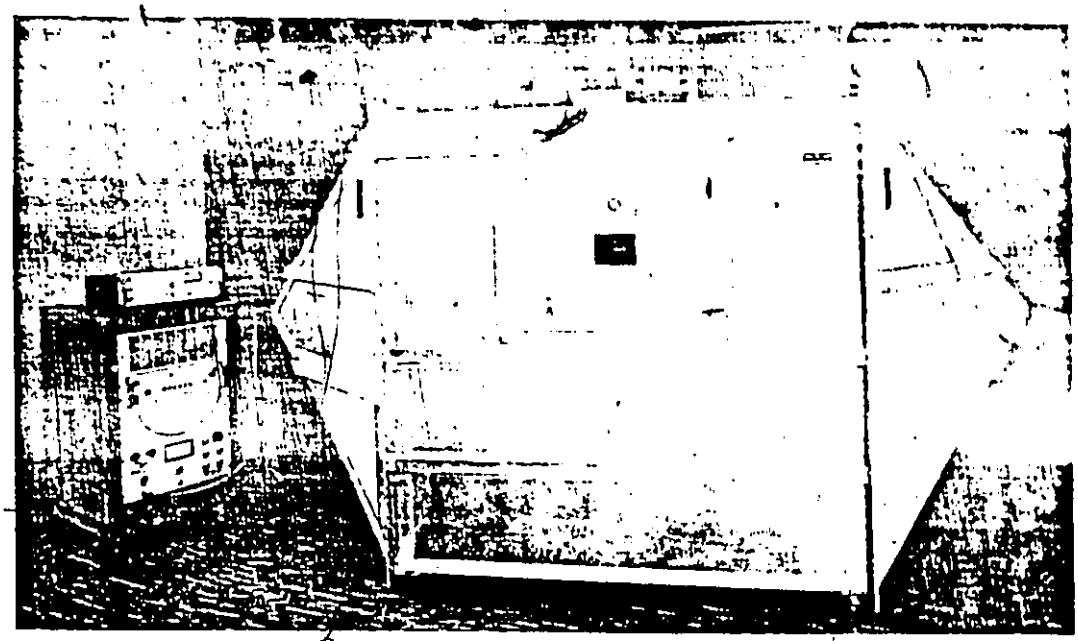

MODEL CC-101S—DC-100 MHz with square center section

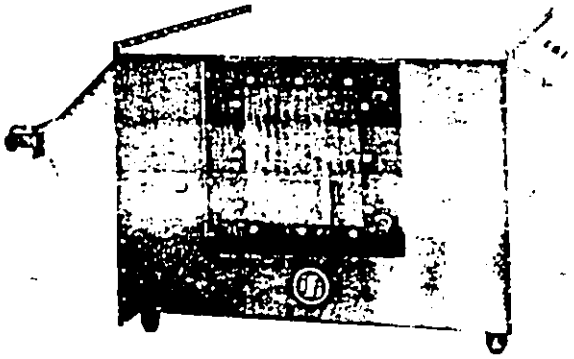

MODEL CC-103
With special
screened
access door

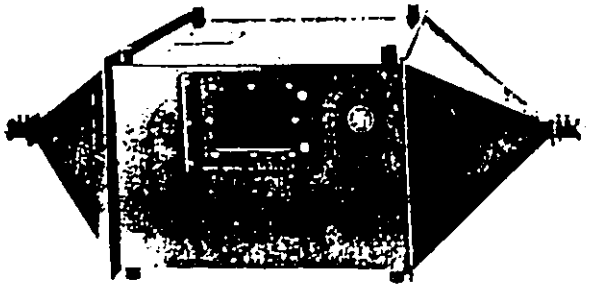

MODEL CC-103

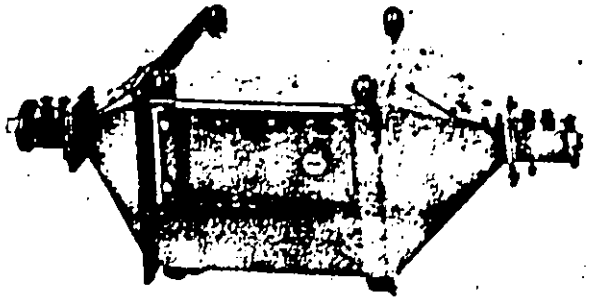

MODEL CC-108

Physical dimensions and frequency ranges of IFI TEM cells .

MODEL	FREQUENCY RANGE	CELL SIZE (outer dimensions)	SEPTUM WIDTH	ACCESS DOOR SIZE	CENTER SECTION HEIGHT-WIDTH (inside dimension)	CONN. PLATE OPENING DIMENSION
CC101	DC - 100 MHz	142 x 73 x 51	54.0	30.5 x 18	47.16 x 70.7	6 x 2.5
CC101.5	DC - 150 MHz	104 x 50 x 34	36.0	16 x 10	31.44 x 47.16	6 x 2.5
CC102	DC - 200 MHz	77 x 38 x 26	27.0	13 x 8	23.6 x 35.4	6 x 2
CC103	DC - 300 MHz	54 x 26 x 18	17.8	8.5 x 6.5	15.7 x 23.6	4.5 x 1.5
CC104	DC - 400 MHz	42 x 20 x 14	13.4	6 x 5	11.8 x 17.7	3.5 x 1.25
CC108	DC - 800 MHz	24 x 11 x 8	6.5	5 x 2.3	5.9 x 8.8	1.5 x 2
CC110	DC - 1000 MHz	18 x 8 x 5	5.2	3 x 2	4.7 x 7.1	1.5 x 2

The Model IFI cc101.5s TEM cell is a modified version of the model IFI cc101.5 cell . The major difference between the two model is that the IFI 101.5s model has a square center section instead of rectangular center section as in the regular IFI 101.5 model TEM cell .

The actual physical dimensions of IFI 101.5s TEM cell are given in the following cross-sectional drawings .

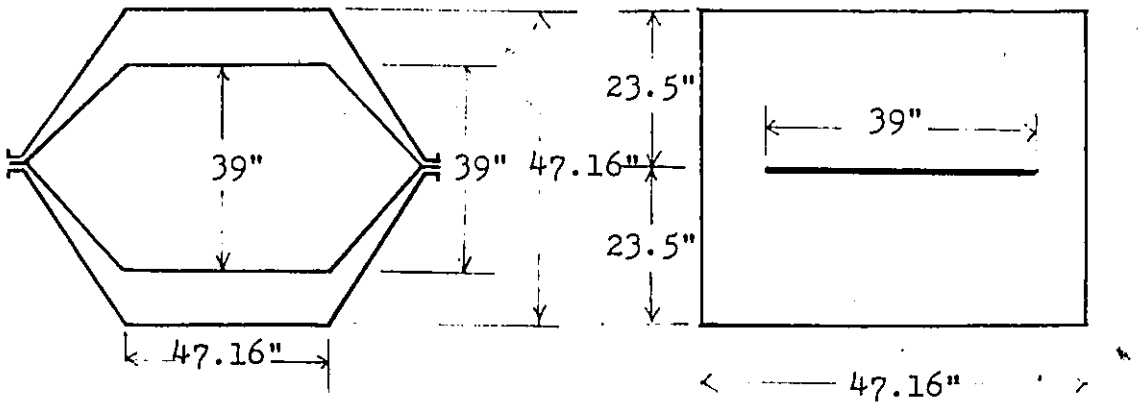

BIBLIOGRAPHY

TEM CELL REFERENCES

[1] P.F.Wilson,M.T.MA, "*Simple Approximate Expressions for Higher Order Mode Cutoff and Resonant Frequencies in TEM Cells*," IEEE Trans. on Electromagnetic Compatibility, vol.EMC-28,No.3,pp125-129 ,August 1986.

[2] T.K.Seshadri,S.K.Das,B.K.Sinha ,"*Studies on Field and Impedance Variation with object height inside*" IEEE 1985 International Symposium on Electromagnetic Compatibility ,IEEE.1985,Wakefield,MA.,USA,pp525-529,August,1985.

[3] N.S. Nahman,M.Kanda,E.B.Larsen,M.L. Crowford,"*Methodology for Standard Electromagnetic field Measurements*"IEEE Trans. on Instrumentation and Measurement , vol. IM-34,No.4,pp490-503,December 1985.

[4] B.N.Das,S.A.Mohan ,"*TEM Cell in Absence of One of the Walls Parallel to the Septum*", IEEE Trans. on Electromagnetic Compatibility ,vol. EMC-27,No.2, pp58-63,May,1985.

[5] B.N.Das,S.A.Mohan ,"*Analysis of a TEM Cell with Septum on a Dielectric Slab*",IEEE Trans.on Electromagnetic Compatibility,vol. EMC-27,No.1,pp1-6,February 1985.

[6] A.Tehori "*Using a TEM Cell for EMP Simulationus*" ,1984 International Symposium on Electromagnetic Compatibility . IEEE .Inst. Electron. & Commun. Eng. Japan. Inst. Electr. Eng. Japan 1984 Tokyo Japan pp627-629,1984.

[7] P.F.Wilson,M.T.Ma ,"*Small Obstacle Loading in a TEM Cell* ",1984 International Sym-

posium on Electromagnetic Compatibility, IEEE Inst. Electron. & Commun. Eng. Japan Inst. Electr. Eng. Japan. 1984 Tokyo,Japan.pp30-35,1984.

[8] P.F. Wilson ,D.C. Chang ,M.T. MA, "*Input Impedance of a Probe Antenna in a TEM Cell* ", IEEE Trans. on Electromagnetic Compatibility ,vol. EMC-26,No.4 ,pp154-161,November,1984.

[9] C.M. Weil ,L.Gruner "*High-Order Mode Cutoff in Rectangular Striplines*",IEEE Trans. on Microwave Theory Tech., vol. MTT-32, no.6, pp638-641,June,1984.

[10] D.A.Hill ,J.A.Walsh,"*Resonance Suppression in a TEM cell*",J.of Microwave Power,vol.18,No.4 , pp325-330,March 1983.

[11] D.A. Hill,"*Bandwith Limitations of TEM Cells due to Resonances*",J.of Microwave Power,vol.18,No.2, pp181-195,January 1983.

[12] M.Kanda,"*Electromagnetic-Field Distortion Due to a Conducting Rectangular Cylinder in a Transverse Electromagnetic Cell*",IEEE Trans. on Electromagnetic Compatibility ,vol. EMC-24, No.3,pp294-301,August 1982.

[13] D.A. Hill ,"*Human Whole-Body Radiofrequency Absorption Studies Using a TEM Cell Exposure System*" ,IEEE Trans. on Microwave Theory and Tech. vol.30,No.11, pp1847-1854,Norvember 1982.

[14] J.K.Daher,E.E.Donaldson,Jr.and J.A.Woody "*Evaluation of Radiated Emission and Susceptibility Measurement Techniques*",IEEE Electromagnetic Compatibility Symposium Record, pp244-251,1982.

[15] I.Sreenivasiah,D.C.Chang,M.T.Ma,"*A Critical Study of Emission and Susceptibility Levels of Electrically small Objects from Tests Inside a TEM Cell*",IEEE Electromagnetic Compatibility Symposium Record ,pp499-501,1981.

[16] M.L. Crowford ,J.L.Workman,C.L.Thomas ,"*Expanding the Bandwidth of TEM Cells for EMC Measurements*", IEEE Trans. on Electromagnetic Compatibility ,vol. EMC-20, No.3,pp368-375,August 1978.

[17] R.E.Hartman,W.A. Kesselman,"*TEM Transmission Line Technique for the Measurement of "Radiated Susceptibility""*,IEEE Electromagnetic Compatibility Symposium Record pp187-190,1978.

[18] C.M. Weil ,"*The Characteristic Impedance of Rectangular Transmission Lines With Thin Center Conductor and Air Dielectric*",IEEE Trans. on Microwave Theory and Tech., vol.MTT-26,No.4,pp238-242,April 1978.

[19] M.L.Crowford,J.L.Workman,C.L.Thomas,"*Generation of EM Susceptibility test fields Using a Large Absorber-Loaded TEM Cell*",IEEE Trans. on Instrumentation and Measurement,vol.IM-26,No.3,pp225-230,September 1977.

[20] M.L. Crawford ,J.L.Workman,"*Asymmetric Versus Symmetric TEM Cells for EMI Measurements*",IEEE Electromagnetic Compatibility Symposium Record pp204-206,1977.

[21] J.C. Tippet ,D.C.Chang ,"*Radiation Characteristics of Electrically Small Devices in a TEM Transmission Cell*",IEEE Trans. on Electromagnetic Compatibility , vol. EMC-18,No.4,pp134-140,Norvember 1976.

[22] M.L.Crawford,"*Generation of Standard EM Fields Using TEM Transmission Cells*",IEEE Trans. on Electromagnetic Compatibility ,vol.EMC-16,No.4,pp189-195,November 1974.

[23] R.R.Gupta,"*Accurate Impedance Determination of Coupled TEM Conductors*",IEEE Trans.on Microwave Theory and Tech. ,vol.17,No.8,pp479-488,August 1969.

[24] O.R.Cruzan,R.V.Garver,"*Characteristic Impedance of Rectangular Coaxial Transmission*

Lines",IEEE Trans. on Microwave Theory and Tech.,vol.MTT-12,pp488-495,September 1964.

[25] D.W.T. ,Crawford M.L.,Wilson W.A.,"Construction of a Transverse Electromagnetic Cell ", NBS Technical Note 1011 November 1978.

[26] P.F.Wilson ,D.C.Chang ,M.T.Ma,"Input Impedance of a Probe Antenna Exciting A TEM Cell",National Bureau of Standards .Technical Note 1040.

[27] M.L.Crowford,J.L.Workman,"Using a TEM cell for EMC Measurements of Electronic Equipment",Nat.Bur.Stand.(U.S) Tech. Note 1013 ,July 1981.

[28] J.C.Tippet ,D.C. Chang ,"Radiation Characteristics of Dipole Sources Located Inside a Rectangular,Coaxial Transmission Line",NBSIR 75-829 ,January 1976.

[29] T.Saad ,"Microwave Engineers' Handbook " ,Artech House Inc. ,1971.

REFERENCES OF NUMERICAL METHODS

[30] H.E. Green,"*The Numerical Solution of some Important Transmission Line Problems*",IEEE Trans. on Microwave Theory and Tech.,vol. MTT-13,No.5,pp676-692,September 1965.

[31] M.V.Schneider ,"*Computation of Impedance and Attenuation of TEM-Lines by Finite-Difference Methods.*",IEEE Trans. on Microwave Theory and Tech.,vol.MTT-13,No.6,pp793-800,November,1965.

[32] A. Wexler ,"*Computation of Electromagnetic Fields*" ,IEEE Trans. on Mirowave Theory and Tech., vol.MTT-17,No.8,pp416-439,August 1969.

[33] B.H. McDonald,M.Friedman,A.Wexller, "*Variational Solution of Integral Equations*", IEEE Trans. on Microwave Theory and Tech.,vol. MTT-22 , No.3, pp237-248,March 1974.

[34] J.F.Botha,G.F.Pinder,"*Fundamental Concepts in the Numerical Solution of Differential Equations*",Wiley & Sons,1983.

[35] E.H.Twizell,"*Computational Methods for Partial Differential Equations*",Wiley & Sons ,1984.

[36] P.P.Silvester ,R.L.Ferrari,"*Finite Elements for Electrical Engineer*", Cambridge university press,1983.

[37] P.P.Silvester,M.V.K.Chari ,"*Finite Elements in Electrical and Magnetic Field Problems*", John Wiley and Sons ,1980.

[38] L.J.Segerlind,"*Applied Finite Element Method Analysis* ", John wiley & sons 1984.

[39] O.C.Zienkiewick,K.Morgan,"*Finite Elements and Approximation*", John Wiley and Sons ,1983.

[40] S.G.Mikhlin,"*Variational Methods in Mathematical Physics*", Pergamon Press,1964.